

2004

The Geology, Geochemistry and Ecology of a Shallow Water Submarine Hydrothermal Vent Bahía Concepción, Baja California Sur, México

Matthew J. Forrest
California State University, Monterey Bay

Follow this and additional works at: https://digitalcommons.csumb.edu/caps_thes

Recommended Citation

Forrest, Matthew J., "The Geology, Geochemistry and Ecology of a Shallow Water Submarine Hydrothermal Vent Bahía Concepción, Baja California Sur, México" (2004). *Capstone Projects and Master's Theses*. 91.

https://digitalcommons.csumb.edu/caps_thes/91

This Master's Thesis is brought to you for free and open access by Digital Commons @ CSUMB. It has been accepted for inclusion in Capstone Projects and Master's Theses by an authorized administrator of Digital Commons @ CSUMB. Unless otherwise indicated, this project was conducted as practicum not subject to IRB review but conducted in keeping with applicable regulatory guidance for training purposes. For more information, please contact digitalcommons@csumb.edu.

THE GEOLOGY, GEOCHEMISTRY AND ECOLOGY OF A
SHALLOW WATER SUBMARINE HYDROTHERMAL VENT IN
BAHÍA CONCEPCIÓN, BAJA CALIFORNIA SUR, MÉXICO

A Thesis

Presented to

The Faculty of the Institute of Earth Systems Science & Policy

California State University Monterey Bay

Through

Moss Landing Marine Laboratories

In Partial Fulfillment

Of the Requirements for the Degree

Master of Science in Marine Science

By

Matthew J. Forrest

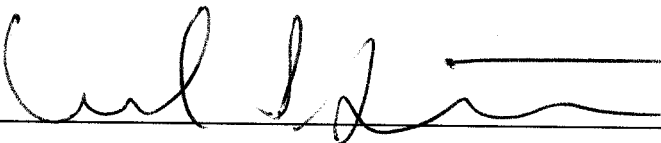
May, 2004

© 2004

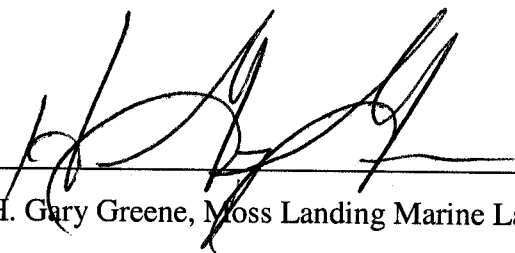
Matthew J. Forrest

ALL RIGHTS RESERVED


APPROVED FOR THE INSTITUTE OF EARTH SYSTEMS
AND SCIENCE POLICY



Dr. Michael S. Foster, Moss Landing Marine Laboratories



Dr. H. Gary Greene, Moss Landing Marine Laboratories



Dr. Kenneth H. Coale, Moss Landing Marine Laboratories

APPROVED FOR THE UNIVERSITY

ABSTRACT

THE GEOLOGY, GEOCHEMISTRY AND ECOLOGY OF A SHALLOW WATER SUBMARINE HYDROTHERMAL VENT IN BAHÍA CONCEPCIÓN, BAJA CALIFORNIA SUR, MÉXICO

By

Matthew J. Forrest

I studied a shallow water (0-13m water depths) hydrothermal vent in Bahía Concepción, Baja California Sur, Mexico. Investigations using side-scan sonar and SCUBA suggested that the submarine hydrothermal activity is mainly controlled by a NW-SE trending onshore-offshore fault. Compared to seawater, vent fluids are enriched in Ca, Mn, HCO₃, SiO₂, B, As, Li, Fe, Rb, and Sr, and depleted in Na, Cl, Mg, and SO₄, with calculated end-member temperatures up to 220°C. The vent gas is primarily nitrogen, carbon dioxide, and methane, and the geochemistry of the gas suggests that it may be derived from the thermal alteration of algal matter. The submarine hydrothermal activity is negatively affecting abundances and diversity of infaunal assemblages. The carbon and nitrogen stable isotope ratios of some of the animals feeding around the vent, particularly the sea cucumber *Holothuria inabilis*, were significantly different than those from the same species collected away from venting activity.

ACKNOWLEDGEMENTS

This thesis would not have been possible without the assistance and contributions of many people. I am particularly indebted to my committee members, Mike Foster, Gary Greene, and Kenneth Coale, who helped me shape the many different facets of my thesis into a more coherent whole. I would also like to thank Bill Ussler, Jorge Ledesma-Vázquez, Rosa Maria Prol-Ledesma, Victoria Orphan, Diana Steller, Ivano Aiello, John Heine, Joan Parker, John and Jocelyn Douglas, Jason Felton, Thomas Pichler, Rob Burton, Paul Koch, Susan von Thun, Peter Slattery, Rusty Fairey, John Goetzel, Autumn Bonnema, Mike Gordon, Bill Watson, Aroon Melwani, Chad King, Laurie McConnico, Mike Graham and the staff, faculty, and students at Moss Landing Marine Labs for their invaluable contributions in the lab and in the field.

Partial funding was provided by generous grants from the Earl and Ethel Myers Oceanographic Trust, the David and Lucille Packard Foundation, and PADI Aware. I am also grateful to my family, especially my father Jack Forrest and my mother Virginia Forrest who provided tremendous love and support. My fieldwork in Bahía Concepción was greatly facilitated by the generous hospitality of Chuck and Kathy Mitchell and the kind and loving people of Baja California Sur.

This by no means represents a complete list of all of the people who helped me with this thesis, but in the interest of brevity I conclude with a huge thank you and muchas gracias to all of the other people who enriched my thesis work and my life.

TABLE OF CONTENTS

Abstract.....	iv
Acknowledgments.....	v
List of Tables.....	vii
List of Figures.....	viii
General Introduction.....	1
 CHAPTER I. THE GEOLOGY AND GEOCHEMISTRY OF A SHALLOW WATER HYDROTHERMAL VENT IN BAHÍA CONCEPCIÓN	
Abstract.....	8
Introduction.....	9
Materials and Methods.....	19
Results.....	23
Discussion.....	25
 CHAPTER II. ECOLOGICAL IMPLICATIONS OF SHALLOW WATER HYDROTHERMAL VENTING IN BAHÍA CONCEPCIÓN	
Abstract.....	35
Introduction.....	36
Materials and Methods.....	42
Results.....	46
Discussion.....	49
Literature Cited.....	63
Tables.....	82
Figures.....	89
Appendices.....	108

LIST OF TABLES

<u>Table</u>		<u>Page</u>
1.	DO, conductivity, salinity, and pH of pore water cores.	82
2.	Vent fluid geochemistry from Bahía Concepción.	83
3.	Calculated subsurface end-member temperatures of vent fluids.	84
4.	Vent gas compositions from Bahía Concepción.	85
5.	Methane and ethane concentrations and ratios of vent gas.	86
6.	Carbon stable isotope ratios from CO ₂ , CH ₄ , and C ₂ H ₆ .	87
7.	Elemental compositions of vent and non-vent <i>Holothuria inhabilis</i> and flocculent material samples.	88

LIST OF FIGURES

<u>Figure</u>		<u>Page</u>
1.	Map of known deep-sea hydrothermal vent regions.	89
2.	The Baja California peninsula and associated tectonic structures.	90
3.	Geologic map of the Bahía Concepción region.	91
4.	Isla El Requesón with tombolo of rhodolith derived sand.	92
5.	El Mono cherts occurring along Concepción Fault Zone.	92
6.	Geological map of Punta Santa Barbara area.	93
7.	Mineral precipitates around intertidal hot springs.	94
8.	Gas and hydrothermal fluids venting in subtidal at 6 m.	94
9.	Locations of side-scan track lines near Punta Santa Barbara.	95
10.	Side-scan track line 13 with close-ups of vent features.	96
11.	Map of interpretive side-scan data.	97
12.	Means of pH profiles in sediments at vent, transitional, and non-vent sites.	98
13.	Means of temperature profiles in sediments at vent, transitional, and non-vent sites.	99
14.	Fraction % of grain sizes from vent, transitional, and non-vent sites.	100
15.	Giggenbach diagram of subtidal and intertidal vent fluids.	101

LIST OF FIGURES (CONT.)

<u>Figure</u>		<u>Page</u>
16.	Methane $\delta^{13}\text{C}$ values and hydrocarbon ratios of natural gases of biogenic and thermogenic origins.	102
17.	Mean infaunal abundances per core separated by phyla.	103
18.	Reduced space and eigenvectors plots of infaunal cores.	104
19.	Reduced space and eigenvectors plots of physical data.	105
20.	Plot of stable isotope ratios from vent and non-vent fauna.	106
21.	Fluorescence microscopy analyses of flocculent materials with DAPI stain and FISH probe.	107

GENERAL INTRODUCTION:

Submarine hydrothermal venting

Submarine hydrothermal venting occurs in diverse tectonically active areas throughout the world. Deep-sea high temperature hydrothermal venting, where heat is transferred from the lithosphere to the ocean, is generally associated with active plate boundaries such as spreading centers, fracture zones, and back-arc spreading centers in subduction zones (Fig. 1) (German et al., 1995). Fault and fracture patterns influence venting activities, as well as the longevity and locations of lower-temperature hydrothermal fluid outlets (Van Dover, 2000), because fractures and faults provide conduits or permeable pathways for fluids (Barton et al., 1995; Orange et al., 1999). Warmer, and therefore lighter, hydrothermal fluids are continuously driven by convective flow toward faults from the host rocks, while stress concentration around faults leads to dilatancy due to pore volume expansion from the formation of micro-cracks, thereby increasing fault-rock porosity (Gudmundsson, 1999). These hydrothermal fluids circulate through the porous top layers of oceanic crust where they react with volcanic rocks and sediments, influencing and altering the elemental composition of the entrained seawater (Dziak and Johnson, 2002). Sea floor spreading centers, where cold seawater circulates through the highly faulted crust and reacts with hot (>300°C) basalts, may be important components of the global chemical mass balance of the oceans over geological time as the fluxes of some elements injected in to, or removed from, the ocean and dispersed via mid-depth circulation may exceed fluxes from fluvial sources (Edmond et al., 1982).

The chemical composition and physical properties of hydrothermal fluids can have significant localized effects on geochemistry, physical geology, and ecological processes. The hydrothermal vents located on the deep (defined here as >1000m water depths) sea floor often support unique ecosystems that rely mainly on sulfide-rich hydrothermal fluids and chemosynthetic bacteria, rather than photosynthesis, to provide energy and nutrition to the animals present (Brooks et al., 1987; Brinkhoff et al., 1999).

Chemosynthesis, or more accurately chemolithoautotrophy, refers to the biosynthesis of organic compounds from carbon dioxide or methane using energy and reducing power from inorganic compounds such as hydrogen sulfide (H₂S) (Conway, et al., 1994). Deep-sea chemosynthetic communities have also been discovered in “cold seep” environments where chemically modified fluids derived from hydrocarbon reservoirs, methane hydrates, pore waters in sediments, and sites of organic enrichment such as whale skeletons on the ocean floor are released at ambient temperatures (Van Dover et al., 2002). Some invertebrates found around these vent and seep environments are “obligate” chemolithotrophic organisms (Barry et al., 1996). These animals harbor symbiotic chemoautotrophic bacteria within their tissues, and these symbionts may provide some or all of the nutritional needs of the host organisms, which in turn provide the bacteria with a constant supply of essential organic and inorganic compounds (Brooks, et al. 1987).

Generally, sulfur-oxidizing chemosynthetic bacteria appear to be the major primary producers in hydrothermal environments, but methanotrophic bacteria are also important in seep environments (Paull et al., 1985; Orphan et al., 2001). Obligate organisms at hydrothermal vents may have simultaneous access to oxygen and reduced compounds as

a result of mixing of the vent fluids with ambient sea-water, while obligate organisms at seep environments often live at the interface between the reducing environments in the sediments, and the overlying oxygenated water (Southward, 1989).

Deep-sea hydrothermal vents are characterized by macrofaunal biomasses so much greater than that of the surrounding deep-sea benthos that they have been referred to as “oases” in the otherwise barren “deserts” of the deep sea floor (Carney, 1994).

Chemosynthetic bacteria at vents and seeps are also present as suspended free-living populations associated with hydrothermal fluid discharge, or as microbial mats growing on hard substrates or sediments. Numerous “regional” (Barry et al., 1996) suspension-feeding, grazing, and deposit feeding species that do not harbor bacterial symbionts may have access to these potential food sources (Van Dover and Fry, 1994). Microbial mats near areas of hydrothermal venting represent the base of complicated food webs, attracting and supporting increased numbers of deposit feeders, resulting in higher numbers of predators and scavengers in the area (Davis and Spies, 1980). Some of these predators and scavengers may reside permanently around the vents, or may act as vagrant species: animals that bridge the gap between vent and non-vent environments by entering the venting areas to forage (MacAvoy et al., 2002).

Competition for space proximal to hydrothermal vents, and differences in tolerances to physical and chemical gradients may be driving forces in structuring vent communities, and biological zonation analogous to that found in some rocky intertidal communities may ensue (Johnson et al., 1994). The character of species interactions varies along a gradient in hydrothermal fluid flux, with inhibitory interactions among

species more prominent in zones with higher temperatures, productivity and faunal densities, while facilitative interactions appear to be more characteristic where temperatures, productivity, and faunal densities are low (Mullineaux et al., 2003). Deep sea hydrothermal communities are often distributed in concentric rings around the vent openings, with bacterial feeders dwelling on, or around, chimneys formed by the precipitation of dissolved metals within the hydrothermal fluids, vent-obligates colonizing intermediate areas experiencing more diffuse flow, and filter-feeding organisms forming the outer ring (Colaco et al., 2002). Although gradients from oxic to anoxic conditions are very sharp in vent environments, dense aggregations of some vent organisms, such as the vent mussel *Bathymodiolus thermophilus* can disperse hydrothermal fluids laterally over several meters, thereby increasing the area of the redox transition zone (Johnson et al., 1994).

On slowly spreading ridge systems such as the Mid-Atlantic Ridge, fluids seem to be derived from a single source, and fluid chemistry is relatively homogenous, but at faster-spreading ridges such as the East Pacific Rise, hydrothermal fluids even a few meters apart can be chemically unique (Van Dover et al., 2001). Habitats around hydrothermal vent sites are patchy and ephemeral, and shifts along ridge axes may occur on decadal time scales at fast-spreading centers, consequently vent communities may face extinctions or bottle-neck effects if fluid flow changes in intensity or ceases (Jollivet, 1996). Additionally, catastrophic events such as volcanic eruptions and earthquakes may create or destroy entire habitats, making disturbance and subsequent primary succession dominant characteristics of deep sea vent ecosystems (Mullineaux et al., 2003).

Hydrothermal fluids mixed with entrained seawater provide the primary thermal and chemical energy that incubate and fuel the microbial subsurface biosphere thriving in the porous upper crustal rocks (Dziak and Johnson, 2002). This subsurface microbial biomass may rival the biomass of the global surface flora and fauna (Van Dover, 2000). Massive sulfide deposits, some up to 45m tall, are common around hydrothermal vents on the East Pacific Rise and the Juan de Fuca Ridge. These deposits, often referred to as “chimneys”, grow as metal sulfides precipitate from the hot (up to 400°C) hydrothermal fluids as they mix with the ambient seawater (Edmond et al., 1982). Sulfide deposits serve as habitat for hyperthermophilic bacterial populations, and microbial populations in plumes of hydrothermal fluids may mediate oxidation-precipitation reactions of hydrothermal plume constituents, thereby enhancing mineral deposition (Juniper et al., 1988; Van Dover, 2000).

Deep-sea hydrothermal vents and seeps support unique communities dependent on primary production via chemosynthetic dietary carbon sources. Bacterial communities around hydrothermal vent systems are essential components of the ecological and geochemical processes that they influence. Deep-sea vent and seep communities are composed of predominately endemic species adapted for living in patchy and ephemeral environments, and sharp gradients in temperature and geochemistry around vents may result in biological zonation and mediate species interactions.

Shallow water submarine hydrothermal venting

Shallow water (defined here as less than 100m deep) hydrothermal venting also

occurs throughout the world's marine environments (Levin et al., 2000). In many cases such venting is associated with volcanic islands and arcs, or occurs on the top of seamounts (e.g. Pichler et al., 1999a; Dando et al., 1995a; Sedwick and Stuben, 1996; Sorokin et al., 1998; Tarasov et al., 1999). Since shallow water vents are usually located within the euphotic zone, primary production via photosynthesis is expected to be the dominant source of dietary carbon to the fauna surrounding these vents. However, chemosynthetic bacterial mats may also be present, and could potentially represent additional sources of primary production to organisms that are capable of consuming and processing the chemosynthetically derived carbon.

A conspicuous feature of shallow water hydrothermal venting is the frequent occurrence of "gasohydrothermal" activity around shallow vents, where gases are discharged in discrete streams along with hydrothermal fluids (Dando et al., 1995b). This type of discrete gaseous venting is not usually present at deep vents because they are subjected to higher hydrostatic pressures, preventing phase separation. In some shallow water venting systems these gases may be acidic, and as they interact with hydrothermal fluids mixed with seawater they leach silica and metal cations from the volcanic sands; the fluid chemistry of these systems may be different from that of deep-sea hydrothermal vents due to differences in the elemental composition of the source rocks and sediments, and the increased effects of magmatic degassing and phase separation under reduced hydrostatic pressure (Sedwick and Stuben, 1996).

While massive sulfides, Mn-oxyhydroxides, Fe III oxyhydroxides and Fe-smectites seafloor deposits are associated with deep-water, high-temperature hydrothermal systems

along mid-ocean ridges and in deep back-arc basins, Fe III oxyhydroxides are the prominent precipitates that form in shallow water, lower temperature hydrothermal systems (Pichler and Veizer, 1999). Fe-oxyhydroxide precipitation is often microbially mediated (Fortin et al., 1998), and the accumulation of Fe III oxides by microbial activity is an important mechanism of iron deposition in the deep oceans (Juniper and Tebo, 1995). Fe III oxyhydroxides are particularly important constituents in marine sediments in volcanically active coastal areas where they can effect the composition of local seawater, and therefore marine life (Pichler et al., 1999b).

Shallow water hydrothermal venting also occurs in continental margin settings affected by intense tectonic extension, such as in western México--particularly within the Gulf of California and along the Baja California Peninsula (Canet et al., 2003). The peninsular fault systems associated with the opening of the Gulf of California typically involve hydrothermal activity (Libbey and Johnson, 1997). Shallow water hydrothermal activity has been reported in Bahía Concepción (McFall, 1968), San Felipe, Punta Estrella, El Coloradito and Puertecitos in the Gulf of California along the eastern shore of the Baja California Peninsula (Barragán et al., 2001), and in Punta Banda on the western shore of Baja near Ensenada (Vidal et al., 1978). Shallow water hydrothermal activity has also been investigated in Punta Mita, near Puerto Vallarta, México (Rubio-Ramos and Prol-Ledesma, 2000; Prol-Ledesma et al., 2002; Taran et al., 2002) (Fig. 2). This thesis will address the structural geology, geochemistry, and ecological implications of a shallow water hydrothermal vent within Bahía Concepción, a prime example of an extensional basin formed in association with the opening of the proto-Gulf of California.

CHAPTER I. THE GEOLOGY AND GEOCHEMISTRY OF A SHALLOW WATER
HYDROTHERMAL VENT IN BAHÍA CONCEPCIÓN

ABSTRACT:

Intertidal hydrothermal activity has been documented at several locations along the western shore of Bahía Concepción. Subtidal venting of hydrothermal fluids and gas is also occurring in depths of 0-14 m along approximately 750 m of coastline near Punta Santa Barbara. Side-scan sonar and *in situ* observations of this subtidal hydrothermal activity suggest that it is primarily controlled by an onshore-offshore fault associated with the fault zone that delineates the western margin of Bahía Concepción, referred to here as El Requesón fault zone. The geochemical characteristics of the gas and fluids being released indicate thermogenic origins. Active manganese and silica precipitation in the intertidal zone near Punta Santa Barbara show similarities with paleo-hydrothermal activity associated with the Concepción Fault Zone on the eastern margin of the bay, and offer a possible mechanism for the formation of El Mono chert. The high concentrations of silica and arsenic in vent fluids are likely due to interactions with local andesitic volcanoclastic rocks. The gas is predominately nitrogen, carbon dioxide, and methane and may be derived in part from thermal alteration of rhodolith and other algal compounds within the sedimentary organic matter. The deep subsurface temperatures of the subtidal vent fluids as calculated by chemical geothermometers range between 106-188°C, and

from 113 -220°C for the intertidal spring fluids. Hydrogen gas geothermometers indicate subsurface temperatures as high as 180°C. These results suggests that the faults associated with El Requesón fault zone are deep-seated, and may be acting as conduits for meteoric water which mixes with seawater and is heated by high local thermal gradients along extensional tectonic structures, similar to other coastal hydrothermal systems reported in Baja and western Mexico.

INTRODUCTION:

Geochemistry of hydrothermal fluids and gases

The relative molar concentrations of the major cations and anions in seawater are virtually constant throughout the world's oceans, varying only as a function of salinity (Millero, 2002). Thermohaline circulation in the oceans occurs with a transit time of approximately 1500 years. The geochemical processes that occur along this pathway strongly affect the chemical evolution, and elemental composition, of seawater (Bricker and Jones, 1995). Processes that occur at hydrothermal vents can result in the addition or removal of elements and constituents to and from seawater. Calcium, copper, zinc, manganese and silica concentrations in hydrothermal vent fluids may be several orders of magnitude greater than natural seawater, whereas high temperature hydrothermal discharges are completely devoid of magnesium due to the formation of Mg silicates

when sea water reacts with molten basalts; these processes can alter elemental concentrations over large temporal scales (Millero, 2002). Hydrothermal fluid circulation in the porous ocean floor is a thermally driven process within a uniform aquifer and can be continuous over thousands of kilometers (Dziak and Johnson, 2002). Subsurface hydrothermal circulation is slow (the global ocean cycles through seafloor hydrothermal systems once every 10-100 million years), but hydrothermal plumes at ridge crests interact with the ocean on much faster time scales (the volume of the global ocean passes through and reacts with hydrothermal plumes approximately every 1000 years (Van Dover, 2000)), and these processes figure prominently in geochemical cycling of elements and the biogeochemistry of deep-ocean waters and sediments.

Active plate margins, particularly fast-spreading centers, are generally sediment starved, therefore the hydrothermal fluid chemistry at these locations is controlled by high temperature sea water-basalt reactions (Edmond et al., 1982). In areas where hydrothermal fluids pass through seafloor sediment cover prior to venting into the water column, physical and chemical interactions between the fluids and sediments enhance mineral deposition (Juniper et al., 1988). Contribution from the overlying sediments at sedimented ridge locations (e.g., the Guaymas Basin in the Gulf of California and the Escanaba Trough in the Gorda Ridge) and back-arc basins (e.g., Mariana and Okinawa Troughs) can also provide strong enrichments in hydrothermal fluids of elements derived from organic matter such as Li, Rb, and Cs (You et al., 1994). The Lau Basin, also a back-arc basin, is characterized by intense and extensive hydrothermal fields with vent fluid chemistry that is very different (lower pH and higher dissolved metal contents of

Mn, Zn, Pb, Cu, and As) relative to spreading center vent fluids, and these differences have been attributed to the greenschist facies interactions of seawater with the andesitic basement in the Lau Basin as opposed to the reaction with basaltic basement at mid-ocean ridge spreading centers (German et al., 1995).

Geothermal vent fluid composition and chemistry are relatively uniform in locations where seawater reacts with basalts, but may differ significantly where the chemical composition of the basement host differs from normal mid-ocean ridge basalts, or where sediment overlies sills of extrusive volcanic rocks, or is buried beneath a basaltic crust (Van Dover, 2000). The fluid chemistry of shallow water hydrothermal systems may be different from that of deep-sea hydrothermal vents due to differences in the elemental composition of the source rocks and sediments, and the increased effects of magmatic degassing and phase separation under reduced hydrostatic pressure (Sedwick and Stuben, 1996). Geothermal fluids are typically classified in three distinct categories based on their Cl^- , SO_4^{2-} , and HCO_3^- contents: highly acidic chloride-sulfate waters, spring waters with associated copious discharge of CO_2 (soda springs), or discharges from deep geothermal wells and associated neutral chloride springs (Giggenbach, 1988). The geochemistry of thermal fluids may be useful in estimating the deep subsurface end-member temperatures in hydrothermal systems. The most widely used vent fluid chemical geothermometers derive from the Na/K, Na/Li, and SiO_2 methods (Verma and Santoyo, 1997).

The composition and geochemistry of gases released in zones of hydrothermal activity can be informative in determining the sources and processes involved in the

generation of these gases (Floodgate and Judd, 1992). The chemical composition of gas mixtures emerging in thermal areas can be used as gas geothermometers to evaluate the deep thermal temperatures (D'Amore and Panichi, 1980). Carbon dioxide is the major component of most of the submarine geothermal gas exhalations that have been sampled (Dando et al, 1995b), but nitrogen and methane may also be present in significant concentrations (e.g. Vidal et al., 1978; Prol-Ledesma et al., 2002). The principal sources of methane in natural gases are either biogenic, created by microbial processes in low-temperature anaerobic environments, or thermogenic where high temperatures ($> 100^{\circ}\text{C}$) are sufficient to break chemical bonds in organic matter (Welhan, 1988). The stable isotope ratios of carbon in methane, along with the ratios of methane to ethane from gas samples can help to determine the origins of the gases (Schoell, 1983). The ratios of the concentrations of methane to C_2 + hydrocarbon gases (i.e. ethane, propane, etc.) are typically in the range of 10^2 in thermogenic systems, and thermogenic methane $\delta^{13}\text{C}$ values are greater than -60‰ (Wiese and Kvenvolden 1993). Isotopic and compositional evidence indicate that the principal sources of methane in most hydrothermal systems are thermogenic, derived from pyrolysis of organic matter at moderate to high temperatures (Schoell, 1988; Welhan, 1988) rather than bacterial methanogenesis. In hydrothermal systems, the formation of hydrocarbons can be a rapid process, occurring in days to years (Simoneit and Kvenvolden, 1994), over temperature ranges from approximately 60° to greater than 400°C (Simoneit, 2000).

The geochemistry of the gas and fluids from hydrothermal vents can offer evidence about the processes involved in their formation and migration. Analyses of the vent fluids

and gas can provide evidence about interactions with host rocks and sediments, and when applied to geothermometers, they allow for estimates of subsurface end-member temperatures. These data may also elucidate whether the shallow water hydrothermal venting in Bahía Concepción is related to the complex tectonic evolution of Baja California.

Bahía Concepción and El Requesón fault zone

The evolution of the Baja California peninsula and the Gulf of California occurred in several distinct phases beginning in the Miocene and continuing through recent times (Oskin et al., 2001). The first phase involved a subduction regime off the Pacific coast, which ended about 12 Ma, concurrent with an active terrestrial volcanic arc where the Gulf of California is presently located (Hausback, 1984; Lonsdale, 1989). This subduction zone was extinguished in jumps from 16 Ma in the north to 12 Ma in the south (Umhoefer et al., 2002). Around 12 Ma, a transform plate boundary, the Tosco-Abrejos strike-slip fault, formed on the west side of the future Baja California peninsula (Spencer and Normark, 1989) (Fig. 1). The second phase was associated with the opening of the Proto-gulf of California, which occurred from about 10-3.5 Ma, and involved major east-northeast crustal extension caused by north-northwest striking normal faults adjacent to the modern Gulf (Stock and Hodges, 1989). Dextral displacement on the southern San Andreas Fault resulted in orthogonal extension, and localization of plate

boundary slip in the gulf and complete transfer of the Baja California peninsula to the Pacific plate occurred rapidly between 6.3 and 4.7 Ma (Oskin et al., 2001).

The Proto-Gulf rift formed a deep marine basin between the Baja Peninsula and mainland Mexico about 8 Ma, but the intense tectonic extension associated with its opening and the related intrusion of magmatic bodies at shallow depths occurred as early as 23-15 Ma (Zanchi, 1994). Marine incursion into the southern Gulf of California at 7.5-8.2 Ma, and in the northern Gulf at 6.5 Ma, probably covered a region of more intense continental extension, as suggested by plate-tectonic reconstructions (Stock and Hodges, 1989; Oskin and Stock 2003). About 3.5 Ma a complex transform boundary was activated within the Gulf, connecting the San Andreas fault system with the East Pacific Rise (Lonsdale, 1989). Between 3.5 Ma and the present, basalts began emerging from the seafloor in the spreading mouth of the Gulf of California, and a new set of westwardly oriented transform faults were generated in the center of the modern Gulf (Hausback, 1984) (Fig 1).

The basic structural element of a continental rift with orthogonal extension is a half-graben, where subsidence occurs along a single fault (Ingersoll and Busby, 1995; Umhoefer et al., 2002). The western margin of the Gulf of California is made up of 50-150 km-scale segments of tectonic blocks, separated by accommodation zones, that alternate in the symmetry of their major normal faults and half-grabens (Axen, 1995). The segment containing Bahía Concepción represents a prime example of the extensional basins and accommodation zones that formed along the Baja California peninsula associated with the opening of the Proto-Gulf. Bahía Concepción's narrow (5-10 Km),

elongate (40 Km) shape (Fig. 3) results from a half-graben controlled by northwest-southeast trending faults [average N 30° W] (Johnson and Ledesma-Vázquez, 2001). The most prominent of these NW-SE faults make up the Concepción Fault Zone on the Peninsula Concepción, which acts as the eastern margin of the bay (McFall, 1968). A pre-Pliocene age for the Concepción Fault Zone is inferred, based on the occurrence of flat-lying marls on the northern tip of Peninsula Concepción that are dated as late Miocene to early Pliocene age due to the presence of the Foraminifera *Globigerinoides obliquus obliquus* and *G. extremus extremus* (Carreño, A.L., 1999; personal communication). The timing of the initiation of a marine connection in Bahía Concepción conforms to the onset of tectonic extension in the Gulf of California region, suggesting that the faults responsible for the development of its half-graben structure were formed during the Late Miocene extensional episode related to the opening of the Proto-Gulf (Ledesma-Vázquez and Johnson, 2001).

Considerable uplift along the Concepción Fault Zone is evident from a 30 km long bajada reaching heights of 600 m derived from sediments in coalescing alluvial fans from the many short canyons dissecting the western shore of Peninsula Concepción (Johnson and Ledesma-Vázquez, 2001), and from exposures of basement granitic rock and offset of Comondú units on the peninsula (McFall, 1968). The Comondú Group includes rocks from the upper Oligocene to the middle Miocene, and is divided into three units. The lower unit consists of continental sandstones and conglomerates with minor felsic tuffs and basaltic lava flows. The middle unit is composed of andesitic lava flows with interbedded debris flows, and the upper unit consists of andesite lava flows and

massive breccias (Hausback, 1984; Umhoefer et al., 2001). The volcanic rocks of the Comondú were produced by forearc magmatism developed during the Tertiary in a pre-rift tectonic setting (Ledesma-Vázquez and Johnson, 2001).

The prominent, steep escarpment along much of the western shore of Bahía Concepción suggests that this side of the bay is also bound by a northwest-southeast trending fault zone (Meldahl et al., 1997a) (Fig. 3). No major offset in the bedrock units on the west side was noted by McFall (1968), which suggests that this fault zone experienced less vertical throw than the Concepción Fault Zone. However, a few smaller alluvial fans are exposed along this margin (Meldahl et al., 1997a; Johnson et al., 1997), and active venting of hydrothermal fluids occurs at discrete locations along the western shore (McFall, 1968). No formal faults controlling these features have been named (Ledesma-Vázquez and Johnson, 2001; Umhoefer et al., 2002). We have suggested the name El Requesón fault zone for the NW-SE trending faults that delineate the western shore of Bahía Concepción (Forrest et al., 2003).

Located just off Mexican Federal Highway 1, 42 km south of Mulegé, Isla El Requesón is a prominent and conspicuous geographical feature attached to the western shore of Bahía Concepción by a 350 m long tombolo of calcareous sand (Fig. 4). The Spanish word “requesón” refers to cottage cheese curds, undoubtedly an allusion to the lumpy, pustular appearance of crushed and bleached rhodolith debris, the main component of the calcareous sand on the tombolo and in the shallow bays adjacent to Isla El Requesón (Hayes, et al. 1993). Rhodoliths are free living non-geniculate calcareous red algae, that occur in “beds”, or aggregations bordered by areas of soft sediments;

generally growing in the form of structurally complex carbonate spheres, they provide important habitat for settlement and development of many organisms (Foster et al., 1997; Steller, 1993). Rhodoliths are major carbonate producers in Bahía Concepción and throughout the Gulf of California (Meldahl, et al. 1997b; Halfar et al., 2001). Beds of living rhodoliths pave the sea floor in 3-12 m depths along much of the bay's western shore, and exposed Pliocene and Pleistocene carbonate deposits in the region contain massive sequences of rhodolith fossils, indicating that they have been an important component of the ecological and sedimentary processes of the area throughout its history as a marine basin (Foster et al., 1997).

The peninsular fault systems associated with the Gulf of California typically involve hydrothermal activity (Libbey and Johnson, 1997). McFall (1968) concluded that manganese veins exploited at the Gavilán mine on the Peninsula Concepción were of hydrothermal origin. Several faults cut across Pliocene strata on a trend parallel to the Concepción Fault Zone at the base of Peninsula Concepción (Johnson et al., 1997). These faults may have acted as conduits for hydrothermal fluids, resulting in paleo-hot spring sites where geothermal fluids rose through, and reacted with, the silica-rich volcanic rocks of the Miocene Comondú Group (Ledesma-Vázquez et al., 1997). These hot, silica-saturated fluids may have transformed Pliocene carbonate-rich mudstones and tuffs to Opal-A and low cristobalite, creating the El Mono chert of the Infierno Formation, a well-bedded 14 m thick unit of cherts and cherty breccias located in the southeast corner of Bahía Concepción (Fig. 5) (Ledesma-Vázquez et al., 1997).

An area of active hydrothermal venting along a near-vertical (dip 80° E), N 10° W trending onshore-offshore normal fault was investigated near Punta Santa Barbara (Fig. 6) using side-scan sonar and SCUBA. Geothermal fluids and gas are being released in the intertidal and shallow subtidal (to 13 m water depths) through rocks and soft sediment in a roughly linear trend extending over 750 m of coastline near Punta Santa Barbara. The seashore is steep and abrupt in this area, and andesitic volcanic rocks of the Miocene Comondú Group (McFall, 1968; Johnson and Ledesma-Vázquez, 2001) are exposed along modern beach cliffs controlled by the El Requesón fault zone. Colluvial debris cover the steepest slopes, and a short canyon with an associated small alluvial fan interrupts the rocky shoreline. A 75 m long fossil bed made up of encrusting red algae is visible along a cliff next to the active vent area (Canet et al., 2003). Several intertidal hot springs lined with mineral precipitates occur along the shoreline (Fig. 7).

Gas and geothermal fluid discharge is also observed offshore, generally in alignment with the onshore fault. In some areas there are pervasive streams of gas bubbles emanating from the seafloor, and the vent fluids flow vigorously enough to create a shimmering effect in the water (Fig. 8). Gas and fluid flow occurs through sediments and pebble-cobble conglomerates, as well as through cracks in bedrock and boulders. In the intertidal, gas and fluids flow is observed through fractures, most of which are aligned with the onshore fault (NW-SE), and through conjugate fractures that intersect the fault aligned fractures at a 60° angle. Fluid flow and mineral precipitation is also observed within a highly fractured breccia layer exposed in the intertidal. This

hydrothermal activity is modifying sediments, cementing clasts, and actively precipitating calcite, cinnabar, manganese, and opal-A (Fig. 7) (Canet et al., 2003).

The location and orientation of the onshore-offshore fault near Punta Santa Barbara suggest that it may be part of El Requesón fault zone, which delineates the western shore of Bahía Concepción. Side-scan and in-situ observations were used to determine the extent that the fault continues offshore, and whether there was any evidence of structural modifications due to hydrothermal activity. Gas and fluids samples were collected in the intertidal and subtidal along the coastal fault to determine whether they suggested a thermogenic source, and to estimate deep subsurface temperatures. Fluids were also collected at another site of intertidal hydrothermal activity near Playa Santispac for comparison, and to determine whether they indicated that the hydrothermal activity within Bahía Concepción is consistent with flow along tectonic structures induced by a high local thermal gradient.

MATERIALS AND METHODS:

Side-scan sonar data were collected along track lines on the western side of Bahía Concepción in the spring of 2001 in the Punta Santa Barbara area (Fig. 9). The area was surveyed using a 100 kHz Klein Digital Side-Scan Sonar System 595. Navigation fixes on the side-scan record were correlated with GPS readings obtained using a Garmin

GPSMAP™ 215 system and mapped on a laptop computer using the ArcNav™ extension of ArcView® software developed by the Monterey Bay Aquarium Research Institute (MBARI). Groundtruthing was performed in areas of interest using SCUBA. Data were collected along four side-scan track lines, which ranged from about 700 to 2000 meters in length, in the area around Punta Santa Barbara. Swath widths were 200 m, and the horizontal resolution was approximately 1 m. Track lines that clearly imaged the groundtruthed vent-related features were computer scanned and georeferenced using TNTMPS® software. Some errors associated with navigation were unavoidable as the navigational charts available for this region are dated, and were originally made without the benefit of precise GPS coordinates. Therefore, routes that were pre-planned for the sidescan track lines had to be modified en-route when the water depths were not sufficient to safely deploy the side-scan, or obstructions were encountered. Additionally, the side-scan sonar system was not equipped with a digital recorder, so the only record generated was on thermal paper. The precision of the GPS readings correlated with features of interest was consequently affected, and a horizontal offset of as much as 10 m may have occurred.

Sediment cores for pore water analyses were collected in order to elucidate any variations in hydrothermal flow, and to examine profiles in temperature and pH within the sediments. Acrylic cores with sampling ports drilled at 1 cm intervals were used to collect discrete samples. Syringes with 10µm Porex rod fittings were inserted into the sediment through these ports and filtered samples of pore water were drawn off. The pH of the pore water samples was determined using a Hanna Piccolo® Plus pH meter

(accuracy +/- 0.01 pH). Dissolved oxygen (DO), conductivity, and salinity were determined using a multi-parameter YSI 556 MPS meter. *In situ* sediment temperatures were measured at 0, 1, 3, 5, 10 and 15 cm depths in the sediment, using a digital thermometer (accuracy +/- 1.0°C) with a 15 cm stainless steel probe encased in a waterproof housing. Pore waters samples were collected at 13-14 m water depths at three actively venting sites, three “transitional sites” at the edges of these vent sites, and at three “non-vent” sites less than one meter away where no venting activities or elevated temperatures were observed. These sites are referred to as Vent, Trans, and Out respectively in the text and figures. Cores of sediment were also collected in the same sites to determine whether the hydrothermal flow was affecting grain sizes. Sediment samples were processed and analyzed using dry sieve analyses (Folk, 1974) at Moss Landing Marine Labs.

SCUBA divers collected hydrothermal fluid samples at 8m, where hot fluids were emanating vigorously through cracks in bedrock and boulders, and through pebble-cobble conglomerates. Fluid samples were collected in Pyrex-glass bottles equipped with two valves that allow vented gas to replace seawater in the bottle. Hydrothermal fluids were sampled by adjusting the input valve to allow venting fluids to displace the vent gas in the bottle. This procedure ensured that very little ambient seawater is collected in the samples. Hydrothermal fluids were also collected at intertidal hot springs where hot fluids vented through sand near Playa Santispac, and at the intertidal springs near Punta Santa Barbara. Seawater was collected at a site within the bay far removed from any hydrothermal influence for comparison. Major cations and trace elements were analyzed

by Inductively Coupled Plasma-Mass Spectrometer (ICP-MS) and anions by ion chromatography (see Pichler et al., 1999a; Prol-Ledesma et al., 2003 for complete methods).

Samples of gas bubbles were collected using inverted funnels to fill 25mL serum vials (Bellco Glass, Vineland, NJ), which were sealed with thick rubber stoppers and secured with aluminum crimp-seals. Gas samples were collected in areas where streams of bubbles were consistently observed in order to facilitate collection. Gas samples were analyzed for gross molecular compositions via gas chromatography by Isotech Laboratories, Inc. (Champaign, IL). Hydrocarbon compositions were also analyzed at MBARI using a Shimadzu mini-2 gas chromatograph equipped with a Carbosieve-G column (80/100 mesh; 1/8" dia x 5 ft stainless steel; Supelco, Bellefonte, PA), and a flame ionization detector. Gas was removed from the serum vials with a hypodermic needle and diluted with ultra-high purity nitrogen before analysis. A C₁-C₄ hydrocarbon gas standard (Scott Speciality Gases, Plumsteadville, PA) was run periodically.

Aliquots of gas were analyzed for the $\delta^{13}\text{C}$ composition of methane, ethane, and carbon dioxide by GC-IRMS at the Department of Marine Sciences, University of North Carolina-Chapel Hill using a Finnagan MAT-252 equipped with an HP 5890 GC and combustion interface using a modification of methods developed by Popp et al. (1995) and Sansone et al. (1997).

RESULTS:

Side-scan sonar records imaged sinuous structures in the sea floor sediment oriented along a linear trend (Fig. 10) aligned sub-parallel to the onshore fault near Punta Santa Barbara. *In situ* SCUBA observations revealed that these structures were areas of slightly elevated sediment, and sites of gas and geothermal fluid venting. These sinuous mounds were invariably covered with yellow and red iron oxide precipitates and flocculent material heavily colonized by morphologically diverse bacteria (see Chapter 2). These structures occupied a depression in the seafloor, bordered by boulders on the onshore (western) side and a rhodolith bed on the offshore (eastern) side. Water depths were approximately 13-14 m where the sinuous vent structures were located, and 11 m where the rhodolith bed began. These observations suggest that the bottom morphology may be indirectly fault controlled in this area since the fault focuses fluid and gas flow and this venting affects the morphology. Side-scan data were interpreted and mapped to show locations of the features that were imaged (Fig. 11).

Vent and transitional pore water samples had lower dissolved oxygen (DO), salinity, conductivity, and pH values than the non-vent (outside) pore water samples (Table 1). Pore water samples had distinct pH profiles with mean values ranging from pH 8.0 outside the vent areas to pH 6.2 within the hydrothermal vent areas (Fig. 12). Temperatures in the sediments ranged from 28°C outside the vents to 87°C in vent areas,

and increased with depth in sediment in vent and transitional areas, but remained constant in non-vent areas (Fig. 13).

All sediment samples had mean grain sizes that classified as medium sand according to Wentworth grain size classes (Fig. 14) (Folk, 1974). All samples were moderately to moderately-well sorted, and the grain sizes were more coarsely skewed in the vent samples. Shell debris were present in all outside and all transitional samples except Trans3, but were absent in all vent samples.

Compared to seawater, the vent fluids are enriched in Ca, Mn, HCO_3 , SiO_2 , B, As, Li, Fe, Rb, and Sr, and depleted in Mg, Na, Cl, and SO_4 (Table 2). The subtidal vent fluid samples were higher in Mg, Na, Cl, and SO_4 than the intertidal samples. All vent fluid samples classify as neutral chloride waters after Giggenbach (1988).

The subsurface temperatures of the hydrothermal system at Bahía Concepción were calculated using Na/K, Na/Li, K/Mg, and SiO_2 geothermometers (Table 3). Calculated subsurface end-member temperatures for submarine vent fluid samples ranged from 106°C to 188°C, and from 113°C to 220°C for the intertidal hot spring samples (Fig. 15).

The gas samples primarily consisted of nitrogen and carbon dioxide, and methane with minor amounts of argon, oxygen, helium, ethane, hydrogen, and propane (Table 4). The mean methane to ethane ratios were 85.41 ($\sigma = 3.46$) (Table 5), mean methane $\delta^{13}\text{C}$ values were -34.30‰ ($\sigma = 2.78\text{‰}$), and ethane $\delta^{13}\text{C}$ values were -15.60‰ ($\sigma = 3.20\text{‰}$) compared to PDB (Table 6). The mean carbon dioxide $\delta^{13}\text{C}$ were -5.85‰ ($\sigma = 0.27\text{‰}$) compared to PDB (Table 6).

DISCUSSION:

The side-scan sonar records and *in situ* observations revealed a linear trend of sediment mounds associated with hydrothermal activity (Figs. 6, 10, and 11). Surface morphology can provide clues to the mechanisms controlling fluid expulsion; when fault zones control fluid flow, the surficial expression is typically in the form of linear seeps aligned with the faults (Orange et al., 1999). The sediment mounds imaged on the side-scan sonar records are sub-parallel to the onshore fault near Punta Santa Barbara, suggesting that the submarine fluid and gas venting is associated with this fault. These vent features occupy a linear depression in the seafloor, offering further evidence that they may be fault influenced. The location and orientation of this fault indicate that it may be part of the larger El Requesón fault zone that delineates the western shoreline of Bahía Concepción. These observations conform with the findings of Barragán et al (2001) that thermal manifestations along the coast of the Baja California Peninsula may be related to convection and heating of seawater mixed with meteoric water along extensional tectonic structures, as observed for submarine hydrothermal vents in the Gulf of California and along the East Pacific Rise. Hydrogeological studies, carried out for geothermal energy exploration purposes, show that the primary permeability of the rocks in this area is very low, and that fluid flow is controlled by the presence of faults (Portugal et al., 2000).

Gas geochemistry

The high concentration of N₂ (Table 4) in the gas samples from Bahía Concepción may be derived from the thermal alteration of sedimentary organic matter (Jenden et al., 1988). Gases from other coastal hydrothermal systems in Mexico also show enrichment in N₂, with concentrations as high as 88% at Punta Mita (Prol-Ledesma et al, 2002), and 44% at Punta Banda (Vidal et al., 1978). Punta Mita and Punta Banda gas samples exhibited far lower concentrations of CO₂ (0.19 and 2.0% respectively) than the gas from Bahía Concepción, however carbon dioxide is the major component of most of the submarine shallow-water hydrothermal gases that have been sampled elsewhere (Dando et al, 1995b). The higher concentrations of CO₂ in the Bahía Concepción samples may reflect higher temperatures at depth as CO₂ can be expected to become the predominant gas in geothermal environments at temperatures > 180°C (Giggenbach, 1997).

The methane stable isotope values (Table 6) and methane to ethane ratios (Table 5) clearly indicate a thermogenic source for the gases (Fig. 16) (Schoell, 1988; Welhan, 1988; Wiese and Kvenvolden 1993). The $\delta^{13}\text{C}$ values of the methane are consistent with derivation of the gas by thermal cracking of marine algal kerogens, or pseudokerogens (Schoell, 1983; Berner et al., 1995; Simoneit, 2000). Kerogens are insoluble bulk organic matter, and are mixtures of high molecular weight organic moieties of various complex structures (Simoneit, 2000). The compositional end members of kerogens sources are coals for terrigenous origins, and alginates for marine sources; however, most sedimentary kerogens are admixtures of all input sources (Simoneit, 2000). Recent

sediments yield pseudokerogens, which are lipidic macromolecular materials that are less complex than ancient kerogens, but related to them (Philp et al., 1978). The massive sequences of rhodolith-derived sediments (Foster et al., 1997), and the high productivity of phytoplankton (Martínez-López and Gárate-Lizárraga, 1994) in Bahía Concepción may provide the necessary algal pseudokerogens, which are subsequently exposed to geothermal fluids in excess of 100°C along conduits provided by the El Requesón fault zone. This results in the instantaneous (in terms of geologic time) generation of nitrogen and methane-rich gases (Kvenvolden, K., 2004; pers. comm.). This model of gas generation is also supported by the high concentrations of HCO_3^- in the submarine vent fluids relative to the intertidal and seawater samples (Table 2). Enrichment in HCO_3^- may be related to interactions between the hot vent fluids and the carbonate within Quaternary sediment layers present in the subtidal areas affected by hydrothermal venting (Proledesma et al., 2003).

The $\delta^{13}\text{C}$ values from the rhodolith carbonates in Bahía Concepción were -0.161‰ to -5.164‰ (mean -2.831‰) (Steller, D., 2004; pers. comm.), close to the mean for $\delta^{13}\text{C}$ values of the CO_2 from the gas samples (-5.85‰) (Table 6). These isotopic values suggest that some of the CO_2 in the gas may be derived from hot, acidic geothermal fluids dissolving rhodolith carbonates because at temperatures $> 100^\circ\text{C}$ isotopic fractionation of $\delta^{13}\text{C}$ from CaCO_3 converted to CO_2 gas is small, on the order of 3‰ (Sano and Marty, 1995). Alternatively, the CO_2 in the gas phase could be derived from an approximately 80/20 mixture of seawater DIC ($\delta^{13}\text{C} = 0\text{‰}$) and DIC from buried marine organic matter that has been broken down by sulfate reduction ($\delta^{13}\text{C} \approx -25\text{‰}$).

The nitrogen to argon ratios of the Bahía Concepción gas samples were 72.91 and 79.12 (Table 4), very similar to the atmospheric ratios of N_2/Ar (40-80) (Jenden et al., 1988). Typically these values would suggest that the nitrogen in the gas samples could be attributed to atmospheric sources such as N_2 entrained in seawater and/or meteoric water (Kroos et al., 1995). However, the relatively high He, H and CO_2 concentrations of the Bahía Concepción vent gases suggest that significant portions of the gases have non-atmospheric, chemically-reduced sources. A simple mass balance calculation, assuming that all of the oxygen in the vent gas samples was derived from atmospheric contamination during sampling, suggests that these gases have only a small component (~0.6%) of atmospheric contamination.

The chemical composition of gas mixtures emerging in thermal areas can be used to evaluate the deep subsurface thermal temperatures (D'Amore and Panichi, 1980). Gas geothermometers are usually applied to subaerial steam emanations in geothermal fields, and may be of limited use in shallow-water submarine systems such as the hydrothermal venting in Bahía Concepción where phase separation is occurring. In the application of gas geothermometers equilibrium is assumed between the gas components, fluid, and rock, and if equilibrium is not attained there will be systematic deviations in the derived values (Giggenbach, 1997). Equilibria in systems containing C-H-O-N-gases likely does not occur under hydrothermal conditions below 250°C, however the H_2-H_2O system is in equilibrium over a temperature range of 100-350°C (Taran, 1986). The deep subsurface temperature estimates of the Bahía Concepción hydrothermal vent using hydrogen gas geothermometers (Taran, 1986) were 165°C and 180°C. These temperatures were far

higher than those directly measured at the vent, and further support the model of CO₂ and N₂ rich gas generation due to the thermal alteration of sedimentary organic matter.

Fluid geochemistry

The geochemistry of the shallow water hydrothermal vent in Bahía Concepción appears to be strongly influenced by interactions with the local andesitic rocks and carbonate and volcanoclastic sediments. The chemical composition of the vent fluid is very similar to those sampled at deep-sea sites (Van Dover, 2000), with some notable exceptions. Magnesium, sulfate and oxygen are generally completely removed from seawater during hydrothermal processes at high temperature “black smoker” vents at deep-sea spreading centers, and their presence in the vent fluids suggests that mixing with seawater has occurred (Edmond et al., 1982). The lower concentrations of Na, Cl, Mg, and Sulfate in the vent and hot spring samples compared with seawater may be a result of sub-seafloor mixing of meteoric waters and seawater (Prol-Ledesma et al., 2002). Boron and Li are generally present only in low concentrations in vent fluids at sediment starved hydrothermal settings along plate margins, but concentrations may be orders of magnitude higher in areas where hydrothermal fluids interact with sediment cover (You et al., 1994). Boron and Li are released from sediments at relatively low temperatures, and complete mobilization of these elements occurs at temperatures less than 150°C (You and Gieskes, 2001). Therefore the lower temperatures associated with this shallow water

vent as compared to those at deep-sea vents would be sufficient to produce the concentrations of B and Li observed.

The high Ca and HCO_3^- concentrations in the vent fluids may be influenced by interactions with the carbonate sediments, which are present in very thick sequences in Bahía Concepción due to the presence of many rhodolith beds. The role of rhodolith-derived sediment may be very important in this system, as they are major contributors to the carbonate sediments of this area (Halfar et al., 2001), and a rhodolith bed actually borders the area where hydrothermal activity occurs (see Figs 10,11). In fact, venting has been observed through some areas covered by rhodoliths (D. Steller, 2000; pers. comm.). Elevated levels of Si and As in the vent samples may be explained by interactions with the andesitic volcanoclastics present in this system (German et al., 1995). Arsenic contents range from 5 to 50 ppb in high-temperature (up to 400°C) vent fluids at ocean ridges underlain by basalt, 20 to 80 ppb at ocean ridges covered by terrigenous sediment, and 450 to 825 ppb at back-arc basins underlain by andesite and rhyodacite; the highest arsenic values (up to 1,050 ppb) in a submarine hydrothermal fluid were measured in CO_2 -rich fluids with temperatures near 100°C that were venting in shallow water on the flanks of a Quaternary arc volcano offshore Papua New Guinea (Pichler et al., 1999a). The arsenic concentrations in the Bahía Concepción submarine hydrothermal fluids are nearly as high as those measured in the Papua New Guinea fluids, up to 974 ppb, and the As concentrations in the intertidal vent samples were nearly twice as high, 2,030 ppb. However, the intertidal vents are more similar to subaerial hydrothermal settings, particularly at low tide where less mixing with seawater is likely to occur.

The subsurface end-member temperatures and geochemistry of the subtidal and intertidal vent fluids indicate that the geothermal fluids being released along the El Requesón fault zone may be of meteoric origin, heated by the high local thermal gradient, and that some mixing with seawater is occurring subtidally. This is supported by the δD and $\delta^{18}O$ values of the geothermal fluids which plot along the local meteoric line derived by Portugal et al. (2000) for the Tres Vírgenes geothermal field (Prol-Ledesma et al., 2003), located approximately 150 km northwest of Bahía Concepción. Alternatively, the geochemistry of the vent fluids may result from the subsurface boiling of seawater entrained along fractures. The concentrations of the constituents from the vent fluids collected in the intertidal springs are more likely to represent the end-member values of fluids in this hydrothermal system because they experience less mixing with seawater. This assumption is supported by the relatively lower concentrations of Mg in the intertidal fluids (Table 2). Therefore, the values in Table 3 and Figure 15 for subsurface end-member temperatures calculated from the intertidal springs (IS), are likely more accurate representations than those calculated for the submarine vent fluids (VF).

Geological implications of modern and paleo-hydrothermal activity

The geothermal fluids venting along faults within Bahía Concepción may provide the necessary mechanisms and geochemistry for the transformation of the carbonate-rich mudstones such as those in the Pliocene Infierno Formation to the cherts found in the El Mono chert (Fig. 5) (see Ledesma-Vázquez et al. (1997) for a detailed description of this

deposit). Acidic solutions (pH 5.7-6.2) that are supersaturated with silica are capable of dissolving and replacing carbonate minerals with silica, allowing for chert formation at low pressures (Hesse, 1989). The geothermal fluids collected along El Requesón fault zone are highly enriched in silica, up to 5.73 mM/L vs. 0.02 mM/L for seawater (Table 2), and are acidic, pH 6.2 vs. pH 7.75 for seawater (Fig. 12). Clearly these geothermal fluids would be capable of the dissolution and conversion of carbonates to cherts, particularly if they experienced little mixing with seawater as they percolated through the mudstones along conduits provided by faults. Additional evidence for a connection between the modern vent geothermal fluids and precipitates along El Requesón fault zone and the paleo-hydrothermal activity associated with the Concepción Fault Zone is the high manganese content of some of the vent precipitates near Punta Santa Barbara (Fig. 7), which represent very rare examples of manganese hydrothermal deposits formed in shallow submarine environments settings (Canet et al, 2003). Similar hydrothermal activity likely created the manganese veins on the Peninsula Concepción (McFall, 1968). These parallels between paleo-hydrothermal activity along the Concepción Fault Zone and modern venting along El Requesón fault zone suggest that both may be associated with hydrothermal flow along conduits provided by extensional tectonic structures in Baja California.

The extensive presence of *Ophiomorpha* ichnofossils and *in situ* root casts of the black mangrove *Avicennia* within the El Mono chert indicate that the original sediment layer was deposited in a shallow lagoon (Ledesma-Vázquez et al., 1997). The mangrove stand at Playa Santispac (Fig. 3), one of the sites of coastal hot spring activity along the

El Requesón fault zone, may provide a contemporary model for the depositional setting of these cherts. A low-lying basin on the west side of the highway at Playa Santispac is surrounded by alluvial fans, and only a slight rise in relative sea level would be necessary to create a small lagoon (Johnson et al., 1997). After sea levels subsided, this lagoon would no longer be a marine setting, and the acidic, silica-rich geothermal fluids from the hot springs could dissolve the carbonate shell and calceolarian material within the lagoon mud and replace them with silica relatively rapidly. The present-day hydrothermal activity along the El Requesón fault zone, particularly in the shallow estuarine setting at Playa Santispac, offer important keys to interpreting the processes along the Concepción Fault Zone which may have resulted in the formation of the Pliocene El Mono chert deposits.

Although this study focused mainly on one fault within El Requesón fault zone, hydrothermal venting occurs in several locations along the western shore of Bahía Concepción (McFall, 1968) (Fig. 3). The geochemistry of the vent fluids from the subtidal and intertidal vents near Punta Santa Barbara was very similar to the fluids collected at an intertidal vent near Playa Santispac, approximately 10 km to the north (Table 2). These findings suggest that the hydrothermal venting in these disparate locations results from the same or similar processes, and support the model of geothermal fluid flow along the faults that make up the western margin of Bahía Concepción. According to Johnson et al (1997), rifting associated with the development of the Gulf of California clearly is related to the formation of the fault zones and hot springs in the Bahía Concepción region. Therefore, the results of this study agree with the conclusions

of Barragán et al (2001) that hydrothermal activity along the coast of the Baja California Peninsula may be related to convection and heating of seawater mixed with meteoric water along extensional tectonic structures.

CHAPTER II. ECOLOGICAL IMPLICATIONS OF SHALLOW WATER HYDROTHERMAL VENTING IN BAHÍA CONCEPCIÓN

ABSTRACT:

Shallow water hydrothermal venting in Bahía Concepción, B.C.S., México appears to be exerting small-scale, localized effects on the surrounding biota. The abundances and diversities of infauna were significantly lower in areas of hydrothermal flow through sediments than in areas not affected by venting activity, mainly due to elevated temperatures. Flocculent materials were observed covering sediments affected by venting. Microscopic analyses revealed that these flocculent materials contained diatoms, silicoflagellates, cyanobacteria, and morphologically diverse bacteria within a mineral and organic-rich matrix. Organisms were observed feeding on these flocculent materials around the vent. The stable isotopes of some of these animals, particularly the sea cucumber *Holothuria inabilis*, were significantly different than those from animals collected away from the vent, suggesting that they were able to assimilate some unique source of carbon related to the hydrothermal activity. Arsenic concentrations within the vent fluids and the flocculent materials were high, yet there was no evidence that this was having detrimental effects on the surrounding biota. Microbially mediated adsorption of arsenic onto Fe(III) oxyhydroxide precipitates may render it biologically unavailable to the organisms around the vent.

INTRODUCTION:

Submarine hydrothermal vents occur at tectonically active regions throughout the world, generally along mid-ocean ridges, back-arc spreading centers, and fault zones (Fig. 1) (Van Dover et al., 2002). In 1976, abundant communities of large benthic organisms were discovered at the Galapagos Rift, and on the crest of the East Pacific Rise at depths of 2500-2925 m clustered near active hydrothermal vents releasing fluids at temperatures as high as 300°C (Lonsdale, 1977). Subsequent studies of hydrothermal vent fauna revealed that some of these organisms assimilate nitrogen and carbon from local sources, distinct from typical deep-sea organisms reliant on slowly sinking photosynthetically derived organic matter (Rau and Hedges, 1979; Rau 1981). It is now understood that the hydrothermal vents and cold seeps located on the deep-sea floor often support unique ecosystems that rely mainly on primary production via chemosynthetic bacteria, rather than photosynthesis, to provide energy and nutrition to the animals present (Childress et al., 1986; Brooks et al., 1987; also see General Introduction to this thesis).

Deep-sea hydrothermal vent and seep communities have been relatively well studied. However, less attention has been focused on the ecological aspects of vent and seep communities at shallower depths. Organisms around shallow water hydrothermal vents and seeps have access to “typical” photosynthetic food sources found within the photic zone. Additionally, the influence of shallow-water hydrothermal effluents may

promote the development of communities with specific photosynthetic and chemosynthetic processes (Tarasov et al., 2003). Shallow water vents may be characterized by communities of sulfur oxidizing microbes that form bacterial mats where vent fluids rich in hydrogen sulfide are discharged (Jacq et al., 1989). Around some subaerial and shallow water hydrothermal vents the high temperatures of the vent fluids encourages the growth of thermophilic cyanobacteria (Lopez-Cortes, 1999; Ward and Castenholz, 2000).

The fauna of hydrocarbon seeps occurring on the continental slope and shelf have been investigated in several locations. In the Gulf of Mexico, communities associated with hydrocarbon seeps at depths from 640-540 m (MacAvoy et al., 2002), and sulfide-rich brine seeps at 72 m (Jensen, 1986), have been studied. The fauna of pockmarks and active gas seeps occurring at depths of 65-250 m in the North Sea were also surveyed (Hovland and Thomsen, 1989; Dando et al., 1991). The infauna at methane seeps on the Oregon margin (590 m water depth), and the northern California slope (520 m), and shelf (31-53 m) have been examined (Levin et al., 2000; Levin and Michener, 2002). Several infaunal community studies of coastal hydrocarbon seeps have also been reported from the Santa Barbara Channel in California at depths ranging from 15-18 m (Davis and Spies, 1980; Spies and Davis, 1979; Spies and DesMarais, 1983; Montagna et al., 1989). Most of these studies suggested that the densities of organisms around seeps were higher than in the surrounding areas. Species diversity, however, tended to be lower relative to surrounding environments, with the fauna dominated by weedy (early colonizers that exhibit rapid growth) organisms tolerant to potentially toxic constituents of seep fluids

such as hydrogen sulfide. Some of the macrofauna and meiofauna found around these seeps belong to genera or families known to bear chemosynthetic symbionts, allowing them to derive energy from hydrogen sulfide and other reducing compounds (see Levin et al., 2000 for a summary). Other animals exhibit physiological adaptations to hydrogen sulfide, which allow them to tolerate exposure to levels of H₂S that would kill less tolerant organisms (Vismann, 1991; Gamenick et al., 1998).

Shallow water hydrothermal vents occur throughout the world's marine environments. In many cases shallow submarine hydrothermal venting is associated with volcanic islands and arcs, or occurs on the top of seamounts (e.g. Fricke et al., 1989; Pichler et al., 1999a; Dando et al., 1995a; Sedwick and Stuben, 1996; Sorokin et al., 1998; Tarasov et al., 1999). Shallow vents also occur in continental margins affected by intense tectonic extension, such as Punta Banda, in Baja California (Vidal et al., 1978), and Punta Mita, near Puerto Vallarta, Mexico (Fig. 2) (Prol-Ledesma et al., 2002). Despite the accessibility of these shallow-water sites, the biota are poorly known when compared to deep-sea vents (Thiermann et al., 1997). The biogeochemical processes around shallow water hydrothermal vents are considerably different than those in surrounding areas not affected by the venting, and their functional characteristics may be more complicated than in deep-sea hydrothermal systems due to the potentially simultaneous occurrence of chemosynthetic and photosynthetic primary production (Tarasov et al., 1999). Bacteria, cyanobacteria, and microalgae can form dense mats and assemblages near shallow water hydrothermal vents throughout the world's oceans (Stein, 1984; Tarasov et al., 1990, 1999, 2003; Dando and Hovland 1992; Jensen et al., 1992;

Kamenev et al., 1993; Brinkhoff et al., 1999), which may contribute significantly to the diet of the regional background species that live near the vents (Stein, 1984; Trager and DeNiro, 1990; Tarasov, 2003).

One of the most thoroughly studied shallow water hydrothermal systems occurs near the island of Milos, Greece, part of the Hellenic Volcanic Arc in the Aegean Sea, where sulfide-rich hydrothermal fluids up to 100°C and gas are released from the littoral zone to depths of 115 m (Dando et al., 1995a; Botz et al., 1996). Surveys of sessile epifauna and plankton around vent and non-vent sites revealed that species richness was higher at sites closest to vents (Morri et al., 1999; Pansini et al., 2000; Bianchi and Morri, 2000; Robinson, 2000). Additionally, the abundance of species with warm-water affinity was apparent in algal (Sartoni and De Biasi, 1999) and animal communities (Pansini et al., 2000), and mounds of the coralline algae *Mesophyllum lichenoides* were conspicuous only at vent sites (Cocito, et al., 2000). In contrast, infaunal diversity was significantly reduced within the sediments affected by venting, a pattern attributed to the elevated temperatures (Dando et al., 1995a; Fitzsimons, et al., 1997; Thiermann et al., 1997). These findings are in agreement with the work of Kamenev et al. (1993), who found that the abundance and diversity of infauna decreased as temperature increased from 17-81°C in zones of hydrothermal activity occurring at depths from 4-200 m in the Bay of Plenty, New Zealand. At coastal hydrothermal vents at 0-27 m in Matupi Harbour, Papua New Guinea, epifauna and infauna were sparse at the vents due to temperatures within the sediment up to 90°C, but the periphery of the vent field was characterized by the richest benthic communities found in the Harbour (Tarasov et al., 1999). This pattern has also

been described around methane seeps in 10-12 m in the Kattegat off the Danish coast, where carbonate-cemented sandstone structures form “bubbling reefs” which support a rich epifauna and flora, but the infauna is depauperate due to the putative toxic effects of hydrogen sulfide within the gases released (Jensen et al., 1992).

Carbon and nitrogen stable isotope analyses have been used to demonstrate chemoautotrophic-based food webs in a variety of deep-sea vent and seep communities (Rau and Hedges, 1979; Rau 1981; Paull et al., 1985; Brooks, et al., 1987; Van Dover and Fry, 1989, 1994; Colaco et al., 2002), and shallow-water communities in reducing environments (Spiro et al., 1986). The non-photosynthetic nature of the base of the food webs at deep-sea hydrothermal vents and seeps was originally established in part by the $\delta^{13}\text{C}$ of the fauna (Conway et al., 1994), which were usually far more negative (Rau and Hedges, 1979; Paull et al., 1985) than the typical range of photosynthetically derived carbon, where CO_2 fixation via the Calvin-Benson pathway results in $\delta^{13}\text{C}$ values between -15 and -22‰ (Gearing et al., 1984). One notable exception to the very light stable carbon isotopes typically found in organisms from vent and seep systems is the tube worm *Riftia pachyptila* sampled from the Galapagos Rift, which had considerably heavier $\delta^{13}\text{C}$ values, around -11‰, perhaps due to CO_2 limitation resulting from internal symbiotic chemosynthesis (Rau, 1981). During uptake and assimilation of organic nitrogen by consumers, nitrogen stable isotopes increase approximately 3.4‰ with each trophic level (Minawaga and Wada, 1984), suggesting the nitrogen isotope ratios can serve as indicators of trophic levels (Conway et al., 1994).

Stable carbon and nitrogen isotope ratios have also been used to demonstrate that some animals foraging around a shallow-water hydrothermal vent near White Point, California derive substantial nutrition from sulfur-oxidizing bacterial mats growing in areas of venting (Trager and DeNiro, 1990). Stable carbon and sulfur isotope studies around petroleum seeps in 15 m of water in the Santa Barbara Channel, also demonstrated that some infaunal organisms are feeding on bacterial mats related to the seeps (Spies and DesMarais, 1983). However, in other areas of shallow water hydrothermal activity and methane seeps, carbon stable isotopes studies did not conclusively demonstrate chemosynthetic contribution to the diets of the regional background species (Dando, et al., 1991; Jensen et al., 1992).

I examined the epifauna and infauna around a shallow-water hydrothermal vent in Bahía Concepción, Baja California Sur, Mexico. Detailed descriptions of the geology and geochemistry of the site is provided in Chapter One of this thesis. Epifaunal organisms observed feeding around flocculent deposits associated with hydrothermal activity were collected and their carbon and nitrogen stable isotopes and elemental contents were analyzed to determine if they differed significantly from the same species collected away from the hydrothermal vents. The flocculent materials were also collected and analyzed. Additionally, infaunal organisms were sampled at vent sites, transitional sites around the vents, and non-vent sites to determine whether the hydrothermal activity influences the community structure within affected sediments.

Since the hydrothermal fluids and gas released at this shallow vent do not contain detectable levels of hydrogen sulfide (see Chapter One), I expected that the abundances

and diversities of the infauna would be influenced mainly by the temperatures within the sediment, which are as high as 92°C in vent areas. The absence of H₂S also should preclude the growth of chemosynthetic sulfur oxidizing bacteria; therefore the bacterial mats present at other vents should not form in this environment. However, other reduced compounds (such as Fe, Mn, and As) that may promote the growth of chemosynthetic bacteria are present within the vent fluid at elevated concentrations compared to seawater (Table 2), and thermophilic cyanobacteria have been isolated from the nearby intertidal hot springs at Santispac (Lopez-Cortes, 1999). Therefore, the macrofauna around the shallow vents in Bahía Concepción may have sources of dietary carbon that are not available to animals in other parts of the bay where hydrothermal vents are not present.

MATERIALS AND METHODS:

Infaunal organisms were sampled at vent sites at 13 m where hydrothermal activity was observed through soft sediments in order to determine whether the vents influence infaunal diversities and abundances. Infauna were collected to 5 cm depths in the sediments using acrylic cores (volume= 400.59 cm³). Two infaunal cores were taken in sediments directly affected by hydrothermal venting (Vent), the transitional areas surrounding these areas (Trans), and immediately outside the venting area (Out) at three distinct vent sites (see Fig. 11 for locations). Therefore, two infaunal cores were collected

per zone (Vent, Trans, Out), at each site (Vent1, Vent2, Vent3). The temperatures occurring at 15 cm within the sediment defined these different zones: Vent zones had temperatures above 70°C, Transitional zones were above 50°C, and Out zones were less than 30°C. All samples were sieved through a 300µm mesh, and the materials retained were initially preserved in 8% buffered formaldehyde and filtered seawater, then transferred after 48 hours into 70% alcohol. In the laboratory, infauna were sorted from sediments using dissecting microscopes, counted, and identified to lowest taxon possible.

In the same locations where the infaunal cores were collected, sediment samples for grain size analyses and pore water samples were collected and analyzed for dissolved oxygen, pH, salinity, and conductivity according to the methods outlined in Chapter One.

Total numbers of organisms and total number of different taxa from each core were compared with blocked Analysis of Variances (ANOVA) (Zar, 1999) using SYSTAT®10 software. Samples were blocked by site, and the two cores collected in each zone were nested. Homogeneity of variances were confirmed *a priori* using Cochran's Test. ANOVA results were compared using post-hoc Tukey Multiple Comparisons tests (Zar, 1999). Biological data were also analyzed with a Principal Components Analysis (PCA) using SYSTAT®10 software. Organisms were grouped according to phyla, and abundances were square root transformed prior to analyses. The physical data from the pore water samples (temperature, pH, salinity, and grain size) of the different zones were also analyzed using PCA. Dissolved oxygen (DO) data were not used in these analyses because the probe used consumes the oxygen in the samples in order to obtain the

readings. The data are thus unlikely to represent absolute values, but may be informative in terms of relative values of DO in each zone.

Selected macrofauna from around the vent areas were collected and their tissues were analyzed to determine whether their carbon and nitrogen stable isotope signatures differed significantly from those of the same species found away from the vents. Animals observed feeding around venting areas at 5-13 m water depths were collected haphazardly using SCUBA in January, June, and October of 2002. The same species were also collected at various locations throughout the bay that were not affected by hydrothermal activity. Smaller organisms were allowed to evacuate their gut contents in filtered seawater for 24 hours, then frozen whole. Larger organisms were dissected, gut contents were examined, and samples of muscle tissue were frozen. Samples of sediments covered with flocculent material were also collected from the same areas around the vents for stable isotope analyses.

Sediment samples and calcified organisms (the coral *Porites californica* and the bryozoan *Bugula neritina*) were treated with 0.5M HCl in order to dissolve carbonates. Tissue samples were treated with a mixture of chloroform, water, and methanol to remove lipids. Samples were thoroughly rinsed in de-ionized water and dried completely at 60°C. Stable isotope analyses for carbon and nitrogen were done using a mass spectrometer. Repeated measurements of a gelatin standard yielded a standard deviation <0.12‰ for both elements. The stable isotope ratios for the same species collected at vent and non-vent sites were compared with one-tailed, two sample standardized T-tests performed using SYSTAT[®]10 software (Systat, Evanston, Illinois, USA). One-tailed T-

tests were used because the hypothesis being tested was whether the stable isotope ratios were different because the organisms around the vent were deriving nutritional benefits by consuming the flocculent materials. Because all vent “sites” were within the same general area, they are not true replicates. Therefore, the hypothesis tested is primarily related to differences in location. However, the magnitude of any significant differences may suggest dietary differences related to vent activity.

Tissue samples from the sea cucumbers *Holothuria inhabilis* and sediments covered with flocculent materials were analyzed to determine whether there was any evidence that elements that were abundant in the flocculent material were being incorporated into the flesh of the *H. inhabilis* that were consuming it. These samples were processed in accordance with EPA Method 200.7 (Telliard and Martin, 2001) and analyzed for their elemental compositions using a Thermo Finnegan Element 2 Inductively Coupled Plasma-Mass Spectrometer (ICP-MS). Elemental analyses were performed on two *H. inhabilis* observed feeding on the flocculent materials at the vent, and two collected away from vent activity. The flocculent materials from vent sites were also analyzed using light microscopes, along with fluorescence microscopy in order to determine whether they contained bacteria. Samples were treated with DAPI (4', 6-Diamidino-2-phenylindole), a fluorescent dye that binds to all DNA, and analyzed with FISH (Fluorescence *in situ* hybridization), using Domain level probes (Eub338 I-III) targeting bacteria (Daims et al., 1999).

RESULTS:

The physical and chemical data from the pore water samples in areas where infaunal cores were collected are discussed in the Results section of Chapter One, and presented in Table 1 and Figures 12, 13, and 14. A taxonomic list of the infauna from all sites and zones is presented in Appendix 1 and summarized in Figure 17. The three sites were not significantly different from each other in terms of mean number of organisms; however, significant differences were found for mean number of organisms per zone (Blocked ANOVA; Site, $F_{2,4}=0.023$, $p=0.977$; Zone, $F_{2,4}=27.348$, $p=0.005$; no significant interaction terms). Zones were also significantly different from each other in terms of numbers of different taxa present (Blocked ANOVA; Site, $F_{2,4}=3.430$, $p=0.136$; Zone, $F_{2,4}=31.738$, $p=0.0035$; no significant interaction terms). Outside zones had the highest diversities and abundances, Transitional zones were intermediate, and Vent zones had the lowest diversities and abundances of infauna. The Tukey Multiple Comparison Tests showed that Vent and Transitional zones were both significantly different from Outside zones, and that Vent and Transitional zones were not significantly different from each other for either total numbers of organisms or numbers of different taxa.

Infaunal cores from Vent zones were dominated by annelids and arthropods. Molluscs were present at Vent1 and Vent3 and echinoderms were only present at Vent1. No sipunculids or nemertean were found in any of the Vent cores. Nematodes were found in some cores from all zones, but were not included in the analyses because many

nematodes are too small to find and separate out with a dissecting microscope.

Transitional cores tended to exhibit greater diversities and abundances of infauna than the Vent cores (Fig. 17), but also were dominated by annelids, arthropods, and molluscs.

Echinoderms were found in Trans2 and Trans3 cores, and sipunculids were found in Trans1 and Trans2 cores, and no nemerteans were found in any Transitional cores.

Outside cores exhibited the highest diversities and abundances.

The Principal Component Analysis revealed that the infauna in the two cores taken per zone at each site were generally similar to each other, and that all cores taken in each zone were similar across sites in terms of the phyla present. The reduced space plot (Fig. 18A) showed that Principal Component 1, plotted on the x-axis, explained 62.9% of the variance in the data, while Principal Component 2, plotted on the y-axis, explained 16.7% of the variance. The reduced space plot represents a projection of the data points into the ordination space defined by the principal component axes. The plot of the eigenvectors (Fig. 18B) demonstrates which taxa are driving the patterns revealed in the reduced space plot. The presence of sipunculids was strongly correlated with the x-axis, and therefore Principal Component 1, and was an important factor driving the differences between the Out cores and the Trans and Vent cores. The Out3 cores were different from the other Out cores mainly due to the presence of more echinoderms and nemerteans. This pattern also explained why the second Out2 core plots closer to the Out3 cores. The Trans3 core 1 plotted closer to the Out samples primarily because it had more arthropods than any of the other Trans or Vent cores.

The Principal Component Analysis of the physical data from the pore water samples (Fig. 19A) also showed that cores taken in the same zone generally grouped together. Principal Component 1 explained 69.3% of the variance, while Principal Component 2 explains 27.1% of the variance. The plot of the eigenvectors (Fig. 19B) revealed which physical factors are responsible for the pattern displayed by the PCA. Vent2 and Vent3 group together due to their higher temperatures, while the three Out samples, and Trans2 and Trans3 group together due to higher pH and salinities. Vent1 and Trans1 grouped together because they had a greater % fraction of finer grain sizes (Fig. 14), and therefore less medium sand.

Two species had significantly different stable carbon and nitrogen isotope ratios between individuals collected at vent and non-vent sites (Appendix 2, Fig. 20): the sea cucumber *Holothuria inhabilis* (one-tailed, two sample T-tests; $P=0.008$ for $\delta^{15}\text{N}$; $P<<0.001$ for $\delta^{13}\text{C}$), and the Cortez Angel, *Pomocanthus zonipectus* (one-tailed, two sample T-tests; $P=0.008$ for $\delta^{15}\text{N}$; $P=0.029$ for $\delta^{13}\text{C}$). *H. inhabilis* were commonly encountered feeding on and around the flocculent material, and their gut contents revealed that they were ingesting the flocculent material. The sea cucumber *Isostichopus fuscus* collected at the vent had significantly different stable carbon isotopes than those collected elsewhere (one-tailed, two sample T-tests; $P=0.036$ for $\delta^{13}\text{C}$), but differences in nitrogen stable isotopes were not significant. The stable isotope ratios of the *Porites californica* collected at the vent sites were not significantly different from those collected away from the vents. *Nassarius* sp., *Bugula neritina*, and *Calamus brachysomus* were not encountered away from the vent sites during the sampling period.

Due to small sample sizes, only trends in elemental compositions of the flocculent material and *Holothuria inhamilis* could be examined. One of the vent *H. inhamilis* samples was determined to be an outlier, and the results were not used because all elements were present in quantities that were less than half of the means of all other samples. The vent *H. inhamilis* had Al, Fe, and As concentrations that were higher than the two non-vent *H. inhamilis*. Al, Fe, and As were also present in high concentrations in the flocculent material (Table 7).

The fluorescence microscopy analyses of the flocculent materials with the FISH probes and DAPI (Fig. 21) revealed that the flocculent material contained morphologically diverse bacteria within a mineral and organic-rich matrix (Orphan, V., 2003; pers. comm.). Most of the DNA that was imaged by the DAPI stain was also bound by the Bacterial Eub 338 probes, indicating that bacteria are common within the flocculent material. Analyses of the flocculent materials using light microscopes also revealed that living diatoms and silicoflagellates were abundant.

DISCUSSION:

The hydrothermal vent appears to be controlling and modifying infaunal assemblages at local scales. Diversities and abundances of infauna within sediments directly affected by hydrothermal activity were significantly lower than in areas less than

one meter away that were not affected by venting. The ANOVA results indicated that Vent and Transitional sites were depauperate and less diverse when compared to the Outside sites. The PCA analysis of physical parameters suggested that temperature is the most important factor controlling the abundances of infauna (Fig. 19). These results agree with the infaunal patterns observed at other shallow-water hydrothermal vents (Kamenev et al., 1993; Dando et al., 1995a; Fitzsimons, et al., 1997; Thiermann et al., 1997; Tarasov et al., 1999).

Infaunal assemblages are also affected by sediment grain size (Levin et al., 2001), sediment toxicity (Long et al., 2001), species interactions (Reise, 2002), pH (Knutzen, 1981), and salinity (Chapman and Wang, 2001). The feeding activities of infauna can affect grain sizes as deposit feeders selectively ingest sediments of particular size classes (Self and Jumars, 1988). Biogenic modification of sediments also occurs when sessile or discretely motile animals build tubes and burrows, which in turn may provide microoxic habitats for diverse assemblages of smaller animals, and because the mucus of motile organisms increases sediment cohesion (Reise, 2002). Burrows and tubes are also micro-environments of chemical significance to sediment-water exchange processes, and burrowing activity may significantly increase the oxic conditions within sediments (Rosenberg, 2001). The grain size distribution of sediments is also an important factor controlling sediment metal concentrations (Chapman and Wang, 2001), as fine-grained particles tend to accumulate higher toxicant concentrations than sandy sediments (Long et al., 2001). Exchange and equilibration between interstitial and overlying water is fast

in sands, but slow in sediments containing high proportions of silts and clays (Chapman and Wang, 2001).

The normal variation of pH in sea water of 35‰ is 7.8-8.2 (Knutzen, 1981), which is approximately the range measured above and below the sediment-water interface of the Outside samples (see Table 1). Below pH 7.0 reduced rates of calcification occur, which may harm or hinder growth of animals with calcified shells, while complete arrest of algal calcification has been demonstrated below pH 6.0-6.3 (Knutzen, 1981). This is consistent with the lack of shell and other calcareous debris observed in sediment cores from vent sites where the pH is as low as 6.1 (Fig. 12). Salinity may also be an important variable controlling infaunal distributions; faunal distributions in estuaries are controlled primarily by salinity, and organisms burrowing in the sediments may be exposed to very different salinity regimes than if they were on the sediment surface (Chapman and Wang, 2001). The infauna around the vents are subjected to salinities as low as 29.7‰ within the sediments, while the overlying seawater salinities are approximately 35‰ (Table 1). In addition to the direct effects of pH and salinity on infauna, changes in salinity and pH can affect the bioavailability and toxicity of metals (Knutzen, 1981; Chapman and Wang, 2001).

The detrimental effects of temperature, pH, and salinity are clearly influencing the patterns and compositions of infaunal assemblages around the hydrothermal vents in Bahía Concepción; infaunal abundances and diversities are lower at vent and transitional sites than outside sites. However, considering the higher temperatures, and lower pH and salinities of interstitial waters at vent and transitional sites, it is remarkable that any

infauna are present in these areas. The infauna at vent and transitional sites may be surviving in these difficult conditions due to habitat modification activities of “ecological engineers” that create tubes and burrows (Rosenberg, 2001; Reise, 2002), and because of the environmental effects of gas and fluid flow (Dando and Hovland, 1992; O’Hara et al., 1995). Tube materials were always present in vent and transitional cores, and these tubes may offer some protection to the organisms that build them, and other animals residing on and inside them. Tubes and burrows also increase exchange of interstitial water with the overlying water (Rosenberg, 2001), perhaps resulting in an influx of water with lower temperature and higher pH and salinity in and around these structures in the sediments. Gas flow through permeable sediments results in an outflow of interstitial water along the axis of the gas flow, which is replaced by an inflow of water from the surrounding sediment and overlying surface water (O’Hara et al., 1995). Channels formed by rising gas bubbles will also increase the exchange rate between the sediment and water column (Dando and Hovland, 1992). Gas and fluid flow through sediments can also result in the displacement of fine-grained sediments (Judd and Hovland, 1992). This also appears to be the case at the vent sites, where sediment grain sizes are skewed to coarse classes, which may enhance water exchange (Chapman and Wang, 2001), and lessen toxicant concentrations (Long et al., 2001).

The tanaid crustacean *Leptochelia dubia* was commonly found in the infaunal cores from Vent sites. *L. dubia* is an ubiquitous species with patchy, dense distributions that constructs tubes, often lined with microbes, with particles sorted by size (Krasnow and Taghon, 1997). Many of the other arthropods that were found in the vent and transitional

sites (*Rutiderma apex*, *Photis* sp., and *Aoridae*) are also tube dwellers, and are often found in disturbed environments (Slattery, P, 2003; pers. comm.). Species from the genus *Photis* are also known to construct tubes in empty gastropod shells (Carter, 1982). This habitat was also used by sipunculids at transitional and outside sites: almost all of the sipunculids were either found in empty gastropod shells (which often also contained abundant stores of the flocculent material from the vent sediments), or in holes in rhodolith debris. This use of shells and other carbonates may represent an adaptation that enables some of the organisms to survive in the hostile environments around the vents.

Some of the annelids found at vent and transitional sites such as the Amphiridae, Sabellidae, Spionidae, Capitellidae, and Nereidae are also tube dwellers. Capitellids and nereids are often found in disturbed areas, and nereids are capable of rapidly moving out of their tubes when conditions become intolerable and building new ones in other areas (Fauchald and Jumars, 1979). Other polychaete annelids found at vent and transitional sites such as the Hesionidae, Nephtyidae and Syllidae are motile predators (Fauchald and Jumars, 1979).

Perhaps the most interesting motile invertebrates at the vent and transitional sites are the nassariid gastropods *Nassarius* spp. Although they were only present in some of the Vent and Trans cores (Appendix 1), these gastropods were commonly observed around all vent sites (pers. obs.). They were likely under-represented in the infaunal cores because the cores were too small to adequately sample them. *Nassarius* are capable of rapid movement, and were frequently observed climbing onto the pore water cores that were left in the sediment for 5 minutes to equilibrate. Nassariids are typically scavengers

that feed on dead and decaying animals (Abbott and Haderlie, 1980). The nassariid gastropods *Cyclope neritea*, and *Nassarius mutabilis* were the only macrofaunal species to be found at the vent outlets and living on top of brine seeps in Milos, Greece (Southward et al, 1997). Additionally, a nassariid gastropod, *Nassarius* sp. was also common around a shallow-water hydrothermal vent in Matupi Harbour in Papua New Guinea (Tarasov et al., 1999). The stable carbon isotope values and gut contents of the *Cyclope neritea* from Milos indicate that this species scavenges the carcasses of less tolerant animals killed by exposure to the hydrothermal fluids, but also grazes on bacterial mats at vents (Southward et al, 1997). The *Nassarius* spp. collected around the vents in Bahía Concepción had carbon stable isotope ratios (-15.65‰) that were closer to the $\delta^{13}\text{C}$ of the flocculent material (-19.8‰) than any of the other organisms sampled (Fig. 20), suggesting that the flocculent material could comprise part of their diet. The nitrogen stable isotopes of the that *Nassarius* spp. (13.73‰) indicate that it is more likely that they were feeding on organisms that were directly consuming the flocculent material ($\delta^{15}\text{N} = 7.38‰$) since nitrogen stable isotopes increase approximately 3.4‰ with each trophic level (Minawaga and Wada, 1984).

The stable isotope ratios of the animals collected around the shallow-water hydrothermal vent in Bahía Concepción (Appendix 2, Fig. 20) suggest that their diets are based mainly on photosynthetically derived sources. The typical range of marine photosynthetically derived carbon results in $\delta^{13}\text{C}$ values between -15 and -22‰ (Gearing et al., 1984), and consumers generally reflect the $\delta^{13}\text{C}$ of their food source plus about 1‰ due to trophic fractionation (Coleman and Fry, 1991). Sulfur-based chemosynthetic

energy sources typically result in $\delta^{13}\text{C}$ values of animal tissues from -30 to -42‰ , and methane-based chemosynthetic sources result in $\delta^{13}\text{C}$ values $<-40\text{‰}$ (Brooks et al., 1987). Chemoautotrophs also tend to have lower $\delta^{15}\text{N}$ values (-5 to -12‰) than heterotrophs (2.8 to 13‰) or marine algal sources (MacAvoy et al., 2002).

The holothurians *Holothuria inabilis* and *Isostichopus fuscus*, particularly those collected away from the vent, did have $\delta^{13}\text{C}$ values that were more positive than -14‰ (Appendix 2, Fig. 20). Typically sea cucumber diets consist of organic detritus, microorganisms, and fecal pellets (Massin, 1982). The non-vent *Holothuria inabilis* had mean $\delta^{13}\text{C}$ values of -9.94‰ , which likely reflects this “typical” diet of these sea cucumbers in Bahía Concepción. The vent *H. inabilis* actually had $\delta^{13}\text{C}$ values more consistent with photosynthetically derived carbon (mean = -13.79‰). The mean $\delta^{13}\text{C}$ of the flocculent material was -19.80 , also consistent with photosynthetically derived carbon. The $\delta^{13}\text{C}$ values of the *H. inabilis* collected around the vent were all very similar ($\sigma = 0.34$), which strongly suggests that they are deriving nutrition from the same carbon source since animals raised on isotopically homogenous food sources in labs have an average standard deviation of about 0.6‰ (Coleman and Fry, 1991). The fact that the $\delta^{13}\text{C}$ values for vent *H. inabilis* were on average 3.85‰ more negative than the non-vent *H. inabilis*, and that the differences in $\delta^{13}\text{C}$ and $\delta^{15}\text{N}$ were both significant, suggests that individuals found around the vents are feeding on distinct carbon sources, such as the bacteria colonizing the flocculent material, that they do not encounter away from the vent. Bacterial concentrations will influence the distribution of holothuroids in a benthic area, and sea cucumbers will remain in an area with abundant food sources (Massin,

1982). Muscle tissue $\delta^{13}\text{C}$ values generally reflect an animal's diet over periods of weeks to months (Tieszen et al., 1983), so these data may indicate that the *H. inhabilis* collected at the vent were foraging elsewhere, then moved into the vent area where they encountered the flocculent material and remained there to feed. Holothurians are also the most common echinoderms found at deep sea hydrothermal vents and cold seep sites (Smirnov et al., 2000), suggesting that these animals are good examples of "regional" species (Barry et al., 1996) that are able to consume and process food sources at vents and seeps.

Although the *Isostichopus fuscus* collected at the vent did have significantly different $\delta^{13}\text{C}$ values than the *I. fuscus* collected away from the vent (Appendix 2, Fig. 20), this difference was driven primarily by the $\delta^{13}\text{C}$ values of one individual. The flocculent material that the *H. inhabilis* collected around the vent were observed feeding on forms mainly where venting activity occurs through soft sediments. *Isostichopus fuscus* were typically found on rock and other hard substrates at both vent and non-vent sites in Bahía Concepción (pers. obs.). Only one *I. fuscus* was encountered on sediments around the flocculent material at the vent site, and its $\delta^{13}\text{C}$ value was -14.71‰ , far closer to the $\delta^{13}\text{C}$ of the flocculent material than the non-vent *I. fuscus*, which had a mean $\delta^{13}\text{C}$ of -11.38‰ . This suggests that *I. fuscus* can also assimilate the carbon in the flocculent material, but may be less likely to do so due to habitat preferences. *Isostichopus fuscus* represents an important economic resource as it supports artisanal fisheries in Mexico. However, populations have been overexploited, and *Isostichopus fuscus* is considered an endangered species in Mexico (Herrero-Pérezrul et al., 1999). Temperature seems to be

one of the most important variables determining the timing of reproduction in *Isostichopus fuscus*, which only reproduce when sea surface temperatures reach 27-30°C (Herrero-Pérezrul et al., 1999). Sea surface temperatures in Bahía Concepción range from 19 to 31°C, and bottom temperatures at 10 m range between 17.5 and 30°C at non-vent areas (Steller, D., 2004; pers. comm.). Vent fluid temperatures as high as 92°C have been measured, and bottom temperatures at 12 m are as high as 50°C at vent sites, and 35°C at transitional sites (see Fig. 13). These elevated temperatures at vent sites are persistent in all seasons, and therefore *Isostichopus fuscus* may be capable of reproduction throughout the year near the vent, suggesting that the vent may have important local effects on this economically important species.

Cortez Angels, *Pomocanthus zonipectus*, were conspicuous and abundant around the vent sites—they were often observed “bathing” in the vent fluid, and rubbing their bodies on the hot sediments (pers. obs.). These fish primarily eat sponges and coral polyps (Bernardi, G., 2004; pers. comm.), which are the most important components of the sessile macrobiota at shallow hydrothermal vents (Pansini et al., 2000). The sponges and corals around vent sites may consume bacteria from the flocculent material that were suspended and transported by geothermal fluid and gas flow, and then pass on this “vent signature” to the *P. zonipectus* foraging around the vent.

The elemental analyses of the vent and non-vent *Holothuria inhabilis* and the flocculent material suggest that some elements are present in greater concentrations within the flesh of the *H. inhabilis* feeding around the hydrothermal vent. These data must be interpreted with caution due to the small sample size, particularly since one of

the vent *H. inhabilis* samples was discarded. However, the vent *H. inhabilis* had Al, Fe, and As concentrations that were higher than the two non-vent *H. inhabilis* (see Table 7), and these elements were also present in relatively high concentrations in the flocculent material, suggesting that the vent *H. inhabilis* may be incorporating some of these elements by feeding on the flocculent material. Three *Holothuria* species (*H. edulis*, *H. impetius*, and *H. fascopundata*) collected in Papua New Guinea (PNG) were analyzed for As and Fe (Maven et al., 1995), and had comparable Fe concentrations (50.10 to 105.60 $\mu\text{g/g}$) to the *H. inhabilis* from Bahía Concepción. However, the As concentrations of the PNG *Holothuria* spp. (0.10 to 0.13 $\mu\text{g/g}$) were an order of magnitude lower than the vent (4.924 $\mu\text{g/g}$) and non-vent (2.104 and 3.228 $\mu\text{g/g}$) *H. inhabilis* samples.

The arsenic levels in *Holothuria inhabilis* were lower than the median concentrations found in mollusc tissues in the USA, 9.1 $\mu\text{g/g}$; in bivalve tissues, As concentrations over 14.5 $\mu\text{g/g}$ are considered to be high (Valette-Silver, 1999). Arsenic is also present in the soft tissues of mussels (*Bathymodiolus puteoserpentis*) at mid-Atlantic Ridge hydrothermal vents at 40 $\mu\text{g/g}$ (Larsen et al., 1997). The As concentrations in the flocculent material forming on sediments at vent sites ranged from 479.8 to 612.3 $\mu\text{g/g}$ (Table 7). Arsenic concentrations of sediments corrected for grain size above 23.9 $\mu\text{g/g}$ are considered to be high (Valette-Silver, 1999). Clearly the As concentrations of the flocculent material far exceed typical levels found in sediments, yet there is little evidence for significant bioaccumulation of arsenic within the flesh of the *H. inhabilis* that were observed feeding on the flocculent material. Ingestion of As-containing foods by biota results in the bio-methylation of inorganic As, and organic forms of As are

rapidly excreted by animals without obvious detrimental effects (US FDA, 1993; Larsen et al., 1997). The arsenic in the vent fluid may also be rendered less toxic to the biota due to the strong affinity between Fe(III) oxyhydroxides and As, which results in the scavenging and adsorption of inorganic arsenic (Pichler et al, 1999b). The precipitates forming around the vent in Bahía Concepción are mainly composed of Fe(III) oxyhydroxides, and As concentrations in these precipitates are high (Canet, C., 2003; pers. comm.). Arsenic adsorption occurs most rapidly and completely at a pH of 6-7 (Pichler et al, 1999b), which are within the ranges of the pH measured at the vent and transitional sites (Fig. 12). It is therefore likely that much of the arsenic within the vent fluids and the flocculent materials is being adsorbed and stored in these Fe(III) oxyhydroxide precipitates, and is not biologically available to the *H. inhabilis* and other organisms feeding around the vent.

Fluorescence and light microscopy indicated that the flocculent material contained diatoms, silicoflagellates, cyanobacteria, and morphologically diverse bacteria within a mineral and organic-rich matrix. The presence of diatoms, silicoflagellates, and cyanobacteria may explain why the carbon stable isotope values are consistent with photosynthetic sources. No hydrogen sulfide has been detected in the vent fluid or gas samples from the hydrothermal vents in Bahía Concepción, precluding the presence of sulfur-oxidizing bacteria in this system. However, iron, manganese, and arsenic are potential electron acceptors depending on their oxidation states, and could therefore drive chemosynthetic pathways in bacteria. Methane is also present in the gas, albeit at relatively low concentrations (see Chapter One). In these shallow-water vent systems, phase separation under reduced hydrostatic pressure may decrease the potential for

methane dissolution within the vent fluids (Sedwick and Stuben, 1996), thereby reducing its availability to methanotrophic bacteria. The FISH molecular probes indicated that the majority of microorganisms colonizing the flocculent materials were bacteria (see Fig. 21). Bacteria stained with the FISH Eub 338 probes are morphologically diverse, including some filamentous microorganisms (Orphan, V., 2003; pers. comm.), however the flocculent material does not appear to represent a true bacterial mat community like those found in other hydrothermal vent and seep systems because it is not exclusively comprised of bacterial cells. The mineral assemblages, textural features, and scanning electron microscope observations of the precipitates forming around the vents in Bahía Concepción suggest that the mineralization processes may be microbially mediated (Canet, C., 2003; pers. comm.). The bacteria within the flocculent materials may be involved in the oxidation and reduction processes controlling the scavenging of As and other toxic elements by Fe(III) oxyhydroxides (eg Pichler et al., 1999b).

The general patterns observed in the biological assemblages around the shallow water hydrothermal vent in Bahía Concepción are similar to those reported from other shallow vents. No vent obligate organisms have been found at any of the shallow water hydrothermal vents that have been studied. Although symbiont-containing species, such as Thyasiridae bivalves (Dando et al., 1994; Tarasov et al., 1999) and Pogonophora (Kamenev et al., 1993; Dando et al., 1994) may be present around shallow vents and seeps, these species commonly occur in other reducing environments in anoxic sediments in shallow waters (Spiro et al., 1986). These species are likely absent from the vents in Bahía Concepción because the sediments are oxic, and hydrogen sulfide is absent from

this system. It does appear that the epifaunal assemblages on rock habitats around this vent are more abundant and diverse than other areas not affected by hydrothermal activity (pers. obs.), a pattern observed at most other shallow water vents and seeps (Jensen et al., 1992; Tarasov et al., 1999; Morri et al., 1999; Pansini et al., 2000; Bianchi and Morri, 2000; Cocito, et al., 2000). This was not tested here because of concerns about pseudoreplication, spatial autocorrelation, and the lack of comparable rock substrate at the same depths away from the vent.

The biota around the shallow water vent in Bahía Concepción are clearly influenced by small-scale variations in hydrothermal fluid flow, which is also one of the most important factors influencing the distribution of biota around deep-sea vents and seeps (Johnson et al., 1988; Fisher et al., 1988; Barry et al., 1997; Colaco et al., 2002; Mullineaux et al., 2003; Levin et al., 2003). The high temperatures within the sediments at vent sites appear to negatively affect the abundances and diversities of infauna around this vent, a pattern that has also been observed at other shallow vents (Kamenev et al., 1993; Dando et al., 1995a; Fitzsimons, et al., 1997; Thiermann et al., 1997; Tarasov et al., 1999). Although the vent fluids from Bahía Concepción also contain high concentrations of arsenic and other potentially toxic elements, the physical modification of the sediments due to vent and fluid flow removing the finer grain sizes, and microbially mediated precipitation may lessen their impact on the biota. The stable isotope ratios of the *Holothuria inhabilis* from around the vent suggest that they are able to assimilate some unique source of carbon related to the hydrothermal activity. This potential enrichment in food availability has also been demonstrated around other shallow vents, where bacterial

and algal mats may contribute significantly to the diet of the regional background species that live near the vents (Stein, 1984; Trager and DeNiro, 1990; Tarasov, 2003). However the vent in Bahía Concepción differs significantly from these other shallow vents because hydrogen sulfide is not present in the vent fluids or gas, and the differences observed in the stable isotopes of the *H. inhabilis* foraging around the vent are more likely to be due to thermophilic bacteria and cyanobacteria incubated by the geothermal fluids.

LITERATURE CITED:

- Abbott, D.P. and Haderlie, E.C. 1980. Prosobranchia: marine snails. Ch. 13. In: Morris, R.H., Abbott, D.P. and Haderlie, E.C. Eds. *Intertidal Invertebrates of California*. Stanford Univ. Press, CA. 690 pp.
- Axen, G. 1995. Extensional segmentation of the main gulf escarpment, Mexico and United States. *Geology* 23: 515-518.
- Barragán R., R.M., Birkle, P., Portugal M., E., Arellano G., V.M., and Alvarez R., J. 2001. Geochemical survey of medium temperature geothermal resources from the Baja California Peninsula and Sonora, México. *Journal of Volcanology and Geothermal Research* 110: 101-119.
- Barry, J.P., Greene, H.G., Orange, D.L., Baxter, C.H., Robison, B.H., Kochevar, R.E., Nybakken, J.W., Reed, D.L., and McHugh, C.M. 1996. Biologic and geologic characteristics of cold seeps in Monterey Bay, California. *Deep-Sea Research I* 43: 1739-1762.
- Barry, J.P., Kochevar, R.E., and Baxter, C.H. 1997. The influence of pore-water chemistry and physiology on the distribution of vesicomid clams at cold seeps in Monterey Bay: implications for patterns of chemosynthetic community organization. *Limnology and Oceanography* 42: 318-328.
- Barton, C.A., Zoback, M.D., and Moos, D. 1995. Fluid flow along potentially active faults in crystalline rocks. *Geology* 23: 683-686.
- Berner, U., Faber, E., Scheeder, G., and Panten, D. 1995. Primary cracking of algal and landplant kerogens: kinetic models of isotope variations in methane, ethane and propane. *Chemical Geology* 126: 233-245.
- Bianchi, C.N. and Morri, C. 2000. Serpuloidea (Annelida: Polychaeta) from Milos, an island in the Aegean Sea with submarine hydrothermalism. *Journal of the Marine Biological Association of the U.K.* 80: 259-269.

- Botz, R., Stuben, D., Winckler, G., Bayer, R., Schmitt, M., Faber, E. 1996. Hydrothermal gases offshore Milos Greece. *Chemical Geology* 130: 161-173.
- Bricker, O.P. and Jones, B.F. 1995. Main factors affecting the composition of natural waters. In: Salbu, B. and Steinnes, E. (eds.) *Trace Elements in Natural Waters*. CRC Press, Boca Raton: 1-17.
- Brinkhoff, T., Sievert, S.M., Kuever, J., Muyzer, G. 1999. Distribution and diversity of sulfur-oxidizing *Thiomicrospira* spp. at a shallow-water hydrothermal vent in the Aegean Sea (Milos, Greece). *Applied and Environmental Microbiology* 65: 3843-3849.
- Brooks, J.M., Kennicutt II, M.C., Fisher, C.R., Macko, S.A., Cole, K. Childress, J.J., Bidigare, R.R., and Vetter, R.D. 1987. Deep-sea hydrocarbon seep communities: evidence for energy and nutritional carbon sources. *Science* 238: 1138-1142.
- Canet, C., Prol-Ledesma, R.M., Rubio-Ramos, M.A., Forrest, M.J., and Torres-Vera, M.A. 2003. Characteristics of Mn-Ba-Hg mineralization at shallow hydrothermal vents in Bahía Concepción, Baja California Sur, Mexico. *Geological Society of America Abstracts with Programs*, Seattle 2003: 579.
- Carney, R.S. 1994. Consideration of the oasis analogy for chemosynthetic communities at Gulf of Mexico hydrocarbon vents. *Geo-Marine Letters* 14: 149-159.
- Carter, J.W. 1982. Natural history observations on the gastropod shell-using amphipod *Photis conchicola* Alderman, 1936. *Journal of Crustacean Biology* 2: 328-341.
- Chapman, P.M. and Wang, F. 2001. Assessing sediment contamination in estuaries. *Environmental Toxicology and Chemistry* 20: 3-22.
- Childress, J.J., Fisher, C.R., Brooks, J.M., Kennicutt II, M.C., Bidigare, R.R., and Anderson, A.E. 1986. A methanotrophic marine molluscan (*Bivalvia*, *Mytilidae*) symbiosis: mussels fueled by gas. *Science* 233: 1306-1308.

- Cocito, S., Bianchi, C.N., Morri, C., and Peirano, A. 2000. First survey of sessile communities on subtidal rocks in an area with hydrothermal vents: Milos Island, Aegean Sea. *Hydrobiologia* 426: 113-121.
- Colaco, A., Dehairs, F., and Desbruyeres, D. 2002. Nutritional relations of deep-sea hydrothermal fields at the Mid-Atlantic Ridge: a stable isotope approach. *Deep-Sea Research I* 49: 395-412.
- Coleman, D.C. and Fry, B., Eds. 1991. *Carbon Isotope Techniques*. Academic Press. San Diego, CA. 274 pp.
- Conway, N.M., Kennicutt II, M.C., and Van Dover, C.L. 1994. Stable isotopes in the study of marine chemosynthetic-based ecosystems. Pp 158-186. In: *Stable Isotopes in Ecology and Environmental Science*. Lajtha, K. and Michener, R.H. Eds. Blackwell Sci. Publ. London, U.K.
- D'Amore, F. and Panichi, C. 1980. Evaluation of deep temperatures of hydrothermal systems by a new gas geothermometer. *Geochimica et Cosmochimica Acta* 44: 549-556.
- Daims, H., Brühl, A., Amann, R., Schleifer, K.H. and Wagner, M. 1999. The domain-specific probe EUB338 is insufficient for the detection of all Bacteria: Development and evaluation of a more comprehensive probe set. *System. Appl. Microbiol.* 22: 434-444.
- Dando, P.R. and Hovland, M. 1992. Environmental effects of submarine seeping natural gas. *Continental Shelf Research* 12: 1197-1207.
- Dando, P.R., Austen, M.C., Burke Jr., R.A., Kendall, M.A., Kennicutt II, M.C., Judd, A.G., Moore, D.C., O'Hara, S.C.M., Scmaljohann, R., and Southward, A.J. 1991. Ecology of a North Sea pockmark with an active methane seep. *Marine Ecology Progress Series* 70: 49-63.

- Dando, P.R., Bussmann, I., Niven, S.J., O'Hara, S.C.M., Shmaljohann, R., and Taylor, L.J. 1994. A methane seep area in the Skagerrak, the habitat of the pogonophore *Siboglinum poseidoni* and the bivalve mollusc *Thyasira sarsi*. *Marine Ecology Progress Series* 107: 157-167.
- Dando, P.R., Hughes, J.A., and Thiermann, F. 1995a. Preliminary observations on biological communities at shallow hydrothermal vents in the Aegean Sea. In: Parson et al. (eds.) *Hydrothermal Vents and Processes*. Geol. Soc. Spec. Publ. 87: 303-317.
- Dando, P.R., Hughes, J.A., Leahy, Y., Niven, S.J., Taylor, L.J., and Smith, C. 1995b. Gas venting rates from submarine hydrothermal areas around the island of Milos, Hellenic Volcanic Arc. *Continental Shelf Research* 15: 913-929.
- Davis, P.H. and Spies, R.B. 1980. Infaunal benthos of a natural petroleum seep: study of community structure. *Marine Biology* 59: 31-41.
- Dziak, R.P. and Johnson, H.P. 2002. Stirring the oceanic incubator. *Science* 296: 1406-1407.
- Edmond, J.M., Von Damm, K.L., McDuff, R.E., and Measures, C.I. 1982. Chemistry of hot springs on the East Pacific Rise and their effluent dispersal. *Nature* 297: 187-191.
- Fauchald, K. and Jumars, P.A. 1979. The diet of worms: a study of polychaete feeding guilds. *Oceanography and Mar. Biol. Ann. Rev.* 17: 193-284.
- Fisher, C.R., Childress, J.J., Arp, A.J., Brooks, J.M., Distel, D.L., Duggan, J.A., Felbeck, H., Fritz, L.W., Hessler, R., Johnson, K.S., Kennicutt II, M.C., Lutz, R.A., Macko, S.A., Newton, A., Powell, M.A., Somero, G.N., and Soto, T. 1988. Variation in the hydrothermal vent clam, *Calyptogena magnifica*, at the Rose Garden vent on the Galapagos spreading center. *Deep-Sea Research* 35: 1811-1831.
- Fitzsimons, M.F., Dando, P.R., Hughes, J.A., Thiermann, F., Akoumianaki, I., and Pratt, S.M. 1997. Submarine hydrothermal brine seeps off Milos, Greece: observations and geochemistry. *Marine Chemistry* 57: 325-340.

- Fletcher, J and Munguía, L. 2000. Active continental rifting in southern Baja California, Mexico; implications for plate motion partitioning and the transition to seafloor spreading in the Gulf of California. *Tectonics* 19: 1107-1123.
- Floodgate, G.D and Judd, A.G. 1992. The origins of shallow gas. *Continental Shelf Research* 12: 1145-1156.
- Folk, R.L. 1974. *Petrology of Sedimentary Rocks*, Hemphill Pub. Co., Austin Texas, 182pp.
- Forrest, M.J., Greene, H.G., Ledesma-Vazquez, J., and Prol-Ledesma, R.M. 2003. Present-day shallow-water hydrothermal venting along the El Requesón fault zone provides possible analog for formation of Pliocene-age chert deposits in Bahía Concepción, B.C.S., Mexico. Geological Society of America abstracts with meeting, Cordilleran Section, Puerto Vallarta 2003.
- Fortin, D., Ferris, F.G., Scott, S.D. 1998. Formation of Fe-silicates and Fe-oxides on bacterial surfaces in samples collected near hydrothermal vents on the Southern Explorer Ridge in the northeast Pacific Ocean. *American Mineralogist* 83: 1399-1408.
- Foster, M.S, Riosmena-Rodriguez, R., Steller, D.L. and Woelkerling, W.J. 1997. Living rhodolith beds in the Gulf of California and their implications for paleoenvironmental interpretation. In: Johnson, M.E. and Ledesma-Vazquez, J., eds. *Pliocene Carbonates and Related Facies Flanking the Gulf of California, Baja California, Mexico*: Boulder, CO. Geol. Soc. of Amer. Special Paper 318.
- Fricke, H., Giere, O., Stetter, K., Alfredsson, G.A., Kristjansson, J.K., Stoffers, P., and Svavarsson, J. 1989. Hydrothermal vent communities at the shallow subpolar Mid-Atlantic ridge. *Marine Biology* 102: 425-429.
- Gamenick, I., Abbiati, M., and Giere, O. 1998. Field distribution and sulphide tolerance of *Capitella capitata* (Annelida: Polychaeta) around shallow water hydrothermal vents off Milos (Aegean Sea). A new sibling species? *Marine Biology* 130: 447-453.

- Gearing, J.N., Gearing, P.J., Rudnick, D.T., Requejo, A.G., and Hutchins, M.J. 1984. Isotopic variability of organic carbon in a phytoplankton-based temperate estuary. *Geochimica et Cosmochimica Acta* 48: 1089-1098.
- German, C.R., Baker, E.T., Klinkhammer, G. 1995. Regional setting of hydrothermal activity. In: Parson et al. (eds.) *Hydrothermal Vents and Processes*. Geol. Soc. Spec. Publ. 87: 3-15.
- Giggenbach, W.F. 1988. Geothermal solute equilibria. Derivation of Na-K-Mg-Ca geothermometers. *Geochimica et Cosmochimica Acta* 52: 2749-2765.
- Giggenbach, W.F. 1997. Relative importance of thermodynamic and kinetic processes in governing the chemical and isotopic composition of carbon gases in high-heatflow sedimentary basins. *Geochimica et Cosmochimica Acta* 61: 3763-3785.
- Gudmundsson, A. 1999. Fluid overpressure and stress drop in fault zones. *Geophys. Res. Ltrs.* 26: 115-118.
- Halfar, J., Godinez-Orta, L., Goodfriend G.A., Mucciarone, D.A., Ingle Jr., J.C., and Holden, P. 2001. Holocene-late Pleistocene non-tropical carbonate sediments and tectonic history of the western rift margin basin of the southern Gulf of California. *Sedimentary Geology* 144: 149-178.
- Hausback, B.P. 1984. Cenozoic volcanic and tectonic evolution of Baja California, Mexico. In: Frizzell, V.A., ed. *Geology of the Baja California Peninsula*. Bakersfield, CA, Pacific Section, Society of Economic Paleontologists and Mineralogists: 219-236.
- Hayes, M.L., Johnson, M.E., and Fox, W.T. 1993. Rocky-shore biotic associations and their fossilization potential: Isla Requesón (Baja California Sur, Mexico). *Journal of Coastal Research* 9: 944-957.
- Hesse, R. 1989. Silica diagenesis: origin of inorganic and replacement cherts. *Earth Science Reviews* 26: 253-284.

- Herrero-Pérezrul, M.D., Reyes Bonilla, H., García-Domínguez, Cintra-Buenrostro, C.E. 1999. Reproduction and growth of *Isostichopus fuscus* (Echinodermata: Holothuroidea) in the southern Gulf of California, México. *Marine Biology* 135: 521-532.
- Hovland, M. and Thomsen, E. 1989. Hydrocarbon-based communities in the North Sea? *Sarsia* 74: 29-42.
- Ingersoll, R.V., and Busby, C.J. 1995. Tectonics of sedimentary basins. In: Busby, C.J. and Ingersoll, R.V. (Eds.) *Tectonics of Sedimentary Basins*. Blackwell Science, Cambridge: 1-52.
- Jacq, E., Prieur, D., Nichols, P., White, D.C., Porter, T., and Geesey, G.G. 1989. Microscopic examination and fatty acid characterization of filamentous bacteria colonizing substrata around subtidal hydrothermal vents. *Archives of Microbiology* 152: 64-71.
- Jenden, P.D., Kaplan, I.R., Poreda, R.J., and Craig, H. 1988. Origin of nitrogen-rich gases in the California Great Valley: evidence from helium, carbon, and nitrogen isotope ratios. *Geochimica et Cosmochimica Acta* 52: 851-861.
- Jensen, P. 1986. Nematode fauna in the sulphide-rich brine seep and adjacent bottoms of the East Flower Garden, NW Gulf of Mexico. *Marine Biology* 92: 489-503.
- Jensen, P., Aagard, I., Burke Jr., R.A., Dando, P.R., Jorgensen, N.O., Kuijpers, A., Laier, T., O'Hara, S.C.M., and Schmaljohan, R. 1992. "Bubbling reefs" in the Kattegat: submarine landscapes of carbonate-cemented rocks support a diverse ecosystem at methane seeps. *Marine Ecology Progress Series* 83: 103-112.
- Johnson, K.S., Childress, and J.J., Beehler. 1988. Short-term variability in the Rose Garden hydrothermal vent field: an unstable deep-sea environment. *Deep-Sea Research* 35: 1711-1721.
- Johnson, K.S., Childress, J.J., Beehler, C.L., and Sakamoto, C.M. 1994. Biogeochemistry of hydrothermal vent mussel communities: the deep-sea analogue to the intertidal zone. *Deep Sea Research I* 41: 993-1011.

- Johnson, M.E., Ledesma-Vázquez, J., Mayall, M.A., and Minch, J. 1997. Upper Pliocene stratigraphy and depositional systems: the Peninsula Concepcion basins in Baja California Sur, Mexico. In: Johnson, M.E. and Ledesma-Vázquez, J., eds. Pliocene Carbonates and Related Facies Flanking the Gulf of California, Baja California, Mexico: Boulder, CO. Geol. Soc. of Amer. Special Paper 318:57-72.
- Johnson, M.E. and Ledesma-Vázquez, J. 2001. Pliocene-Pleistocene rocky shorelines trace coastal development of Bahía Concepción, gulf coast of Baja California Sur (Mexico). *Palaeogeography, Palaeoclimatology, Palaeoecology* 166: 65-88.
- Jollivet, D. 1996. Specific and genetic diversity at deep-sea hydrothermal vents: an overview. *Biodiversity and Conservation* 5: 1619-1653.
- Judd, A.G. and Hovland, M. 1992. The evidence of shallow gas in marine sediments. *Continental Shelf Research* 12: 1081-1095.
- Juniper, S.K., Tunnicliffe, V., and Fontaine, A.R. 1988. Biological influences on mineral deposition at deep-sea hydrothermal vents. In: De Luca, M.P. and Babb, I. (Eds.) *Global Venting, Midwater, and Benthic Ecological Processes*. Nat. Undersea Res. Program Res. Report 88: 99-118.
- Juniper, S.K. and Tebo, B.M. 1995. Microbe-metal interactions and mineral deposition at hydrothermal vents. In: Karl, D.M. (Ed.) *The Microbiology of Deep-Sea Hydrothermal Vents*. CRC Press, Boca Raton, FL: 219-253.
- Kamanev, G.M., Fadeev, V.I., Selin, N.I., Tarasov, V.G., and Malakhov, V.V. 1993. Composition and distribution of macro- and meiobenthos around sublittoral hydrothermal vents in the Bay of Plenty, New Zealand. *NZ Journal of Marine and Freshwater Res.* 27: 407-418.
- Knutzen, J. 1981. Effects of decreased pH on marine organisms. *Marine Pollution Bulletin* 12: 25-29.
- Krasnow, L.D. and Taghon, G.L. 1997. Rate of tube building and sediment particle size selection during tube construction by the tanaid crustacean, *Leptochelia dubia*. *Estuaries* 20: 534-546.

- Krooss, B.M., Littke, R., Muller, B., Frielingsdorf, J., Schwochau, K., Idiz, E.F. 1995. Generation of nitrogen and methane from sedimentary organic matter: implications on the dynamics of natural gas accumulations. *Chemical Geology* 126: 291-318.
- Larsen, E.H., Quetel, C.R., Munoz, R., Fiala-Medioni, A., and Donard, O.F.X. 1997. Arsenic speciation in shrimp and mussel from the Mid-Atlantic hydrothermal vents. *Marine Chemistry* 57: 341-346.
- Ledesma-Vázquez, J., Berry, R.W., Johnson, M.E., and Gutierrez-Sanchez, S. 1997. El Mono chert: a shallow-water chert from the Pliocene Infierno Formation, Baja California Sur, Mexico. In: Johnson, M.E. and Ledesma-Vazquez, J., eds. *Pliocene Carbonates and Related Facies Flanking the Gulf of California, Baja California, Mexico*: Boulder, CO. Geol. Soc. of Amer. Special Paper 318: 73-81.
- Ledesma-Vázquez, J., Johnson, M.E. 2001. Miocene-Pleistocene tectono-sedimentary evolution of Bahía Concepción region, Baja California Sur (Mexico). *Sedimentary Geology* 144: 83-96.
- Levin, L.A., James, D.W., Martin, C.M., Rathburn, A.E., Harris, L. H., and Michener R.H. 2000. Do methane seeps support distinct macrofaunal assemblages? Observations on community structure and nutrition from the northern California slope and shelf. *Marine Ecology Progress Series* 208: 21-39.
- Levin, L.A., Etter, R.J., Rex, M.A., Gooday, A.J., Smith, C.R., Pineda, J., Stuart, C.T., Hessler, R.R., and Pawson, D. 2001. Environmental influences on regional deep-sea species diversity. *Ann. Rev. Ecol. Syst.* 32: 51-93.
- Levin, L.A. and Michener, R.H. 2002. Isotopic evidence for chemosynthesis-based nutrition of macrobenthos: the lightness of being at Pacific methane seeps. *Limnological Oceanography* 47: 1336-1345.
- Levin, L.A., Ziebis, W., Mendoza, G.F., Growney, V.A., Tryon, M.D., Brown, K.M., Mahn, C., Gieskes, J.M., and Rathburn, A.E. 2003. Spatial heterogeneity of macrofauna at northern California methane seeps: influence of sulfide concentration and fluid flow. *Marine Ecology Progress Series* 265: 123-139.

- Libbey, L.K. and Johnson, M.E. 1997. Upper Pleistocene rocky shores and intertidal biotas at Playa La Palmita (Baja California Sur, Mexico). *Journal of Coastal Research* 13: 216-225.
- Long, E.R., Hong, C.B., and Severn, C.G. 2001. Relationships between acute sediment toxicity in laboratory tests and abundance and diversity of benthic infauna in marine sediments: a review. *Environmental Toxicology and Chemistry* 20: 46-60.
- Lonsdale, P. 1977. Clustering of suspension-feeding macrobenthos near abyssal hydrothermal vents at oceanic spreading centers. *Deep-Sea Research* 24: 857-863.
- Lonsdale, P. 1989. Geology and tectonic history of the Gulf of California. In: Winterer, E.L., Hussong, D.M., and Decker, R.W., eds., *The Eastern Pacific Ocean and Hawaii*. Boulder, CO. Geological Society of America, *The Geology of North America*, v.N.: 499-521.
- Lopez-Cortes, A. 1999. Marine cyanobacteria from Bahía Concepción, BCS, Mexico. In, Charpy, Larkum eds. *Marine Cyanobacteria*. Bull. Inst. Ocean., Monaco. No. 19: 87-93.
- MacAvoy, S.E., Carney, R.S., Fisher, C.R., and Macko, S.A. 2002. Use of chemosynthetic biomass by large, mobile, benthic predators in the Gulf of Mexico. *Marine Ecol. Prog. Series* 225: 65-78.
- Martínez-López, A. and Gárate-Lizárraga, I. 1994 Quantity and quality of the particulate organic matter in Concepcion Bay during the spawning season of the scallop *Argopecten circularis* (Sowerby, 1835). *Ciencias Marinas* 20: 301-320.
- Massin, C. 1982. Food and feeding mechanisms: Holothuroidea. In: *Echinoderm Nutrition*. Langoux, M. and Lawrence, J.M. Eds. Balkema Rotterdam. Pp 43-55.
- Maven, H., Sunder Rao, K., Benko, W., Alam, K., Huber, M.E., Rali, T., and Burrows, I. 1995. Fatty acid and mineral composition of Papua New Guinea echinoderms. *Fishery Technology* 32: 50-52.

- McFall, C. C., 1968. Reconnaissance Geology of the Concepcion bay area, Baja California, Mexico. *Stanford Univ. Publ., Geol. Soc.* 10: 1-25.
- Meldahl, K.H., Yajimovich, O.G., Empedocles, C.D., Gustafson, C.S., Hidalgo, M.M., and Reardon, T.W. 1997a. Holocene sediments and molluscan faunas of Bahia Concepcion: a modern analog to Neogene rift basins of the Gulf of California. In: Johnson, M.E. and Ledesma-Vazquez, J., eds. *Pliocene Carbonates and Related Facies Flanking the Gulf of California, Baja California, Mexico*: Boulder, CO. *Geol. Soc. of Amer. Special Paper* 318: 39-56.
- Meldahl, K.H., Flessa, K.W., and Cutler, A.H. 1997b. Time-averaging and postmortem skeletal survival in benthic fossil assemblages: quantitative comparisons among Holocene environments. *Paleobiology* 23: 207-229.
- Millero, F.J. 2002. Seawater as an Electrolyte. In: Gianguzza et al., (eds.) *Chemistry of Marine Waters and Sediments*. Springer, Berlin: 3-34.
- Minagawa, M. and Wada, E. 1984. Stepwise enrichment of ^{15}N along food chains: further evidence and the relation between $\delta^{15}\text{N}$ and animal age. *Geochimica et Cosmochimica Acta* 48: 1135-1140.
- Montagna, P.A., Bauer, J.E., Hardin, D., and Spies R.B. 1989. Vertical distribution of microbial and meiofaunal populations in sediments of a natural coastal hydrocarbon seep. *Journal of Marine Research* 47: 657-680.
- Morri, C., Bianchi, C.N., Cocito, S., Peirano, A, De Biase, A.M., Aliana, S., Pansini, M., Boyer, M., Ferdeghini, F., Pestarino, M., and Dando, P. 1999. Biodiversity of marine sessile epifaunal at an Aegean island subject to hydrothermal activity: Milos, eastern Mediterranean Sea. *Marine Biology* 135: 729-739.
- Mullineaux, L.S., Peterson, C.H., Micheli, F., and Mills, S.W. 2003. Successional mechanism varies along a gradient in hydrothermal fluid flux at deep-sea vents. *Ecological Monographs* 73: 523-542.

- O'Hara, S.C.M, Dando, P.R., Schuster, U., Bennis, A., Boyle, J.D., Chui, F.T.W., Hatherell, T.V.J., Niven, S.J., and Taylor, L.J. 1995. Gas seep induced interstitial water circulation: observations and environmental implications. *Continental Shelf Research* 15: 931-948.
- Orange, D.L., Greene, H.G., Reed, D., Martin, J.B., McHugh, C.M., Ryan, W.B.F., Maher, N., Stakes, D., Barry, J. 1999. Widespread fluid expulsion on a translational continental margin: mud volcanoes, headless canyons, and organic-rich substrate in Monterey Bay, California. *GSA Bulletin* 111: 992-1009.
- Orphan, V.J., House, C.H., Hinrichs, K.-U., McKeegan, K.D., DeLong, E.F. 2001. Methane-consuming Archaea revealed by directly coupled isotopic and phylogenetic analysis. *Science* 293: 484-487.
- Oskin, M., Stock, J., and Martin-Barajas, A. 2001. Rapid localization of Pacific-North America plate motion in the Gulf of California. *Geology* 29: 459-462.
- Oskin, M. and Stock, J. 2003. Marine incursion synchronous with plate-boundary localization in Gulf of California. *Geology* 31: 23-26.
- Pansini, M., Morri, C., and Bianchi, C.N. 2000. The sponge community of a subtidal area with hydrothermal vents: Milos Island, Aegean Sea. *Estuarine, Coastal, and Shelf Science* 51: 627-635.
- Paull, C.K., Jull, A., Toolin, L., and Linick, T. 1985. Stable isotope evidence for chemosynthesis in an abyssal seep community. *Nature* 317: 709-711.
- Philp, R.P., Calvin, M., Brown, S., and Yang, E. 1978. Organic geochemical studies on kerogen precursors in recently deposited algal mats and oozes. *Chemical Geology* 22: 207-231.
- Pichler, T., and Dix, G.R. 1996. Hydrothermal venting within a coral reef ecosystem, Ambitle Island, Papua New Guinea. *Geology* 24: 435-438.

- Pichler, T., and Veizer, J. 1999, Precipitation of Fe(III) oxyhydroxide deposits from shallow-water hydrothermal fluids in Tutum Bay, Ambitle Island, Papua New Guinea: *Chemical Geology* 162: 15-31.
- Pichler, T., Veizer, J., and Hall, G.E.M., 1999a. The chemical composition of shallow-water hydrothermal fluids in Tutum Bay, Ambitle Island, Papua New Guinea and their effect on ambient seawater: *Marine Chemistry* 64: 229-252.
- Pichler, T., Veizer, J., and Hall, G.E.M. 1999b. Natural input of arsenic into a coral-reef ecosystem by hydrothermal fluids and its removal by Fe(III) oxyhydroxides. *Environmental Science & Technology* 33: 1373-1378.
- Popp, B.N., Sansone, F.J., Rust, T.M., and Merritt, D.A., 1995. Rapid method for determining abundance and carbon isotopic composition of dissolved methane in sediments and nearshore waters. *Anal. Chem.* 67: 405-411.
- Portugal, E., Birkle, P., Barragan, R.M., Arellano, V.M., Tello, E., and Tello, M., 2000. Hydrochemical–isotopic and hydrogeological conceptual model of the Las Tres Vírgenes geothermal field, Baja California Sur, México. *Journal of Volcanology and Geothermal Research*, 101: 223–244.
- Prol-Ledsma, R.M., Canet, C. Melgarejo, J.C., Tolson, G., Rubio-Ramos, M.A., Cruz-Ocampo, J.C., Ortega-Osorio, A., Torres-Vera, M.A., and Reyes, A. 2002. Cinnabar Deposition in submarine coastal hydrothermal vents, Pacific Margin of Central Mexico. *Economic Geology* 97:1-10.
- Prol-Ledesma, R.M., Canet, C., Torres-Vera, M.A., Forrest, M.J., and Armienta, M.A. 2003. Vent fluid chemistry in Bahia Concepcion coastal submarine hydrothermal system, Baja California, Mexico. *Geological Society of America abstracts with meeting, Cordilleran Section, Puerto Vallarta 2003.*
- Rau, G.H. and Hedges, J.I. 1979. Carbon-13 depletion in a hydrothermal vent mussel: suggestion of a chemosynthetic food source. *Science* 203: 648-649.
- Rau, G.H. 1981. Low $^{15}\text{N}/^{14}\text{N}$ in hydrothermal vent animals: ecological implications. *Nature* 289: 484-485.

- Riese, K. 2002. Sediment mediated species interactions in coastal waters. *Journal of Sea Research* 48: 127-141.
- Robinson, C. 2000. Plankton gross production and respiration in the shallow water hydrothermal system of Milos, Aegean Sea. *Journal of Plankton Research* 22: 997-906.
- Rosenberg, R. 2001. Marine benthic faunal successional stages and related sedimentary activity. *Scientia Marina* 65: 107-119.
- Rubio-Ramos, M.A. and Prol-Ledesma, R.M. 2000. Estudio preliminar petrografico y de inclusiones fluidas en ventilas hidrotermales, Punta Mita, Mexico. *Union Geofis. Mex. GEOS* 20: 250-251.
- Sano, Y and Marty, B. 1995. Origin of carbon in fumarolic gas from island arcs. *Chemical Geology* 119: 265-274.
- Sansone, F.J., Popp, B.N., and Rust, T.M., 1997. Stable carbon isotopic analysis of low-level methane in water and gas. *Anal. Chem.* 69: 40-44.
- Sartoni, G. and De Biasi, A.M. 1999. A survey of the marine algae of Milos Island, Greece. *Cryptogamie, Algol.* 20: 271-283.
- Schoell, M. 1983. Genetic characterization of natural gases. *American Association of Petroleum Geologists Bulletin* 67: 2225-2238.
- Schoell, M. 1988. Multiple origins of methane in the earth. *Chemical Geology* 71: 1-10.
- Sedwick, P. and Stuben, D. 1996. Chemistry of a shallow submarine warm spring in an arc-volcanic setting: Vulcano Island, Aeolian Archipelago, Italy. *Marine Chemistry* 53: 147-161.
- Self, R.F.L. and Jumars, P.A. 1988. Cross-phyletic patterns of particle selection by deposit feeders. *Journal of Marine Research* 46: 119-143.

- Simoneit, B.R.T and Kvenvolden, K.A. 1994. Comparison of ^{14}C ages of hydrothermal petroleum: Organic Geochemistry 21: 525-529.
- Simoneit, B.R.T. 2000. Submarine and continental hydrothermal systems—a review of organic matter alteration and migration processes, and comparison with conventional sedimentary basins. Reviews in Economic Geology 9: 193-215.
- Smirnov, A.V., Gebruk, A.V., Galkin, S.V., and Shank, T. 2000. New species of holothurian (Echinodermata: Holothuroidea) from hydrothermal vent habitats. J. Mar. Biol. Ass. U.K. 80: 321-328.
- Sorokin, Y.I., Sorokin, P.Y., Zakuskina, O.Y. 1998. Microplankton and its functional activity in zones of shallow hydrotherms in the Western Pacific. Journal of Plankton Research 20: 1015-1031.
- Southward, A.J. 1989. Animals fuelled by chemosynthesis: Life at hydrothermal vents, cold seeps and in reducing sediments. Journal of the Zoological Society of London 217: 705-709.
- Southward, A.J., Southward, E.C., Dando, P.R., Hughes, J.A., Kennicutt II, M.C., Alcalá-Herrera, J., and Leahy, Y. 1997. Behaviour and feeding of the Nassariid gastropod *Cyclope Neritea*, abundant at hydrothermal brine seeps off Milos (Aegean Sea). J. Mar. Biol. Assoc. U.K. 77: 753-771.
- Spencer, J.E. and Normark, W.R. 1989. Neogene plate-tectonic evolution of the Baja California Sur continental margin and the southern Gulf of California, Mexico. In: Winterer, E.L., Hussong, D.M., and Decker, R.W., eds. The Eastern Pacific Ocean and Hawaii: Boulder, CO, Geological Society of America. The Geology of North America v. N: 489-497.
- Spies, R.B and Davis, P.H. 1979. The infaunal benthos of a natural oil seep in the Santa Barbara Channel. Marine Biology 50: 27-237.
- Spies, R.B. and DesMarais, D.J. 1983. Natural isotope study of trophic enrichment of marine benthic communities by petroleum seepage. Marine Biology 73: 67-71.

- Spiro, B., Greenwood, P.B., Southward, A.J., and Dando, P.R. 1986. $^{13}\text{C}/^{12}\text{C}$ ratios in marine invertebrates from reducing sediments: confirmation of nutritional importance of chemoautotrophic endosymbiotic bacteria. *Mar. Ecol. Prog. Ser.* 28: 233-240.
- Stein, J.L. 1984. Subtidal gastropods consume sulfur-oxidizing bacteria: evidence from coastal hydrothermal vents. *Science* 223: 696-698.
- Steller, D.L. 1993 Ecological studies of rhodoliths in Bahía Concepción, Baja California Sur, Mexico. M.S. Thesis Moss Landing Marine Labs. 89 pp.
- Stock, J.M. and Hodges, K.V. 1989. Pre-Pliocene extension around the Gulf of California and the transfer of Baja California to the Pacific Plate. *Tectonics* 8: 99-115.
- Taran, Y.A. 1986. Gas geothermometers for hydrothermal systems. *Geochemistry International* 23: 111-126.
- Taran, Y.A., Inguaggiato, S., Marin, M., and Yurova, L.M. 2002. Geochemistry of fluids from submarine hot springs at Punta de Mita, Nayarit, Mexico. *Journal of Volcanology and Geothermal Res.* 115: 329-338.
- Tarasov, V.G., Propp, M.V., Propp, L.N., Zhirmunsky, A.V., Namsaraev, B.B., Gorlenko, V.M., and Starynin, D.A. 1990. Shallow-water gaseohydrothermal vents of Ushishir volcano and the ecosystem of Kraternaya bight. *P.S.Z.N.I: Marine Ecology* 11: 1-23.
- Tarasov, V.G., Gebruk, A.V., Shulkin, V.M., Kamenev, G.M., Fadeev, V.I., Kosmynin, V.N., Malakhov, V.V., Starynin, D.A., and Obzhurov, A.I. 1999. Effect of shallow-water hydrothermal venting on the biota of Matupi Harbour. *Cont. Shelf Res.* 19: 79-116.
- Tarasov, V.G., Bogovski, S., and Muzyka, V. 2003. Biochemical characteristics of algal-bacterial mats and invertebrates from shallow-water hydrothermal fields of the West Pacific Ocean. *Aquatic Sciences* 65: 73-80.

- Telliard, W.A and Martin. T. 2001. Trace elements in water, solids, and biosolids by inductively coupled plasma-atomic emission spectrometry. Method 200.7. Rev. 5.0. U.S. Environmental Protection Agency. Washington D.C.
- Thiermann, F., Akoumianaki, I., Hughes, J.A., and Giere, O. 1997. Benthic fauna of a shallow-water gaseohydrothermal vent area in the Aegean Sea (Milos, Greece). *Marine Biology* 128: 149-159.
- Tieszen L.L., Boutton T.W., Tesdahl K.G., and Slade N.A. 1983. Fractionation and turnover of stable carbon isotopes in animal tissues: implications for ^{13}C analysis of diet. *Oecologia* 57: 32-37.
- Trager, G.C. and De Niro, M.J. 1990. Chemoautotrophic sulfur bacteria as a food source for mollusks at intertidal hydrothermal vents: evidence from stable isotopes. *Veliger* 33(4): 359-362.
- Umhoefer, P.J., Dorsey, R.J., Willsey, S., Mayer, L., Renne, P., 2001. Stratigraphy and geochronology of the Comondú Group near Loreto, Baja California Sur, Mexico. *Sedimentary Geology* 144: 125-147.
- Umhoefer, P.J., Mayer, L. and Dorsey, R.J. 2002. Evolution of the margin of the Gulf of California near Loreto, Baja California peninsula, Mexico. *GSA Bulletin* 114: 849-868.
- US FDA. 1993. Guidance document for arsenic in shellfish. Washington DC: Center for Food Safety and Applied Nutrition.
- Valette-Silver, N.J., Riedel, G.F., Crecelius, E.A., Windom, H., Smith, R.G., and Dolvin, S.S. 1999. Elevated arsenic concentrations in bivalves from the southeast coasts of the USA. *Marine Environmental Research* 48: 311-333.
- Van Dover, C.L. and Fry, B. 1989. Stable isotopic compositions of hydrothermal vent organisms. *Marine Biology* 102: 257-263.
- Van Dover, C.L. and Fry, B. 1994. Microorganisms as food resources at deep-sea hydrothermal vents. *Limnol. Oceanography* 39: 51-57.

- Van Dover, C.L. The Ecology of Deep-Sea Hydrothermal Vents. 2000. Princeton Univ. Press, NJ. 424 pp.
- Van Dover, C.L., Humphris, S.E., Fornari, D., Cavanaugh, C.M., Collier, R., Goffredi, S.K., Hashimoto, J., Lilley, M.D., Reysenbach, A.L., Shank, T.M., Von Damm, K.L., Banta, A., Gallant, R.M., Gotz, D., Green, D., Hall, J., Harmer, T.L., Hurtado, L.A., Johnson, P., McKiness, Z.P., Meredith, C., Olson, E., Pan, I.L., Turnipseed, M., Won, Y., Young III, C.R., Vrijenhoek, R.C. 2001. Biogeography and ecological setting of Indian Ocean hydrothermal vents. *Science* 294: 818-823.
- Van Dover, C.L., German, C.R., Speer, K.G., Parson, L.M., and Vrijenhoek, R.C. 2002. Evolution and biogeography of deep-sea vent and seep invertebrates. *Science* 295: 1253-1257.
- Verma, S.P. and Santoyo E. 1997. New improved equations for Na/K, Na/Li and SiO₂ geothermometers by outlier detection and rejection. *Journal of Volcanology and Geothermal Research* 79: 9-23.
- Vidal, V.M.V, Vidal, F.V., Isaacs, J.D., and Young, D.R. 1978. Coastal submarine hydrothermal activity off Northern Baja California. *Journal of Geophysical Research* 83(B4):1757-1774.
- Vidal, F.V., Welhan, J.A., and Vidal, V.M.V. 1982. Stable isotopes of helium, nitrogen and carbon in a coastal submarine hydrothermal system. *Journal of Volcanology and Geothermal Research* 12: 101-110.
- Vidal, V.M.V, Vidal, F.V., and Isaacs, J.D. 1981. Coastal submarine hydrothermal activity off Northern Baja California 2. evolutionary history and isotope geochemistry *Journal of Geophysical Research* 86: 9451-9468.
- Vismann, B. 1991. Sulfide tolerance: physiological mechanisms and ecological implications. *Ophelia* 1: 1-27.
- Ward, D.M. and Castenholz, R.W. 2000. Cyanobacteria in geothermal habitats. In: *The Ecology of Cyanobacteria*. Whitton, B.A. and Potts, M. eds. Kluwer Academic Publishers, Netherlands. pp 37-59.

- Welhan, J.A. 1988. Origins of methane in hydrothermal systems. *Chemical Geology* 71: 183-198.
- Wiese, K. and Kvenvolden, K. A., 1993. Introduction to microbial and thermal methane. In: Howell, D. G.; Wiese, K.; Fanelli, M.; Zink, L. L.; Cole, F. (Eds.). (The future of energy gases). U. S. Geological Survey Professional Paper, Report: P 1570, pp.13-20.
- You, C.F., Butterfield, D.A., Spivak, A.J., Gieskes, J.M., Gamo, T. and Campbell, A.J. 1994. Boron and halide systematics in submarine hydrothermal systems; effects of phase separation and sedimentary contributions. *Earth and Planetary Science Letters* 123: 227-238.
- You, C.F. and Gieskes, J.M. 2001. Hydrothermal alteration of hemipelagic sediments: experimental evaluation of geochemical processes in shallow subduction zones. *Applied Geochemistry* 16: 1055-1066.
- Zanchi, A. 1994. The opening of the Gulf of California near Loreto, Baja California, Mexico: from basin and range extension to transtensional tectonics. *Journal of Structural Geology* 16: 1619-1639.
- Zar, J.H. 1999. *Biostatistical Analysis*. Fourth Ed. Prentice Hall. New Jersey. 663 pp.

Table 1. Dissolved Oxygen (DO), conductivity, salinity, and pH of pore water samples from sediment cores at 13-14 m. Overlying Water represents the water drawn from the core above the sediment. Pore Water is the water drawn from 0-5cm in the sediment.

	Site One			Site Two			Site Three		
	Vent	Trans	Outside	Vent	Trans	Outside	Vent	Trans	Outside
Overlying Water	2.2	3.2	3.34	2.72	2.39	2.81	2.72	2.64	2.77
DO (mg/l)	51.3	54	53.4	52.9	53.3	53.4	54.1	53.4	53.4
Conductivity(mS)	33.5	35.4	35	34.6	34.9	35.2	35.5	34.9	34.9
Salinity (ppt)	7.89	8.02	8.04	8.00	8.04	8.02	7.97	8.04	8.03
pH	1.39	3.0	2.93	1.74	2.29	2.98	1.84	2.64	2.53
Pore Water	46.2	48.6	55	49.7	51.1	53.6	46.8	54.2	54.5
DO (mg/l)	29.7	31.4	36.1	32.1	33.3	35.1	30.2	35.5	35.5
Conductivity(mS)	6.41	6.59	7.87	6.38	7.23	7.9	6.7	7.21	7.7
Salinity (ppt)									
pH									

Table 2. Vent fluid geochemistry data from Bahía Concepción. Major ion concentrations reported in mM/L. Trace component concentrations reported in $\mu\text{M/L}$. * represents value below detectable limits, n.d.= not determined. All Vent Fluid data from samples collected at subtidal vent near Punta Santa Barbara. Intertidal Spring1 was collected at intertidal hot spring near Playa Santispac. Intertidal Spring2 and Intertidal Spring3 were collected at intertidal hot springs near Punta Santa Barbara. Non-Vent Seawater was collected within Bahía Concepción at a location not affected by hydrothermal venting. Data referenced as R.P.L. are from Prol-Ledesma et al., 2003. T.P are from T. Pichler (unpublished).

Sample	Cl (mM/L)	Na (mM/L)	Mg (mM/L)	Ca (mM/L)	SO ₄ (mM/L)	K (mM/L)	HCO ₃ (mM/L)	Si (mM/L)	Reference
Vent Fluid1	458.39	394.48	35.79	23.28	16.95	12.66	4.86	3.08	R.P.L.
Vent Fluid2	500.71	414.71	41.92	19.36	21.18	12.51	4.28	2.14	R.P.L.
Vent Fluid3	493.65	408.87	40.20	20.59	20.62	12.54	4.48	2.39	R.P.L.
Vent Fluid4	493.82	452.37	37.70	27.94	17.38	12.86	3.52	2.56	T.P.
Vent Fluid5	492.05	404.09	33.21	26.45	17.29	11.79	3.88	2.53	T.P.
Vent Fluid6	497.21	448.02	36.05	26.45	17.99	12.07	3.95	2.74	T.P.
Intertidal Spring1	409.03	334.02	25.00	28.92	12.35	12.17	1.95	4.54	R.P.L.
Intertidal Spring2	388.12	321.88	2.70	39.17	2.92	15.93	1.72	5.73	T.P.
Intertidal Spring3	364.74	267.51	2.26	35.43	1.66	13.45	1.84	4.56	T.P.
Non-Vent Seawater	527.50	485.86	58.35	9.80	26.55	12.37	1.65	0.02	R.P.L.

Sample	Br ($\mu\text{M/L}$)	B ($\mu\text{M/L}$)	Li ($\mu\text{M/L}$)	Rb ($\mu\text{M/L}$)	Sr ($\mu\text{M/L}$)	Mn ($\mu\text{M/L}$)	Fe ($\mu\text{M/L}$)	As ($\mu\text{M/L}$)	Cs ($\mu\text{M/L}$)	Ba ($\mu\text{M/L}$)	I ($\mu\text{M/L}$)	Hg ($\mu\text{M/L}$)
Vent Fluid1	2203.00	828.86	344.38	299.29	173.93	64.81	40.64	10.41	4.35	2.98	3.63	0.49
Vent Fluid2	2178.00	645.70	253.60	290.16	149.85	43.15	33.12	6.14	3.76	2.59	3.31	0.69
Vent Fluid3	2215.00	630.90	275.22	306.31	172.91	52.07	35.63	9.34	4.26	2.88	2.66	6.93
Vent Fluid4	775.97	*	n.d.	n.d.	684.78	32.77	32.23	13.00	n.d.	1.75	n.d.	n.d.
Vent Fluid5	772.22	*	n.d.	n.d.	661.95	25.49	37.60	12.56	n.d.	1.42	n.d.	n.d.
Vent Fluid6	788.49	*	n.d.	n.d.	719.01	20.03	21.49	8.00	n.d.	1.05	n.d.	n.d.
Intertidal Spring1	1055.00	685.48	370.32	387.97	218.33	79.01	17.55	3.74	2.90	2.47	0.84	0.12
Intertidal Spring2	603.25	2081.41	n.d.	n.d.	1198.36	25.49	*	27.10	n.d.	10.70	n.d.	n.d.
Intertidal Spring3	510.64	943.57	n.d.	n.d.	890.21	29.13	*	18.42	n.d.	6.54	n.d.	n.d.
Non-Vent Seawater	2541.00	356.15	67.72	259.97	53.87	0.10	16.47	*	0.01	0.11	2.14	*

Table 3. Calculated subsurface end-member temperatures in °C from geothermometers applied to Bahía Concepción hydrothermal vent fluid samples. References as in Table 1. t_{kn} and t_{km} represent the K/Na and K/Mg geothermometers (Giggenbach, 1988), t_{SiO2}, t_{Na/K}, and t_{Na/Li} represent the SiO₂, Na/K, and Na/Li geothermometers after Verma and Santoyo (1997). n.d.-not determined because Li data are not available.

Sample	t _{kn}	t _{km}	t _{SiO2}	t _{Na/K}	t _{Na/Li}
Vent Fluid1	188.13	108.61	129.43	174.73	134.92
Vent Fluid2	184.04	106.01	110.75	170.57	115.57
Vent Fluid3	185.13	106.67	116.13	171.68	120.60
Vent Fluid4	180.24	108.33	119.78	166.71	n.d
Vent Fluid5	181.89	107.65	119.06	168.39	n.d
Vent Fluid6	176.80	107.15	123.25	163.22	n.d
Intertidal Spring1	196.71	112.66	151.38	183.46	149.04
Intertidal Spring2	218.88	157.97	165.79	206.08	n.d
Intertidal Spring3	220.08	155.02	151.62	207.30	n.d

Table 4. Gas compositions in % volume from hydrothermal vent near Punta Santa Barbara in Bahía Concepción. C₁ represents methane, C₂ ethane, C₃ propane.

Sample	He %	H ₂ %	Ar %	O ₂ %	CO ₂ %	N ₂ %	CO %	C ₁ %	C ₂ %	C ₃ %
BCa	0.0439	0.0045	0.684	0.121	42.88	54.12	0	2.13	0.0177	0.002
BCb	0.0413	0.0091	0.722	0.241	44.05	52.64	0	2.28	0.0179	0.002

Table 5. Methane and ethane concentrations and ratios from gas samples from hydrothermal vent near Punta Santa Barbara in Bahía Concepción.

Sample	CH ₄ (μmoles/L)	CH ₄ (ppm)	C ₂ H ₆ (ppm)	CH ₄ / C ₂ H ₆
BC1	547.78	13365.82	161.10	82.96
BC2	727.22	17744.27	222.24	79.84
BC3	765.07	18667.64	287.35	64.97
BC4	707.21	17255.97	233.69	73.84
BC5	576.61	14069.25	160.15	87.85
BC6	732.98	17884.78	239.50	74.68

Table 6. Carbon dioxide, methane, and ethane carbon stable isotope ratios (in ‰) from gas samples from hydrothermal vent near Punta Santa Barbara in Bahía Concepción.

Sample	CO ₂ δ ¹³ C	CH ₄ δ ¹³ C	C ₂ H ₆ δ ¹³ C
BC7	-5.59	-31.9	-12.23
BC8	-5.7	-36.23	-18.61
BC9	-6.16	-29.75	-15.95
BC10	-6.22	-35.82	
BC11	-5.63	-35.96	
BC12	-5.8	-36.16	

Table 7. Elemental compositions (in $\mu\text{g}/\text{kg}$) of vent and non-vent *Holothuria inhamilis* and flocculent material samples.

Element	Non-Vent <i>H. inhamilis</i> 1	Non-Vent <i>H. inhamilis</i> 2	Vent <i>H. inhamilis</i>	Flocculent Material 1	Flocculent Material 2
Na	2768.2	2516	3679	1318.8	1220.5
Mg	12223.1	9340.3	10236.5	2562.5	2476.6
Al	291.1	139.5	405.7	17910	17918
P	209.5	172.7	249.4	1229.4	1486.2
S	195.8	166.2	232	23	22.7
K	226.7	185	271.8	468.7	381
Ca	32417.6	31929.9	34122.7	1950.5	1959.9
Ti	6.93	4.17	10.48	325.7	295.1
Mn	114.9	73.6	107.7	55.3	59.7
Fe	69.15	45.62	128.3	11133	10177
As	3.23	2.1	4.92	479.8	612.3
Sr	1002.4	866	922.5	206.4	217.8

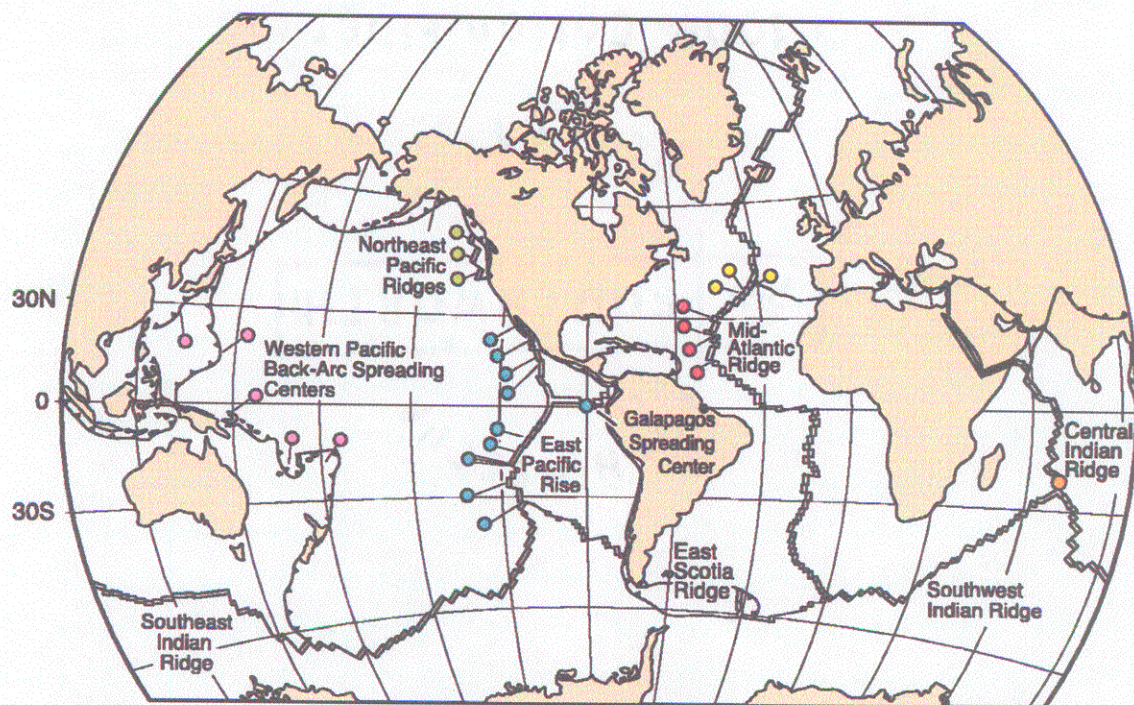
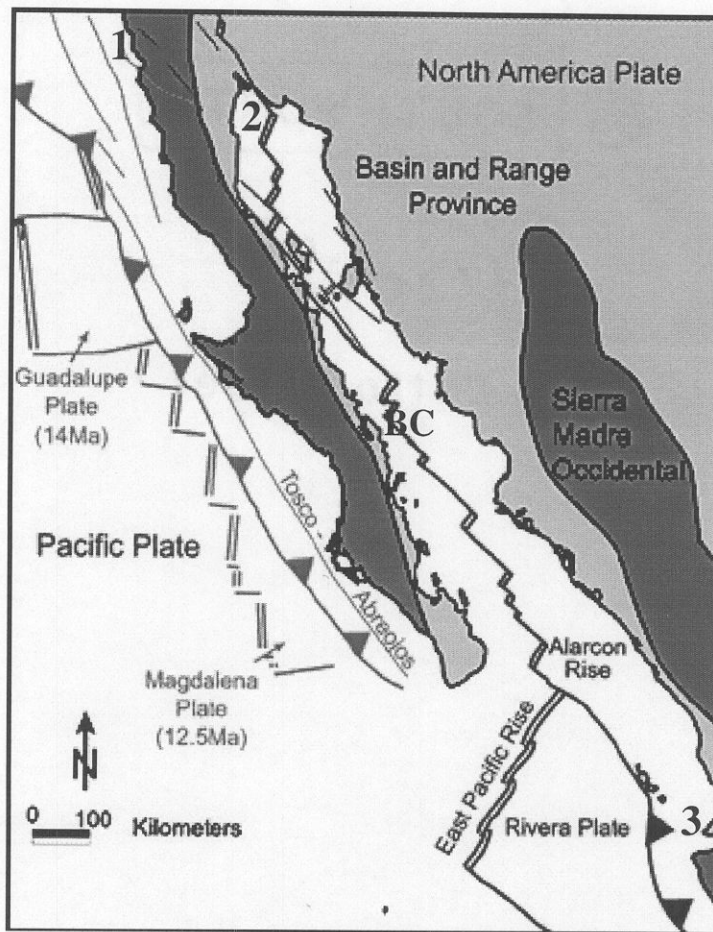


Figure 1. Map of known deep-sea hydrothermal vent regions associated with active plate boundaries. Pink, western Pacific; green, northeast Pacific; blue, East Pacific Rise; yellow, Azores; red, Mid-Atlantic Ridge; orange, Indian Ocean. From Van Dover et al., 2002.







-  Subduction and Paleo-Subduction Zones.
-  Thrust teeth on over-riding plate.
-  Spreading center.
-  Strike-slip faults.

Figure 2. The Baja California peninsula and associated tectonic structures. BC is Bahía Concepción. Numbers represent other coastal hydrothermal systems referred to in the text: 1) Punta Banda, 2) San Felipe, Punta Estrella, El Coloradito, and Puertecitos, 3) Punta Mita. Dates under Guadalupe and Magdalena Plates represent the timing of the cessation of paleo-subduction. Adapted and modified from Fletcher and Munguía, 2000.

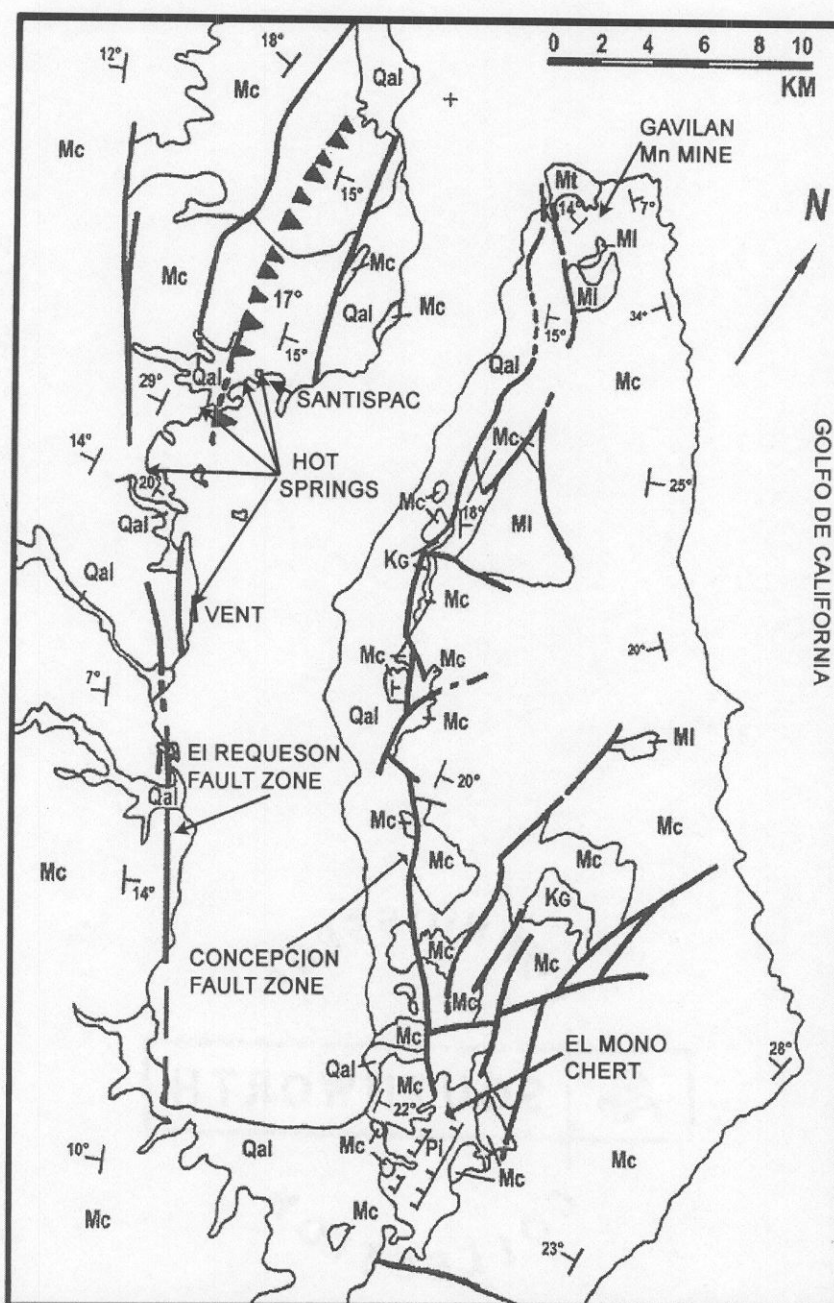


Figure 3. Geologic map of the Bahía Concepción region. Dipping symbols represent average attitude on the Comondú Group. Thick lines represent faults. Hydrothermal vent near Punta Santa Barbara [VENT]; Intertidal hot springs [HOT SPRINGS]; Cretaceous granitoids [KG]; Miocene Comondú Group [Mc]; Miocene undifferentiated intrusive [MI]; Miocene Tirabuzon Formation [Mt]; Pliocene Infierno Formation [Pi]; Quaternary alluvium [Qal]. Modified from McFall (1968) and Ledesma-Vázquez and Johnson (2001).



Figure 4. Isla El Requesón with 350m long tombolo of rhodolith-derived carbonate sand. From Johnson and Ledesma-Vázquez (eds.), 1997.

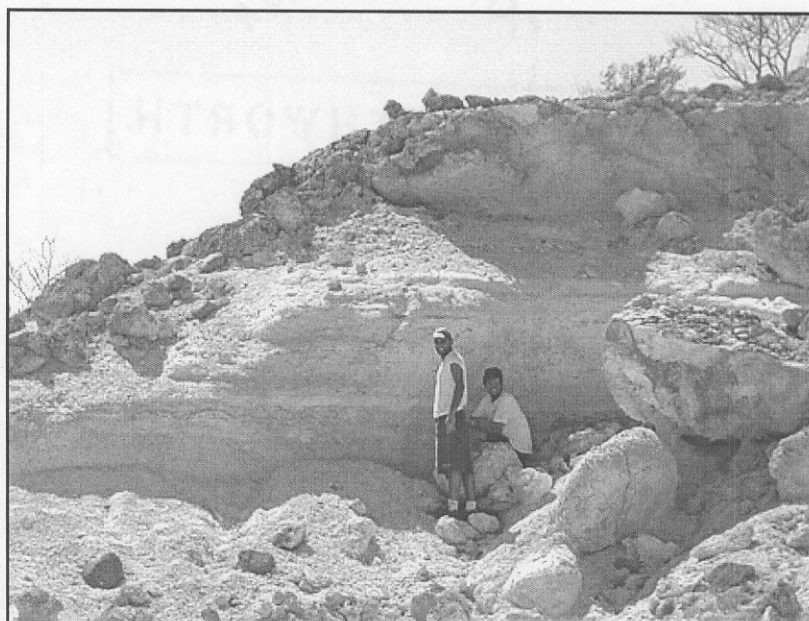


Figure 5. El Mono cherts occurring along Concepción Fault Zone on Peninsula Concepción.

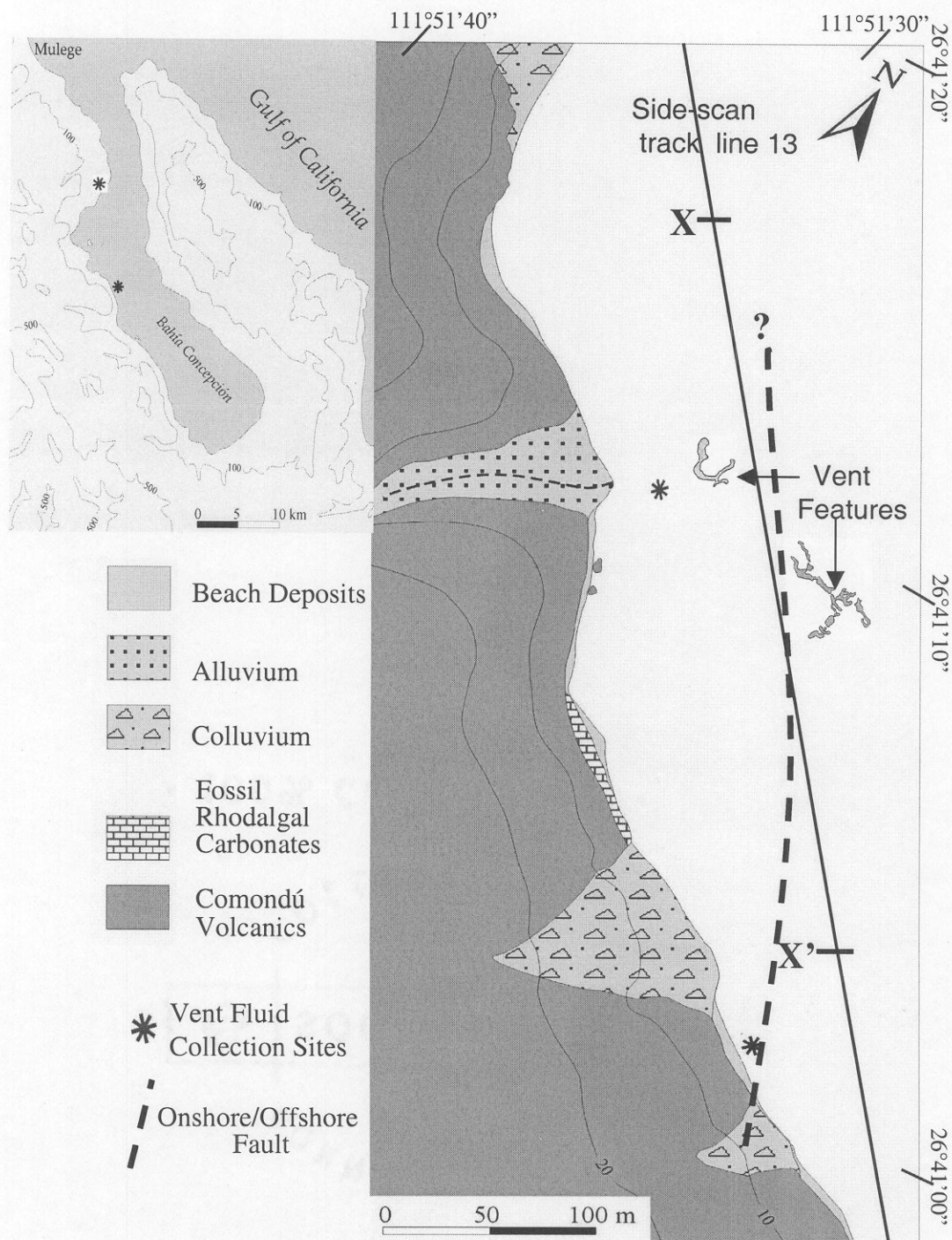


Figure 6: Geological map of the Punta Santa Barbara area with onshore/offshore fault associated with El Requesón fault zone acting as conduit for hydrothermal fluids and gas. See text for features used to define fault. Vent Features (not to scale) are sinuous mounds of sediment associated with fluid and gas venting. X and X' correspond to fixes on Figure 10.



Figure 7. Mineral precipitates around intertidal hot springs near Punta Santa Barbara. Thermometer reads 75.8°C, and is 15 cm in height.



Figure 8. Gas and hydrothermal fluids venting in rocky area at 6 m along El Requesón fault zone near Punta Santa Barbara. White funnel in foreground is 20 cm in height. (Photos courtesy of R. Price).

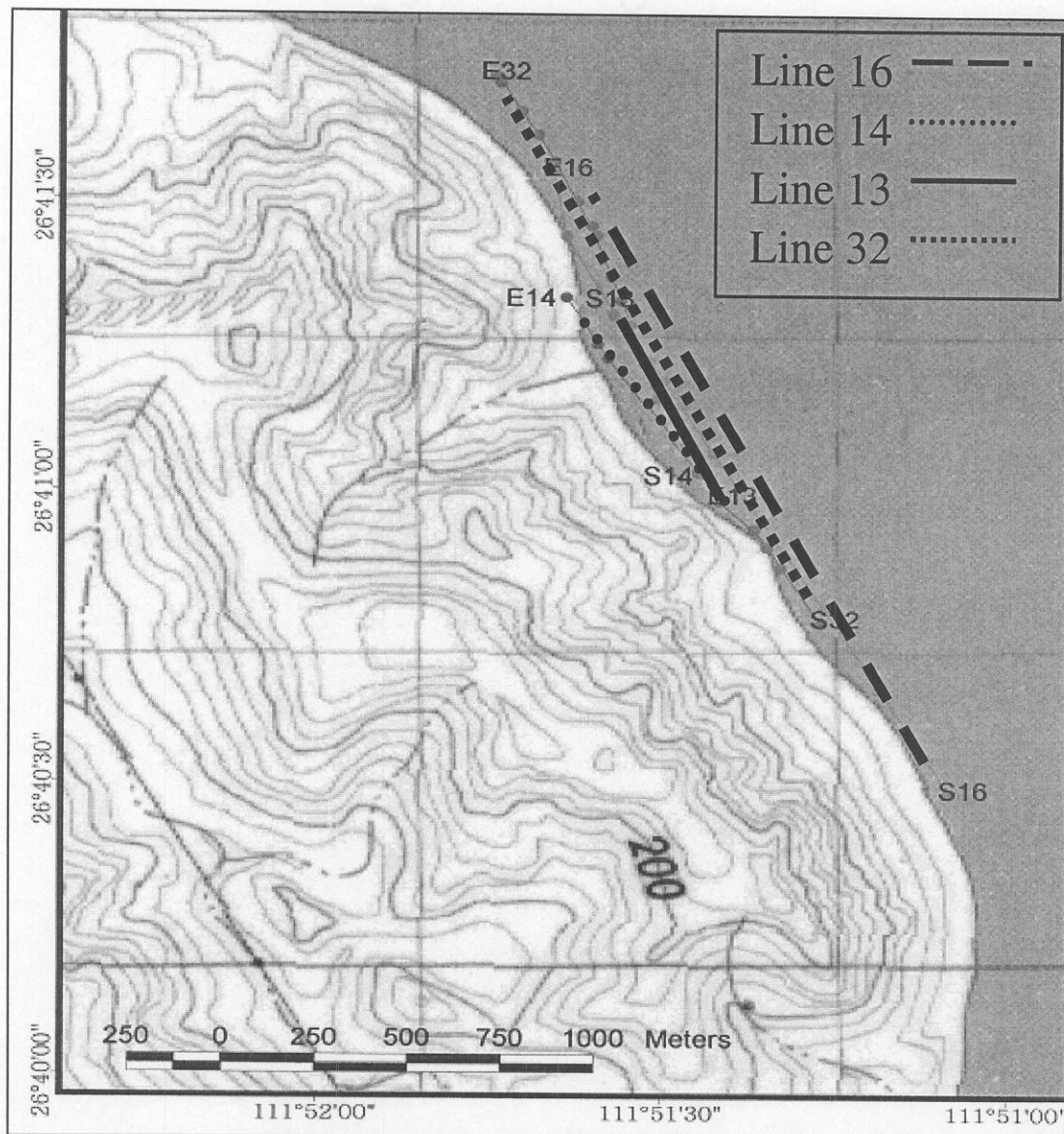


Figure 9. Locations of side-scan track lines from the Punta Santa Barbara area. S13 and E13 represent the start and end of track line 13.

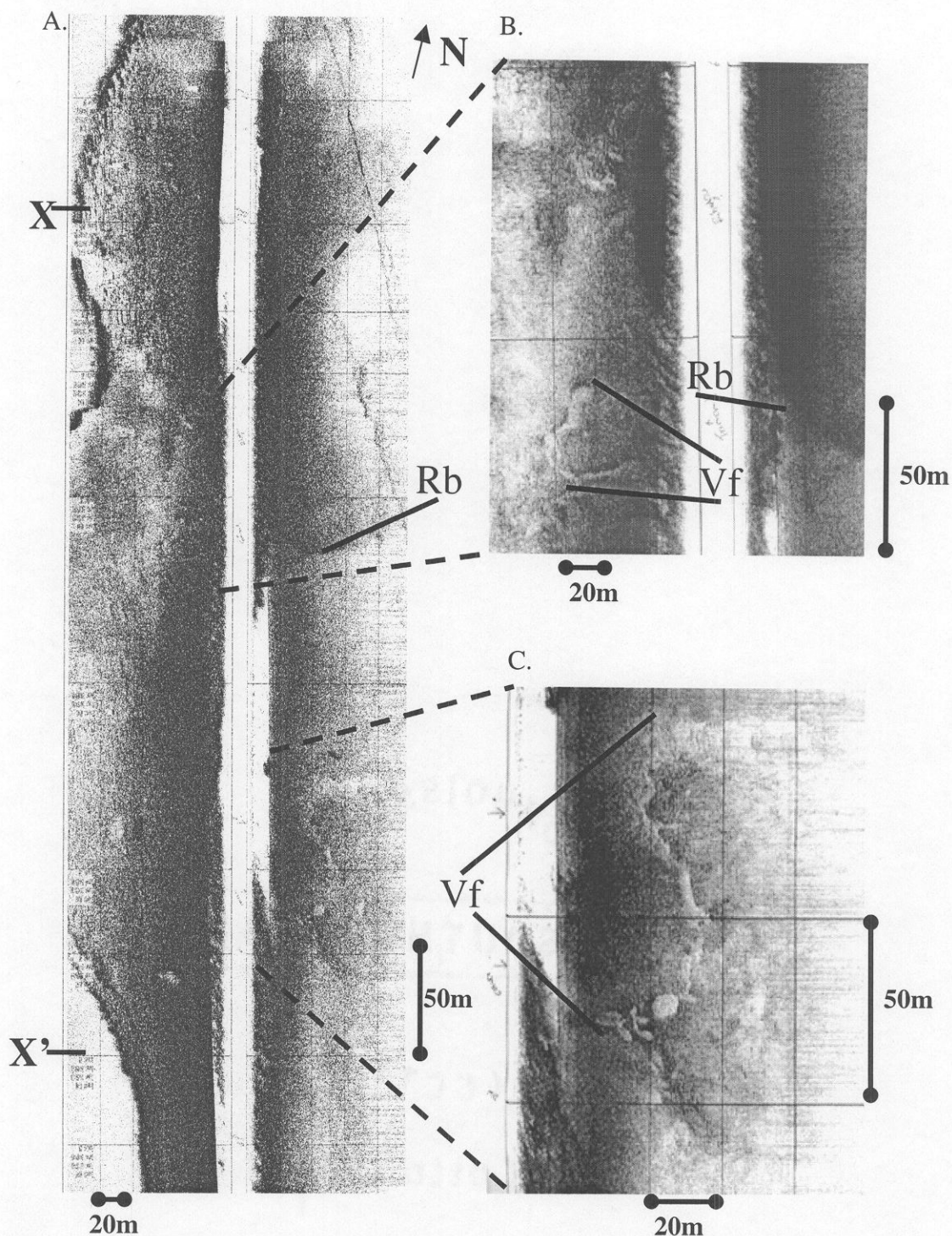


Figure 10. (A) Side-scan Sonar track line 13, illustrates coastline and offshore vent features from subtidal hydrothermal vent area near Punta Santa Barbara. (B) and (C) are close-up views of vent features (Vf) appearing on side-scan. Rb represents the edge of a rhodolith bed. X and X' correspond to fixes on Figure 6.

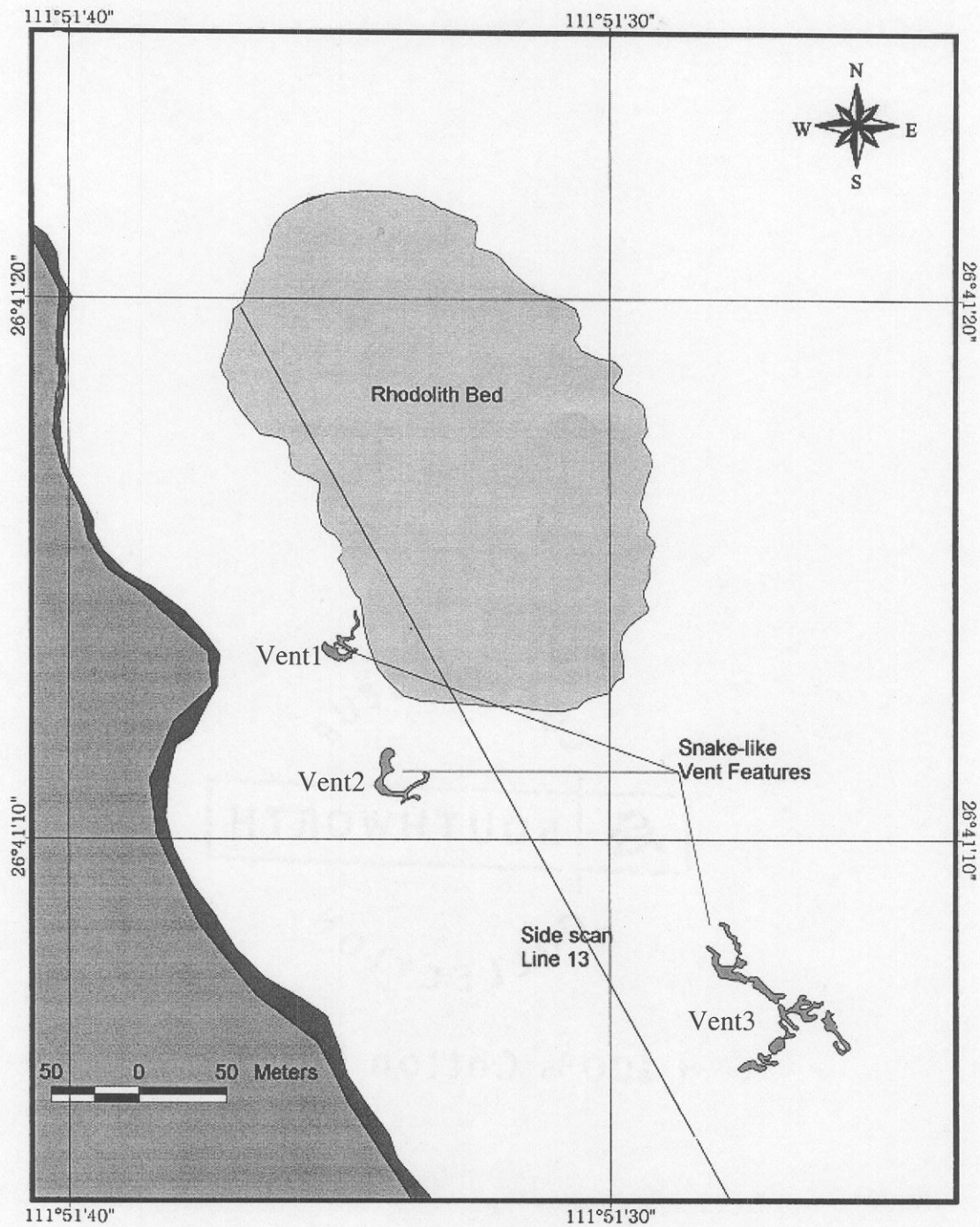


Figure 11. Interpretive side-scan data mapped to show locations and relationships of vent features and rhodolith bed appearing on side-scan track line 13. Vent1, Vent2, and Vent3 represent the three different locations where cores were collected for grain size analyses and to determine physical parameters of pore waters.

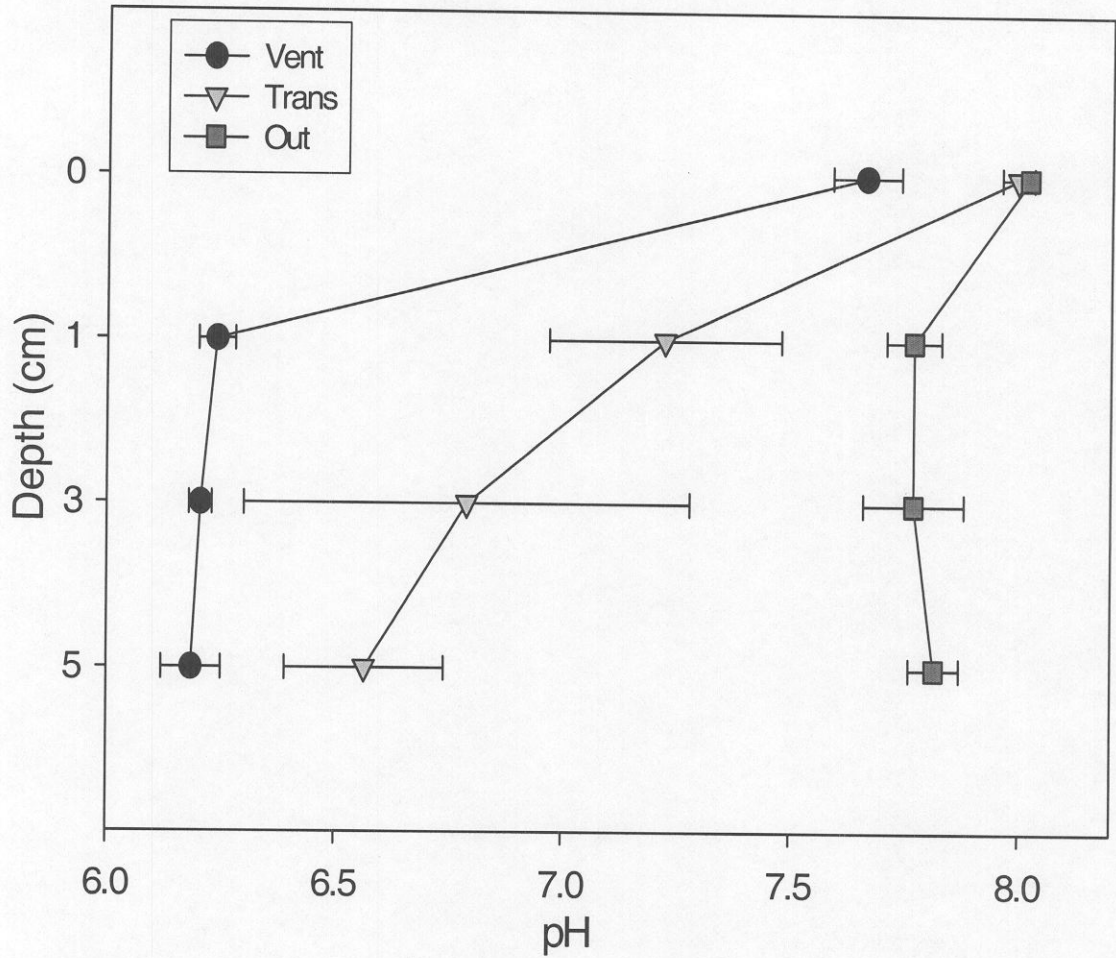


Figure 12. Means of pH profiles in sediments for vent, transitional, and outside (non-vent) samples at 0,1,3 and 5 cm depths. Error bars represent standard errors.

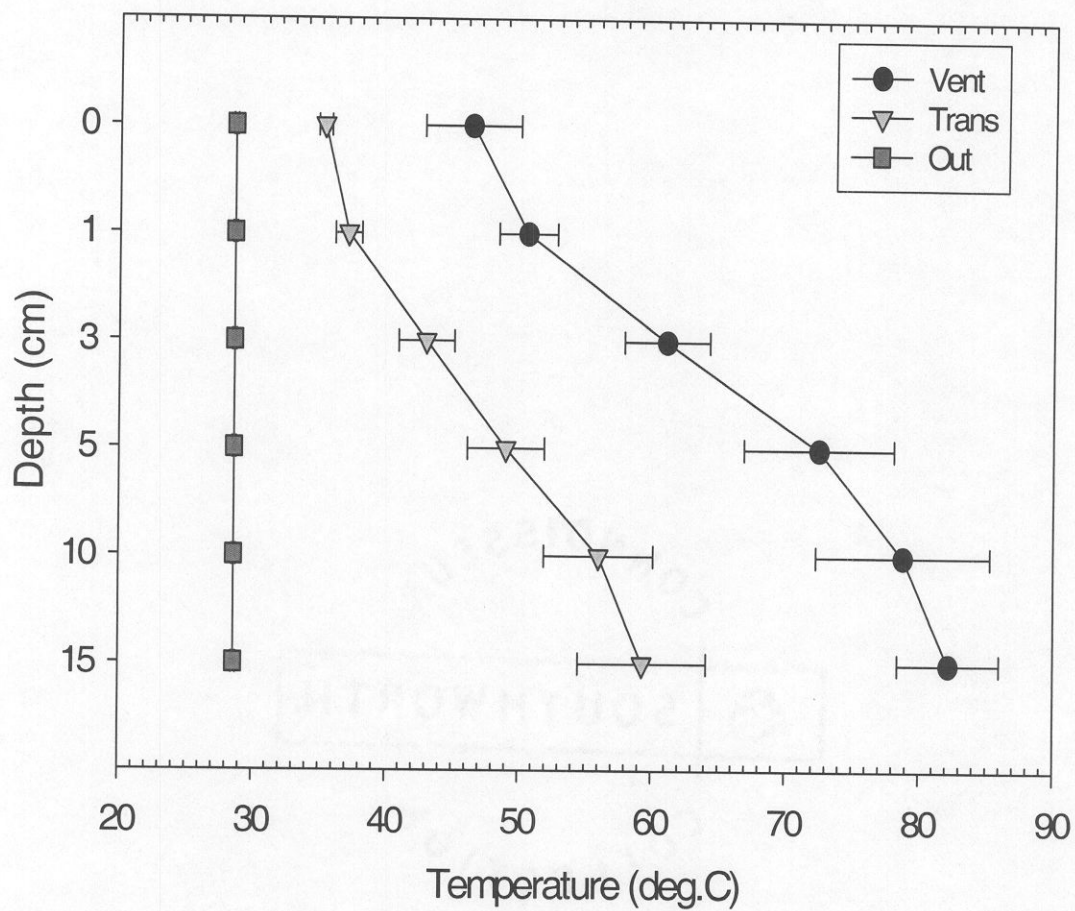


Figure 13. Means of temperature profiles in sediments for vent, transitional, and outside (non-vent) samples at 0,1,3,5, 10, and 15 cm depths. Error bars represent standard errors.

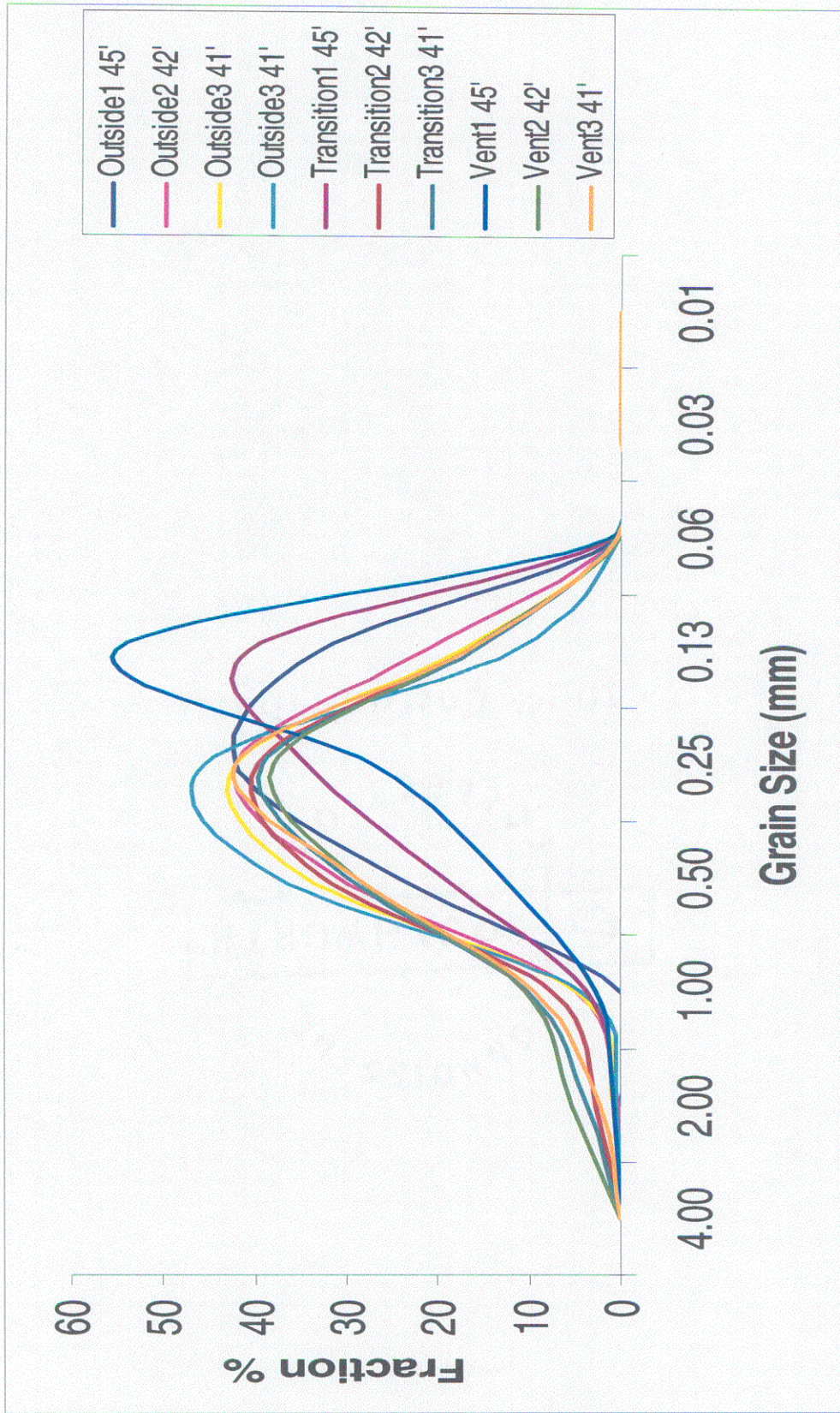


Figure 14. Fraction % of grain sizes (in mm) from Vent, Transitional, and Outside zones from cores collected at three different locations around areas affected by hydrothermal flow of gas and fluids through sediments. See Figure 11 for locations.

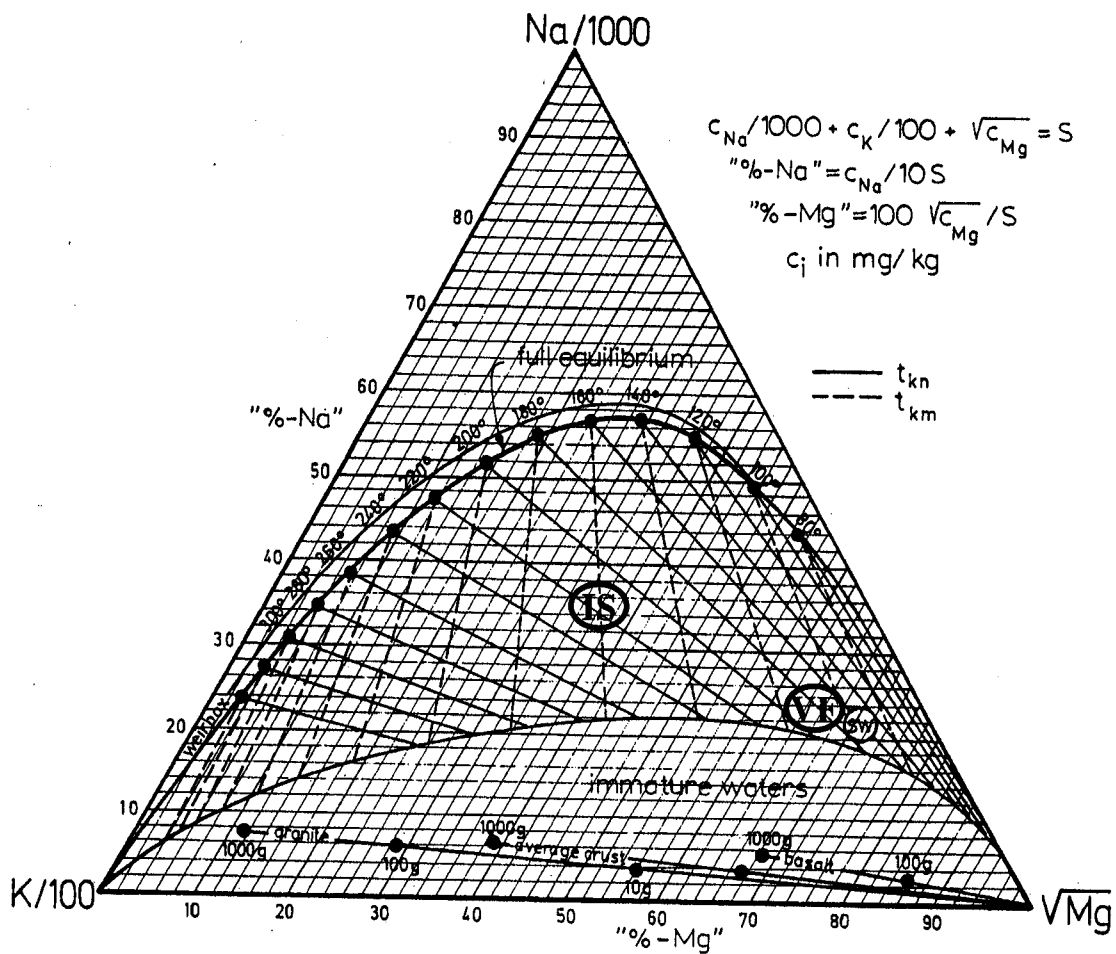


Figure 15: Diagram for the evaluation of Na/K and K/Mg equilibration temperatures after Giggenbach (1988). IS plotted on diagram refer to hydrothermal fluids from Intertidal Springs 2 and 3 located near Punta Santa Barbara, while VF represents values from subtidal vents. SW is seawater.

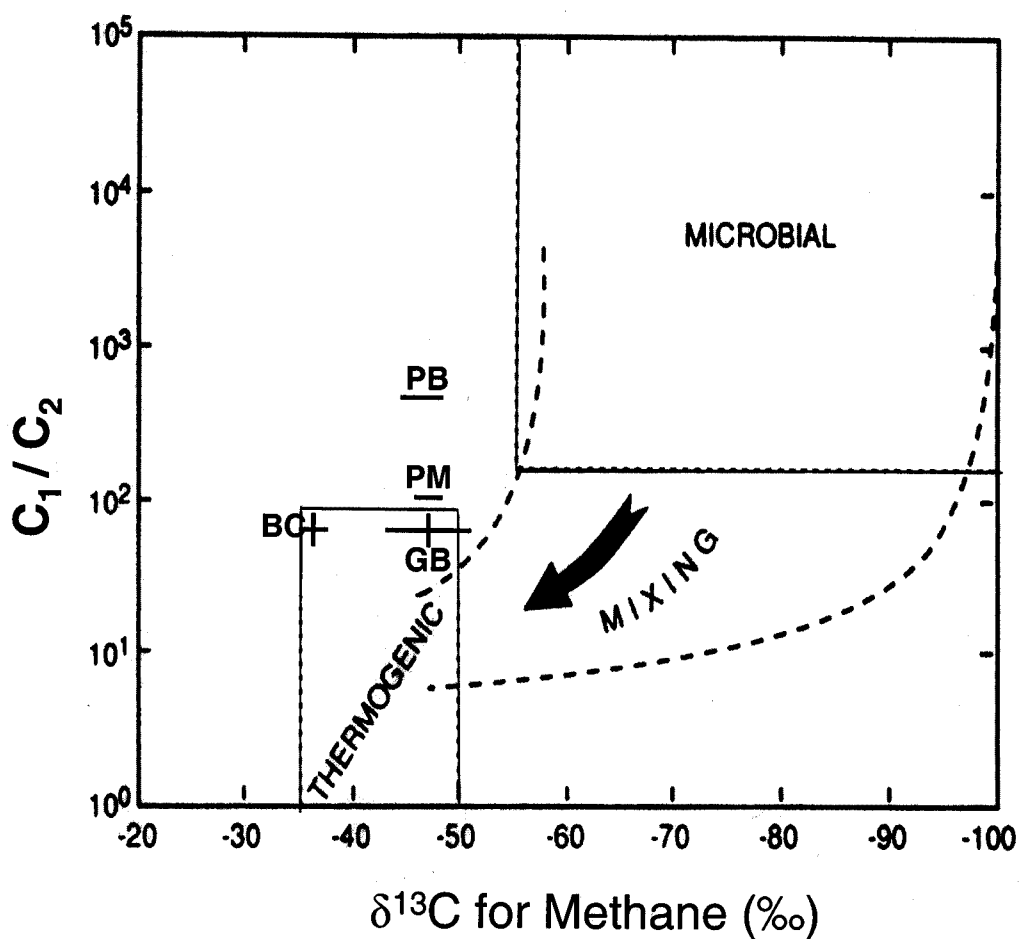


Figure 16. Methane $\delta^{13}C$ values and hydrocarbon ratios of natural gases of biogenic and thermogenic origins. Adapted from Wiese and Kvenvolden (1993). BC represents gas samples from Bahía Concepción (this study), GB is Guaymas Basin (Welhan, 1988), PM is Punta Mita (Taran et al., 2002), PB is Punta Banda (Vidal and Vidal 1981; Vidal, et al. 1982). Error bars represent standard deviations of measured values. No error bars are shown for hydrocarbon ratios of PB and PM samples because only one value was reported.

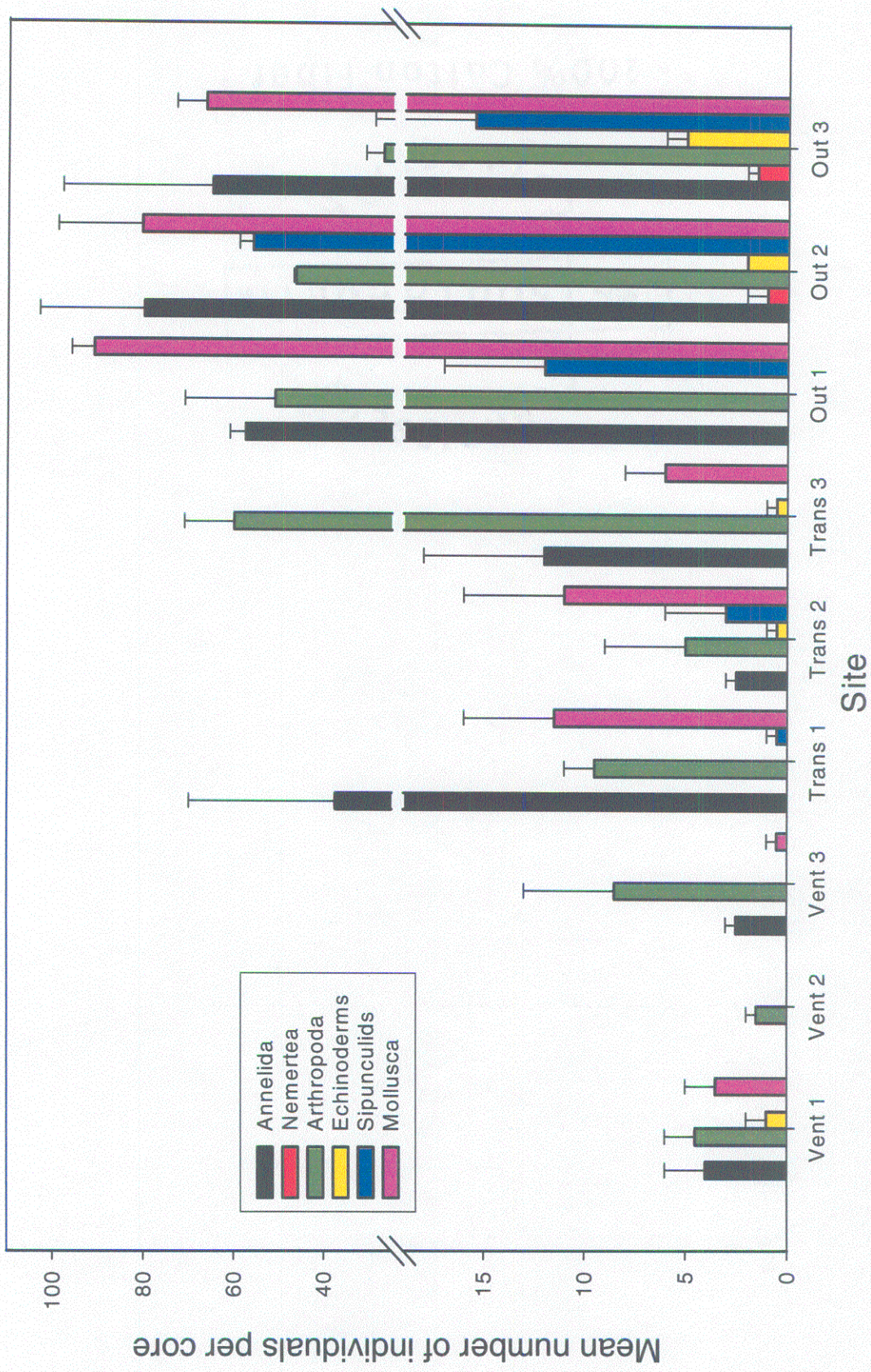


Figure 17. Mean infaunal abundances per core (n=2) separated by phyla. Error bars represent +1 standard error. Infaunal cores collected to 5 cm depths in sediments; total volume of cores = 400.59 cm³.

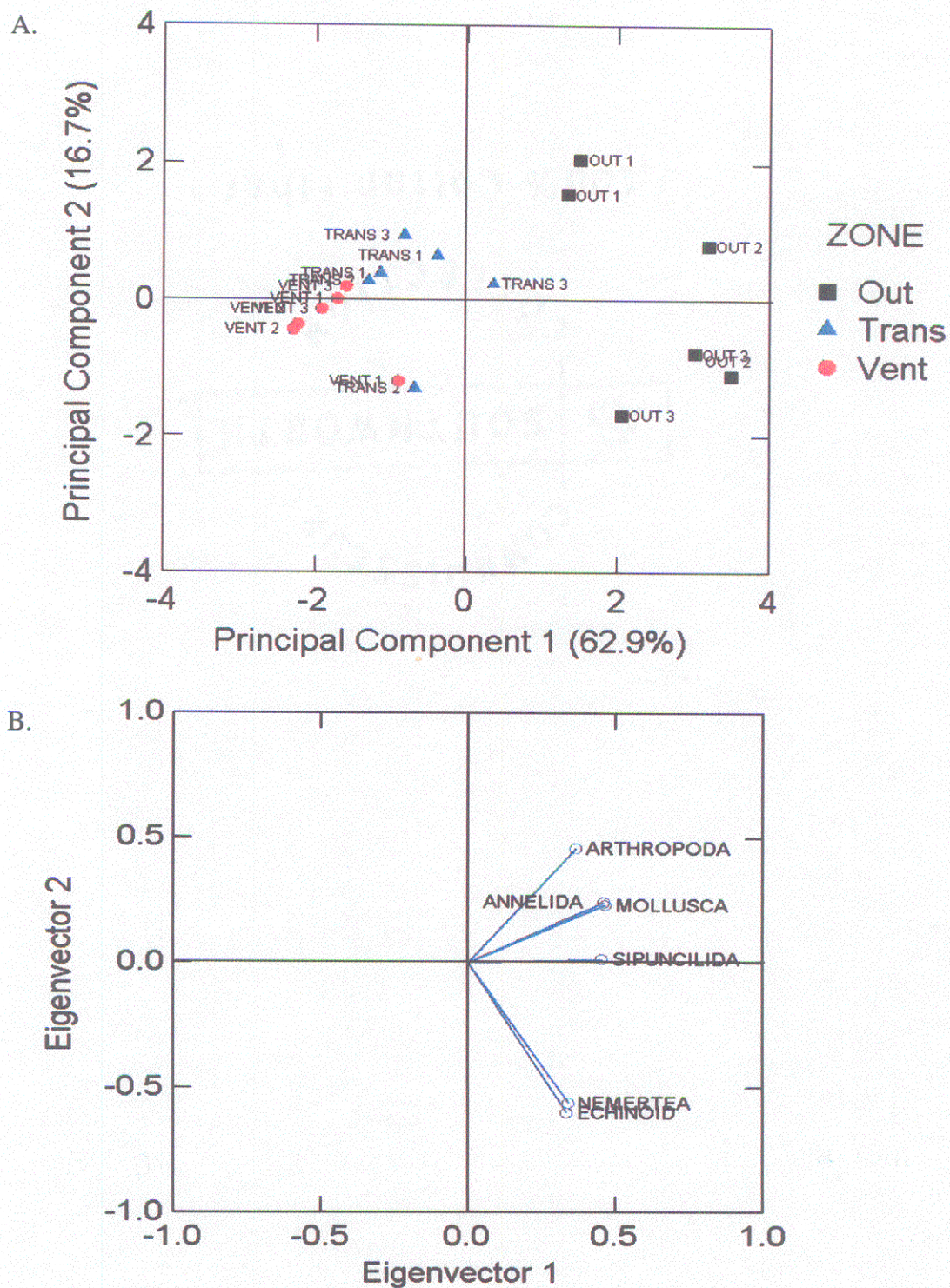


Figure 18: (A) Reduced space plot of Principal Component Analysis of the infaunal cores. (B) Plot of the eigenvectors from the Principal Component Analysis of the infaunal cores.

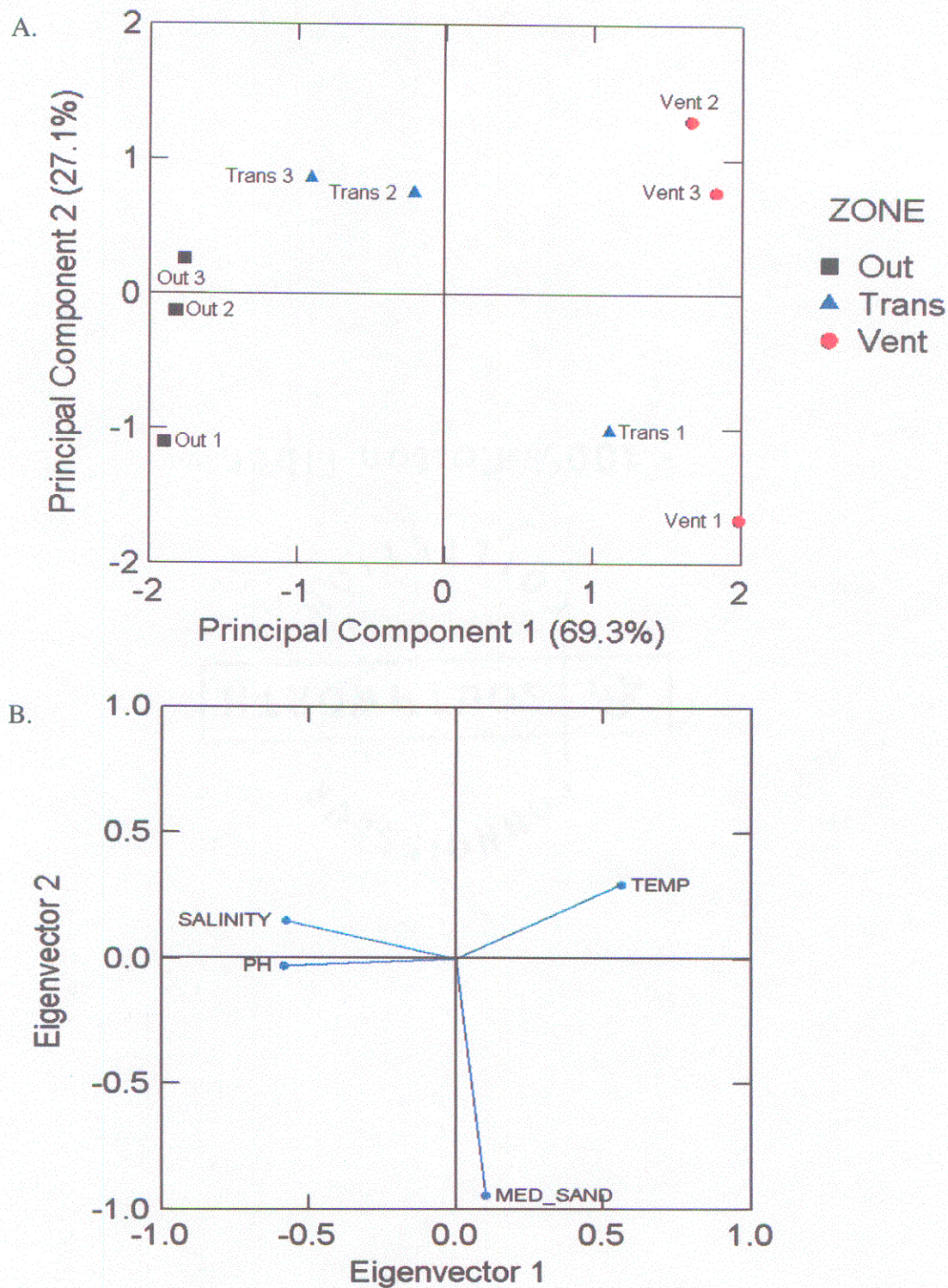


Figure 19: (A) Reduced space plot of Principal Component Analysis of the physical data from the pore water samples. (B) Plot of the eigenvectors from the Principal Component Analysis of the physical data from the pore water samples.

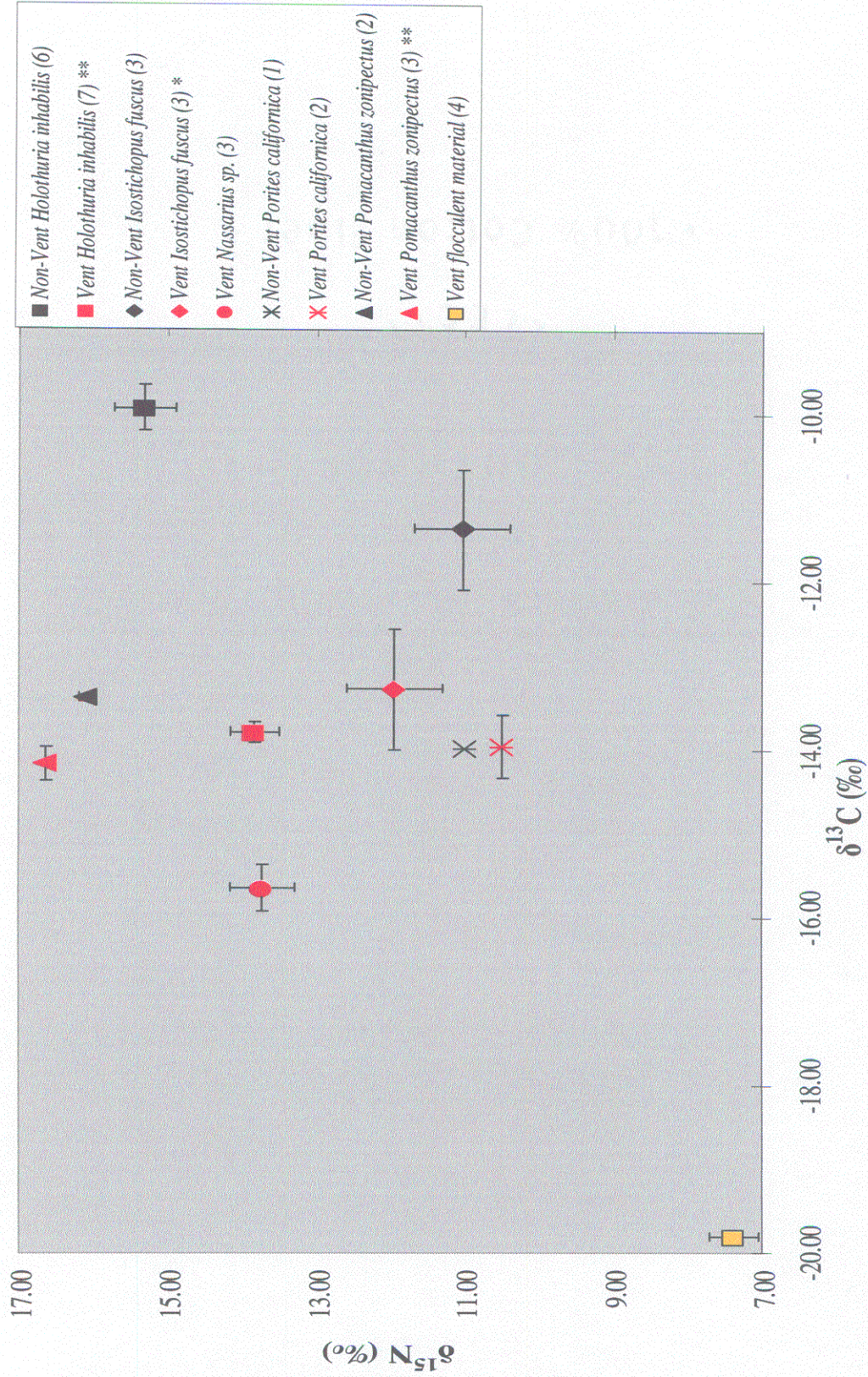


Figure 20. Stable isotope ratios from vent and non-vent fauna. Sample sizes in parentheses. ** $\delta^{13}\text{C}$ and $\delta^{15}\text{N}$ values of vent animals both significantly different ($p < 0.05$) than non-vent animals. * only $\delta^{13}\text{C}$ values significantly different.

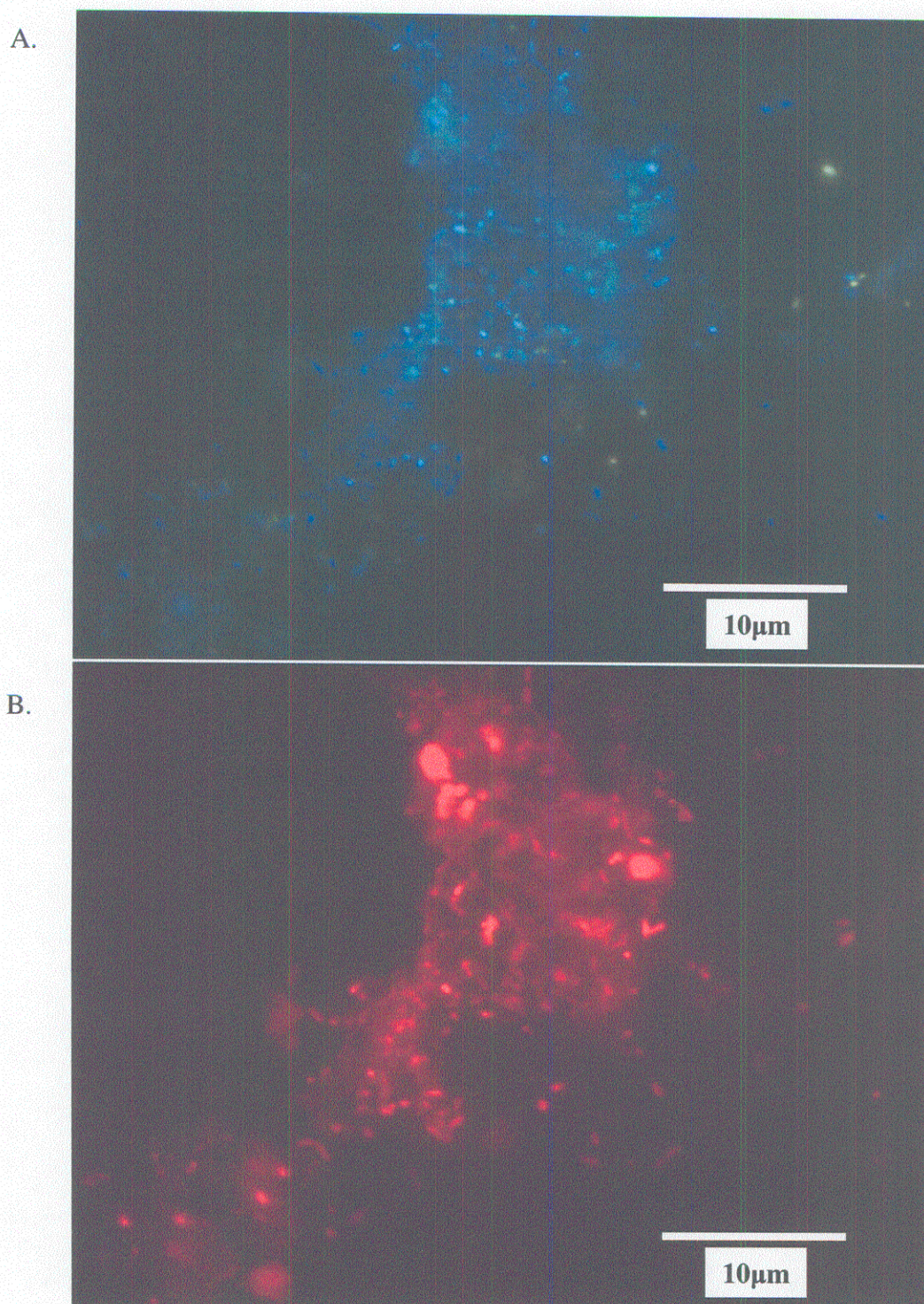


Figure 21. (A) Fluorescence microscopy analyses of the flocculent materials with DAPI stain imaging all DNA in a sample of the flocculent material. (B) FISH image, same field of view from (A) hybridized with Eub338 (a probe targeting bacteria). Images Courtesy of Victoria Orphan, NASA Ames.

Appendix 1: Taxonomic list of organisms from infaunal cores around shallow water hydrothermal vent in Bahía Concepción. V1C1 represents core 1 (of two) from the site Vent1, T1C1 represents core 1 from the site Transicional1, and O1C1 represents core 1 from the site Outside1 (see Figure 11 for locations).

taxa	V1 C1	V1 C2	V2 C1	V2 C2	V3 C1	V3 C2	T1 C1	T1 C2	T2 C1	T2 C2	T3 C1	T3 C2	O1 C1	O1 C2	O2 C1	O2 C2	O3 C1	O3 C2
ANNELEIDA	5	3	0	0	3	2	70	5	2	3	18	5	61	54	103	57	98	32
Ampharetidae	0	0	0	0	0	0	0	0	0	0	1	0	0	0	0	0	0	0
Capitellidae	0	1	0	0	0	0	0	2	0	0	0	0	0	0	0	2	3	0
Chrysopetalidae	0	0	0	0	0	0	0	0	0	0	0	0	4	2	1	0	1	1
Cirratulidae	0	0	0	0	0	0	0	0	0	0	0	0	0	0	0	0	0	1
Dorvilleidae	0	0	0	0	0	0	0	0	0	0	0	0	2	1	0	0	5	0
Eunicidae	0	0	0	0	0	0	0	0	0	0	0	0	0	0	1	0	0	0
Glyceridae	0	0	0	0	0	0	0	0	0	1	2	0	11	15	16	13	7	7
Hesionidae	0	0	0	0	1	0	0	0	0	0	1	0	1	0	0	0	0	0
Lumbrineridae	0	0	0	0	0	0	0	0	0	0	0	0	0	0	1	0	1	1
Megeledonidae	0	0	0	0	0	0	0	0	0	0	0	0	0	0	0	0	2	0
Nephtyidae	0	0	0	0	0	0	0	1	0	0	1	0	0	0	0	0	0	0
Nereidae	2	0	0	0	2	1	0	0	0	1	0	2	0	0	0	0	0	0
Onuphidae	0	0	0	0	0	0	0	0	0	0	0	0	0	0	1	0	0	2
Ophelidae	0	0	0	0	0	1	0	0	0	0	1	0	0	0	0	0	0	1
Paraonidae	0	0	0	0	0	0	0	0	0	0	0	0	0	0	1	0	1	1
Questidae	0	0	0	0	0	0	0	0	0	0	0	0	0	0	30	0	6	0
Sabelidae	0	0	0	0	0	0	0	0	2	1	0	0	29	25	30	25	59	8
Spionidae	1	1	0	0	0	1	0	0	0	0	7	2	0	0	0	2	0	3
Syllidae	2	1	0	0	0	0	1	1	0	0	4	1	6	8	17	6	12	7
N/A Scale Worm	0	0	0	0	0	0	0	0	0	0	0	0	0	0	0	0	1	0
Oligochaeta	0	0	0	0	0	0	68	1	0	0	1	0	8	3	5	9	0	0
NEMATODA	0	0	0	0	0	40	0	0	1	0	1	2	0	0	21	0	3	0
NEMERTEA	0	0	0	0	0	0	0	0	0	0	0	0	0	0	0	2	1	2
ECHINODERMATA	2	0	0	0	0	0	0	0	0	1	1	0	0	0	2	2	4	6
<i>Ophiactis savignyi</i>	2	0	0	0	0	0	0	0	0	1	1	0	0	0	0	1	0	0
<i>Agassizia scrobiculata</i>	0	0	0	0	0	0	0	0	0	0	0	0	0	0	1	0	1	0
Echinoid Juvenile	0	0	0	0	0	0	0	0	0	0	0	0	0	0	1	0	0	1

Appendix 1 (cont.):

taxa	V1 C1	V1 C2	V2 C1	V2 C2	V3 C1	V3 C2	T1 C1	T1 C2	T2 C1	T2 C2	T3 C1	T3 C2	O1 C1	O1 C2	O2 C1	O2 C2	O3 C1	O3 C2
<i>Ophiocoma</i> sp.	0	0	0	0	0	0	0	0	0	0	0	0	0	0	0	0	1	0
<i>Ophioderma</i> sp.	0	0	0	0	0	0	0	0	0	0	0	0	0	0	0	1	0	0
Ophuroid spp.	0	0	0	0	0	0	0	0	0	0	0	0	0	0	0	0	2	0
<i>Pentamera chierchia</i>	0	0	0	0	0	0	0	0	0	0	0	0	0	0	0	0	0	3
<i>Ophiactis</i> sp.	0	0	0	0	0	0	0	0	0	0	0	0	0	0	0	0	0	2
ARTHROPODA	3	6	1	2	4	13	8	11	9	1	71	49	31	71	46	47	31	23
<i>Ampelisca cristata</i>	0	0	0	0	0	0	0	0	0	0	1	0	3	0	1	1	0	0
<i>Ampelisca lobata</i>	0	0	0	0	0	0	0	0	0	0	1	0	0	0	0	0	0	0
Amphitochidae	0	0	0	0	0	0	0	0	0	0	0	1	0	0	0	1	0	0
Aoridae	0	0	0	0	1	0	0	1	0	0	0	0	0	0	0	1	0	0
Apseudidae	0	0	0	0	0	0	0	0	0	0	0	0	0	12	0	0	0	0
Callioptidae	0	0	0	0	1	1	0	0	0	0	13	6	0	0	0	0	0	0
cf. <i>Cyclaspis</i> sp.B	0	0	0	0	0	0	0	0	1	0	0	0	0	0	0	0	2	1
cf. <i>Sarsiella</i> sp. C	0	1	0	0	0	0	0	0	0	0	0	0	0	0	0	0	0	0
Corophioidae	0	0	0	0	0	0	0	0	0	0	0	1	0	0	0	0	0	0
<i>Cumella californica</i>	0	0	0	0	0	0	0	0	1	0	0	0	0	0	0	0	0	0
<i>Cumella</i> sp.	1	0	0	0	0	1	0	0	0	0	3	1	0	0	0	0	2	0
<i>Cyclaspis</i> sp.B	0	0	0	0	0	0	0	0	0	0	0	0	0	0	0	0	0	0
Cylindroleberidae	0	0	0	0	0	0	0	0	0	0	0	1	0	0	0	0	0	0
<i>Edotea sublittoralis</i>	0	0	0	0	0	0	0	0	0	0	0	0	1	0	0	0	0	0
<i>Erichthonius</i> sp.	0	0	0	0	0	0	0	0	0	0	3	1	0	0	0	0	0	0
<i>Eusiridae</i> sp.A	0	0	0	0	0	0	0	0	0	0	0	0	0	0	0	0	0	0
<i>Eusiridae</i> sp.B	0	0	0	0	0	0	0	0	0	0	0	0	0	0	0	0	0	1
<i>Excorallana</i> cf. <i>kathae</i>	0	0	0	0	0	0	0	0	0	0	0	0	0	0	0	0	0	1
<i>Garosyrhoe bigarra</i>	0	0	0	0	0	0	0	0	0	0	0	0	0	1	0	0	0	0
<i>Heptacarpus</i> sp.	0	0	0	0	0	0	0	0	0	0	1	0	0	1	0	0	0	1
<i>Kalliapseudes crassus</i>	0	0	0	0	0	0	0	0	0	0	0	0	2	0	0	0	2	0
<i>Leptochelia dubia</i>	0	0	1	1	1	6	0	0	1	0	0	3	0	0	0	0	0	1
<i>Leucon</i> sp.	0	0	0	0	0	0	0	0	0	0	0	1	0	0	0	0	0	0
<i>Leuroleberis</i> sp.	0	0	0	0	0	0	0	0	0	0	1	0	0	0	0	0	0	0
<i>Listriella</i> sp.	0	0	0	0	0	0	0	0	0	0	0	0	1	0	0	0	0	1

Appendix 1 (cont.):

taxa	V1 C1	V1 C2	V2 C1	V2 C2	V3 C1	V3 C2	T1 C1	T1 C2	T2 C1	T2 C2	T3 C1	T3 C2	O1 C1	O1 C2	O2 C1	O2 C2	O3 C1	O3 C2
<i>Mayerella banksia</i>	0	0	0	0	0	1	0	0	0	0	0	0	0	0	0	0	0	0
Megalopa	0	1	0	0	0	0	0	0	1	0	0	0	0	0	0	0	0	0
<i>Mysidopsis</i> sp.	0	1	0	0	0	1	1	0	0	0	0	0	0	0	0	1	0	0
Mysids	0	0	0	0	0	0	0	0	0	0	0	0	0	0	0	2	0	0
Mysid (juvenile)	0	0	0	0	0	0	1	0	0	0	0	0	0	0	0	0	0	0
<i>Neasiacilla californica</i>	0	0	0	0	0	0	0	0	0	0	0	4	0	0	0	0	0	1
<i>Orchomene magdalenis</i>	0	0	0	0	0	0	0	0	0	0	0	0	1	0	0	0	0	0
<i>Pagurapseudes laevis</i>	0	0	0	0	0	0	0	0	0	0	0	0	2	0	0	0	0	0
<i>Paracerceis</i> sp.	0	0	0	0	0	0	0	0	0	0	1	0	0	0	0	0	0	0
<i>Paranthurus elegans</i>	0	0	0	0	0	0	0	0	0	0	0	0	1	0	0	2	0	0
<i>Photis</i> sp.	0	0	0	0	0	2	0	0	0	0	2	10	0	0	2	1	0	1
<i>Podocerus</i> sp.	0	0	0	0	0	0	0	0	0	0	0	1	0	0	0	0	0	0
<i>Pontogeneia</i> sp.	1	0	0	1	0	0	0	0	0	1	0	6	0	0	0	0	0	0
<i>Pontogeneia rostrata</i>	0	0	0	0	0	0	0	0	0	0	27	0	0	0	0	0	0	0
Portunidae (juv)	1	0	0	0	0	0	0	0	0	0	0	0	0	0	0	0	0	0
<i>Rucilembooides stenopropodus</i>	0	3	0	0	0	0	6	2	0	0	17	10	1	0	6	13	11	6
<i>Rutiderma apex</i>	0	0	0	0	0	0	0	0	0	0	0	0	9	36	17	17	0	1
<i>Rutiderma</i> sp.	0	0	0	0	1	0	0	0	0	0	0	0	0	0	0	0	0	0
<i>Serolis</i> cf. <i>carinata</i>	0	0	0	0	0	0	0	0	0	0	0	0	0	4	0	1	2	0
Shrimp	0	0	0	0	0	0	0	0	0	0	1	0	0	0	0	0	0	1
Sphaeromatidae	0	0	0	0	0	0	0	0	0	0	0	2	0	0	0	0	0	0
Synopiidae	0	0	0	0	0	0	0	0	0	0	0	0	0	0	0	2	0	0
<i>Syrhoe</i> sp.	0	0	0	0	0	0	0	0	0	0	0	0	1	0	0	0	0	0
<i>Ostroroda</i> sp.A	0	0	0	0	0	1	0	6	2	0	0	0	2	0	9	0	6	4
<i>Ostroroda</i> sp.B	0	0	0	0	0	0	2	3	0	0	0	0	6	15	11	2	1	0
<i>Ostroroda</i> sp.C	0	0	0	0	0	0	0	0	0	0	0	1	3	0	0	1	0	0
SIPUNCULA	0	0	0	0	0	0	1	0	0	6	0	0	17	7	59	53	29	2
<i>Phascolosoma</i> sp.	0	0	0	0	0	0	1	0	0	6	0	0	16	7	58	53	28	2
<i>Sipunculus nudus</i>	0	0	0	0	0	0	0	0	0	0	0	0	1	0	1	0	1	0

Appendix 1 (cont.):

taxa	V1 C1	V1 C2	V2 C1	V2 C2	V3 C1	V3 C2	T1 C1	T1 C2	T2 C1	T2 C2	T3 C1	T3 C2	O1 C1	O1 C2	O2 C1	O2 C2	O3 C1	O3 C2
	5	2	0	0	0	0	7	16	16	6	8	4	86	96	99	62	60	73
MOLLUSCA																		
Bivalve sp.1	0	0	0	0	0	0	0	0	0	0	0	0	1	0	0	3	0	0
Bivalve sp.10	0	0	0	0	0	0	0	0	0	0	0	0	1	1	0	0	0	1
Bivalve sp.11	0	0	0	0	0	0	0	0	0	0	0	0	0	0	1	0	0	3
Bivalve sp.12	0	0	0	0	0	0	0	0	0	0	0	0	0	1	0	0	0	0
Bivalve sp.14	0	0	0	0	0	0	0	0	0	0	0	0	0	2	0	0	0	0
Bivalve sp.15	0	0	0	0	0	0	0	0	0	0	0	0	0	1	0	0	0	0
Bivalve sp.16	0	0	0	0	0	0	0	0	0	0	0	0	0	0	0	0	0	2
Bivalve sp.17	0	0	0	0	0	0	0	0	0	0	0	0	0	0	0	0	1	0
Bivalve sp.4	0	0	0	0	0	0	0	0	0	0	0	0	0	0	0	0	0	0
Bivalve sp.5	0	0	0	0	0	0	0	0	0	0	0	0	0	0	5	2	0	0
Bivalve sp.6	0	0	0	0	0	0	0	0	0	0	4	0	0	0	0	0	0	0
Bivalve sp.7	0	0	0	0	0	0	0	0	1	0	0	0	0	0	0	0	0	0
Bivalve sp.8	0	0	0	0	0	0	0	0	0	0	0	0	0	0	0	0	0	0
Bivalve sp.9	0	0	0	0	0	0	0	0	0	0	0	0	1	0	0	0	0	0
Juvenile Bivalve	1	0	0	0	0	0	0	0	0	0	0	1	0	2	1	1	0	0
<i>Laevicardium elatum</i>	0	0	0	0	0	0	0	0	3	0	3	0	0	5	14	14	25	44
<i>Megapitaria squalida</i>	0	0	0	0	0	0	0	0	0	0	0	0	1	0	0	0	0	0
<i>Crucibulum spinosum</i>	1	0	0	0	0	0	0	0	0	0	0	0	0	0	0	0	0	0
Mytilidae	0	0	0	0	0	0	0	0	0	0	0	0	0	0	0	0	1	0
Gastropod sp.1	0	0	0	0	0	0	1	0	0	0	0	0	1	0	0	0	0	0
Gastropod sp.2	0	0	0	0	0	0	0	0	0	0	0	0	0	0	1	0	0	0
Nassarius sp.A	0	0	0	0	0	0	0	0	0	0	1	0	0	1	2	0	2	2
Gastropod sp.5	0	0	0	0	0	0	0	0	0	0	0	0	0	0	0	0	0	1
Gastropod sp.6	0	0	0	0	0	0	0	0	0	0	0	0	1	0	0	0	0	0
Nassarius sp.B	0	0	0	0	0	1	0	1	0	1	0	0	0	0	0	0	1	0
Nassarius sp.C	0	1	0	0	0	0	1	0	1	0	0	0	0	0	0	0	1	0
Gastropod sp.9	0	0	0	0	0	0	0	0	0	0	0	0	0	0	0	0	1	0
Juvenile Gastropod	3	0	0	0	0	0	0	1	4	3	0	3	0	0	2	0	0	0
Olividae	0	0	0	0	0	0	0	0	2	0	0	0	2	0	1	0	1	0
Caecum sp.A	0	1	0	0	0	0	5	14	5	2	0	0	77	80	70	36	22	20
Caecum sp.B	0	0	0	0	0	0	0	0	0	0	0	0	0	2	2	4	1	0
Caecum sp.C	0	0	0	0	0	0	0	0	0	0	0	0	0	1	0	2	1	0

Appendix 2: Carbon and nitrogen stable isotope ratios of vent and non-vent fauna.

Sample	$\delta^{13}\text{C}$	$\delta^{15}\text{N}$
Non-Vent <i>Holothuria inabilis</i> 1	-9.99	16.12
Non-Vent <i>Holothuria inabilis</i> 2	-10.42	15.35
Non-Vent <i>Holothuria inabilis</i> 3	-10.96	13.91
Non-Vent <i>Holothuria inabilis</i> 4	-9.37	14.62
Non-Vent <i>Holothuria inabilis</i> 5	-9.72	16.72
Non-Vent <i>Holothuria inabilis</i> 6	-9.17	15.24
Vent <i>Holothuria inabilis</i> 1	-13.98	13.41
Vent <i>Holothuria inabilis</i> 2	-14.06	13.5
Vent <i>Holothuria inabilis</i> 3	-13.58	13.38
Vent <i>Holothuria inabilis</i> 4	-13.86	12.68
Vent <i>Holothuria inabilis</i> 5	-13.11	15.31
Vent <i>Holothuria inabilis</i> 6	-13.98	14.18
Vent <i>Holothuria inabilis</i> 7	-13.95	14.44
Non-Vent <i>Isostichopus fuscus</i> 1	-11.47	11.02
Non-Vent <i>Isostichopus fuscus</i> 2	-11.87	10.67
Non-Vent <i>Isostichopus fuscus</i> 3	-10.8	11.41
Vent <i>Isostichopus fuscus</i> 1	-12.6	11.93
Vent <i>Isostichopus fuscus</i> 2	-12.53	10.85
Vent <i>Isostichopus fuscus</i> 3	-14.71	13.09
Vent <i>Nassarius</i> sp. 1	-15.83	14.56
Vent <i>Nassarius</i> sp. 2	-16.03	13.08
Vent <i>Nassarius</i> sp. 3	-14.71	14.60
Vent <i>Nassarius</i> sp. 4	-16.03	12.67
Non-Vent <i>Porites californica</i>	-13.98	11
Vent <i>Porites californica</i> 1	-13.59	10.48
Vent <i>Porites californica</i> 2	-14.33	10.51
Vent <i>Bugula neritina</i>	-18.86	11.25
Non-Vent <i>Pomacanthus zonipectus</i> 1	-13.36	16.19
Non-Vent <i>Pomacanthus zonipectus</i> 2	-13.43	16.05
Vent <i>Pomacanthus zonipectus</i> 1	-14.07	16.65
Vent <i>Pomacanthus zonipectus</i> 2	-14.56	16.77
Vent <i>Pomacanthus zonipectus</i> 3	-13.89	16.52
Vent <i>Calamus brachysomus</i>	-11.42	15.98
Vent flocculent material 1	-19.77	7.7
Vent flocculent material 2	-19.72	7.84
Vent flocculent material 3	-19.75	7.56
Vent flocculent material 4	-19.96	6.41